Shedding Light on Photosynthesis: The Impacts of Atmospheric Conditions and Plant Canopy Structure on Ecosystem Carbon Uptake

by

Susan J. Cheng

A dissertation submitted in partial fulfillment
of the requirements for the degree of
Doctor of Philosophy
(Ecology and Evolutionary Biology)
in the University of Michigan
2016

Doctoral Committee

Professor Knute J. Nadelhoffer, Co-Chair
Associate Professor Allison L. Steiner, Co-Chair
Associate Professor William S. Currie
Professor Peter S. Curtis, The Ohio State University
Professor Deborah E. Goldberg

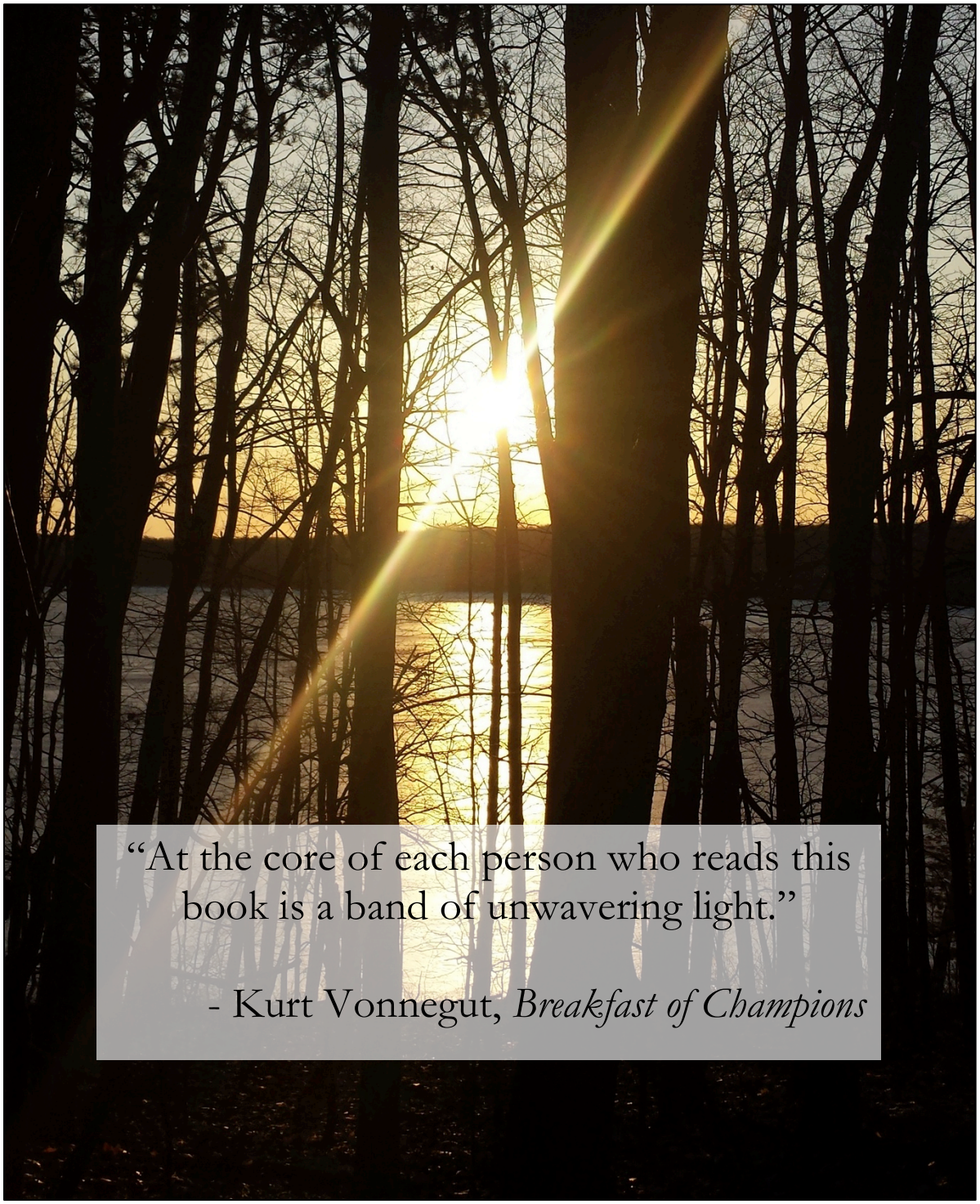

Photo looking onto Douglas Lake at the University of Michigan Biological Station. Reprinted as the dissertation frontispiece with permission from the photographer, James Le Moine. Quotation reprinted under Fair Use Guidelines.

DEDICATION

To my mom, dad, grandma, and big sisters, for giving me the opportunity and strength to keep pushing the boundaries of the world I know. And for teaching me the value of the gifts given by immigrant and first generation college families that embolden younger generations.

獻詞

獻給我的媽媽爸爸，阿嬤和姊姊。是你們賜予給我機會與力量，讓我得以拓展我對於這個世界的認識。同時也是你們教會了我，作為新移民的付出而得以用高等教育培養下一代，是多麼的有價值並需要被傳承下去。

ACKNOWLEDGEMENTS

Words can't capture my gratitude for the extraordinary generosity in time, ideas, and resources that many people have given me over the last six years. I hope to keep living by the lessons you've taught me and honor them in some small way by sharing them with others.

My advisors, Knute Nadelhoffer and Allison Steiner, have played the biggest role in shaping me into the scientist I am today. Knute always encouraged my "big picture" thinking and ambition to explore unexpected connections across disciplines. He is also the best example I could have for how to use science to change the world. I'm convinced Allison has superpowers—I always leave her office with solutions that she's nearly instantaneously thought of and with the inspiration to push my work one step further. She also taught me the importance of staying authentic to myself, both as a scientist and as a person. George Kling was a generous mentor, who was always there to provide emergency pep talks. George's advice was often delivered in the form of memorable proverbs and kept me focused and resilient during tough times. His long lists of suggestions after my presentations at lab meetings made me a better writer, speaker, and teacher.

I couldn't have asked for a better set of committee members than Bill Currie, Peter Curtis, and Deborah Goldberg. I loved committee meetings and I'm probably the only grad student who wishes we were required to have more than one a year. Bill's shared enthusiasm for the physics of ecosystems made me feel like I had a real place in ecology. Peter's calm and collected demeanor encouraged me to explore ideas without fear, with him often reminding me that, "It's just logistics." I have to thank Deborah for pushing me to ask questions in more interesting ways and for building a department where I was in the company of many strong women.

The Kling and Nadelhoffer lab members (2010-present) provided feedback on my research, evening work camaraderie, and much-needed laughter. Many thanks to Buck Castillo (for carrying me through the woods after I sprained my ankle doing field work), Jim Le Moine (for all his community building and last minute editing of papers, applications, and posters), Nicholas Medina, Jacqueline Popma, Luke Nave, Apolline Auclerc, Pierre-Joseph Hatton, Chris Cook, and Marian Schmidt. A special thank you goes to Jasmine Crumsey for showing me how to move through the world with grace (and yoga) and to Jason Dobkowski for showing me the art in everyday paper and discarded lab equipment.

The Steiner Research Group and others in AOSS (I'm calling the department this forever) kept me linked to atmospheric science and gave me support in programming and modeling. Many thanks to Alex Bryan, Stacey Kawecki, Kirsti Ashworth, Yang Li, Matt Wozniak, Thanos Tsikerdekis, Dori Mermelstein, Sam Pennypacker, Sam Basile, and Weiye Yao. A big thank you goes to Kristen Mihalka, who dragged me from her office to meet Allison before I had even chosen which grad schools to apply to. With Ahmed Tawfik and Dan Gershman, the three of you gave me the unique experience of building a family through "Friendship!"

The community at the University of Michigan Biological Station helped me stay positive during several long field seasons. Many thanks to Chris Gough, Meghan Gough, Dave Karowe, Gil Bohrer, Valeriy Ivanov, Tony Sutterly, Richard Spray (who taught me how to drive Zeke), Renee Kinney, Karie Slavik, Peggy Meade, Alicia Farmer, Jason Tallant, Mark Hunter, MaryCarol Hunter, Mike Grant, Sheryn Lowe (who patched me up on my first day at UMBS after a disastrous Fourth of July relay race that happened *before* I met Knute for the first time), Sherry Webster, and Bob Vande Kopple. I'm honored that Jean Wilkening was my first mentee and am very proud of how much she has accomplished so far. An *extra* special thank you goes to Chris Vogel, whose patience, understanding, and ingenuity made it possible for me to collect the data I needed for my dissertation. There is not enough gourmet coffee in the world I could bring to thank you.

My cohort and fellow grad students shared their ideas, time, and thoughts on science and reminded me of the joys in art, social justice, politics, and movies (and puppies): Rachel

Cable, Alison Gould, KC Semrau, Jason Dobkowski, Rafael D'Andrea, Rob Massatti, John Guittar, Jen-Pan Huang, Micaela Martinez-Bakker, Cindy Bick, Sahar Haghighat, Bill Webb, Iman Sylvain, Lauren Stadler, Tara Smiley, Lauren Cline, Missy Stults, Rebecca Mandell, Nick Rajkovich, Tommy Jenkinson, Andréa Thomaz, Pámela Martinez, Jordan Bemmels, Katherine Crocker, Senay Yitbarek, and James Hammond. I'd also like to thank JP Huang and Wei-Chin Ho for translating the dedication in this dissertation for my family.

Thank you to those who gave me the very special experience of becoming friends with my heroes: Liz Wason, Jasmine Crumsey, Fernanda Santos, Brady Getson-Hardiman, and Ed Baskerville.

I'd also like to thank Jo Kurdziel, Laura Eidietis, and Don Zak for showing me by example how to be a better teacher. Jane Sullivan, Cindy Carl, and Sonja Botes were always to the rescue whether it was to troubleshoot problems or to keep me and other grad students calm while we waited for the Chair or our committees to make decisions. Carol Solomon and Amber Stadler were generous and patient with funding and reimbursement needs.

Finally, I'm grateful for the donors and managers of the following funding sources that allowed me to pursue the work in this dissertation: The Rackham Graduate School, the University of Michigan EEB block grant and Helen Olsen Brower Fellowship in Environmental Studies, the University of Michigan Graham Institute Doctoral Sustainability Fellowship, the Michigan Space Grant Consortium, and the University of Michigan Biological Station Marian and David Gates Graduate Fund, Dr. Ralph E. Bennett Endowment Fund, and Henry A. Gleason Fellowship.

It has truly meant a lot to have so many people be a part of my Ph.D. experience. Having this unwavering band of support has helped light my path forward, and I hope to do the same for others in my field. Thank you.

TABLE OF CONTENTS

LIST OF TABLES

LIST OF FIGURES

LIST OF APPENDICES

ABSTRACT

The Earth's climate is influenced by complex interactions of physical, chemical, and biological processes that link terrestrial ecosystems and the atmosphere. One of these interactions involves the use of light in photosynthesis, which allows plants to remove CO_2 from the atmosphere and slow the unprecedented rate of climate change the Earth is experiencing. However, modeling future climate remains challenging, in part because of limited knowledge of mechanisms controlling the effects of light on gross ecosystem CO_2 uptake (conceptually, photosynthetic activity integrated across all leaves in a plant canopy). Unlike previous studies, this dissertation uses data from atmospheric science, ecosystem ecology, and plant physiology to provide evidence for mechanistic links between physical, biophysical, and ecological controls on the effects of light on processes tied to gross ecosystem CO_2 uptake—specifically, ecosystem gross primary production (GPP) and leaf photosynthesis. First, this dissertation empirically demonstrates that the dominant effect of clouds is to reduce total light above canopies. However, optically thin clouds increase scattered, diffuse light, which canopies use more efficiently than they use direct light. This offsets reductions in total light and results in no net change in GPP under thin clouds, while GPP decreases under optically thick clouds because both diffuse and direct light decrease. Second, ground-based measurements indicate that the rate of increase in GPP with diffuse light changes throughout the day. The magnitude of increase depends on how canopies interact with the angle of incoming light to biophysically alter the distribution of light within canopies and thus, the proportions of leaves contributing to GPP. Third, the distribution of species and light within one forest canopy leads to differences in some of the rate-limiting biochemical reactions in leaf photosynthesis. These field-based data indicate which assumptions representing canopies in Earth system models may not have support *in situ*, and could be contributing to errors in model estimates of future climate. Overall, this dissertation identifies mechanisms through which clouds and plant canopy structure alter land-atmosphere CO_2 fluxes and subsequently, Earth's climate. It also provides an important interdisciplinary framework for testing assumptions about the feedbacks that living organisms form with their environment.

Chapter 1

Introduction

1.1 Impacts of Land-Atmosphere Interactions on Climate

The Earth system consists of a complex set of physical, chemical, and biological interactions that shape our environment and form feedbacks with climate (Bonan 2015). Globally, atmospheric circulation controls precipitation and surface temperature patterns (Ropelewski and Halpert 1987, Halpert and Ropelewski 1992, Hurrell 1996, Dai and Wigley 2000), which influence the distribution of plant species and functional traits (Westoby and Wright 2006, Kreft and Jetz 2007). In turn, the global productivity of plants influences climate in several ways, including through the carbon cycle (Bonan 2008). Currently, terrestrial ecosystems remove the equivalent of ~25% of annual anthropogenic CO_2 emissions from the atmosphere and store it as organic carbon in plant biomass and soil (Friedlingstein et al. 2014). Through this process, terrestrial ecosystems play an important role in slowing the Earth's unprecedented rate of climate change (IPCC 2013).

However, the scientific community has a limited understanding of the mechanisms controlling land-atmosphere interactions and how they will respond to climate change (Peñuelas et al. 2013, Richardson et al. 2013, Bahn et al. 2014). This affects how accurately Earth system models simulate concentrations of atmospheric greenhouse gases and limits confidence in future projections of climate. In phase 5 of the Coupled Model Intercomparison Project (CMIP5), Earth system models project a range of atmospheric CO_2 fluxes into terrestrial ecosystems of anywhere from -6 to 9 Pg C yr^{-1} for the year 2100 (Friedlingstein et al. 2014). This level of uncertainty is predominately attributed to differences in how models represent the terrestrial carbon cycle. Improving this representation relies on identifying the mechanisms that mediate land-atmosphere interactions and quantifying how they change leaf photosynthesis and ecosystem uptake of CO_2.

My dissertation extends our understanding of how land-atmosphere interactions affect climate by empirically testing assumptions about how light (i.e., photosynthetically active radiation; 400-700 nm) affects gross ecosystem CO_2 uptake (Figure 1.1). Historically, definitions for terms describing photosynthesis at leaf and ecosystem scales differ among scientific disciplines (Wohlfahrt and Gu 2015). In this dissertation, gross ecosystem CO_2 uptake refers to the conceptual integration of leaf photosynthesis for all leaves within a plant canopy. The datasets in individual chapters define leaf photosynthesis or gross ecosystem CO_2 uptake differently than the conceptual definition of gross ecosystem CO_2 uptake because of measurement limitations. However, the data describe processes related to gross ecosystem CO_2 uptake within the context of each question addressed. Analyzing these datasets therefore adds to our understanding of how plants use CO_2 at the leaf and ecosystem scales. Overall, this dissertation achieves this by combining theory, tools, and data from atmospheric science, ecosystem ecology, and plant physiology to examine the following: 1) the physical mechanisms through which clouds alter the amount and type of light available for plant canopies to use in the process of photosynthesis, 2) how the biophysical features of plant canopies control the distribution of light available to leaves within the canopy, and 3) how ecological variation in canopies changes the photosynthetic limitations of terrestrial ecosystems.

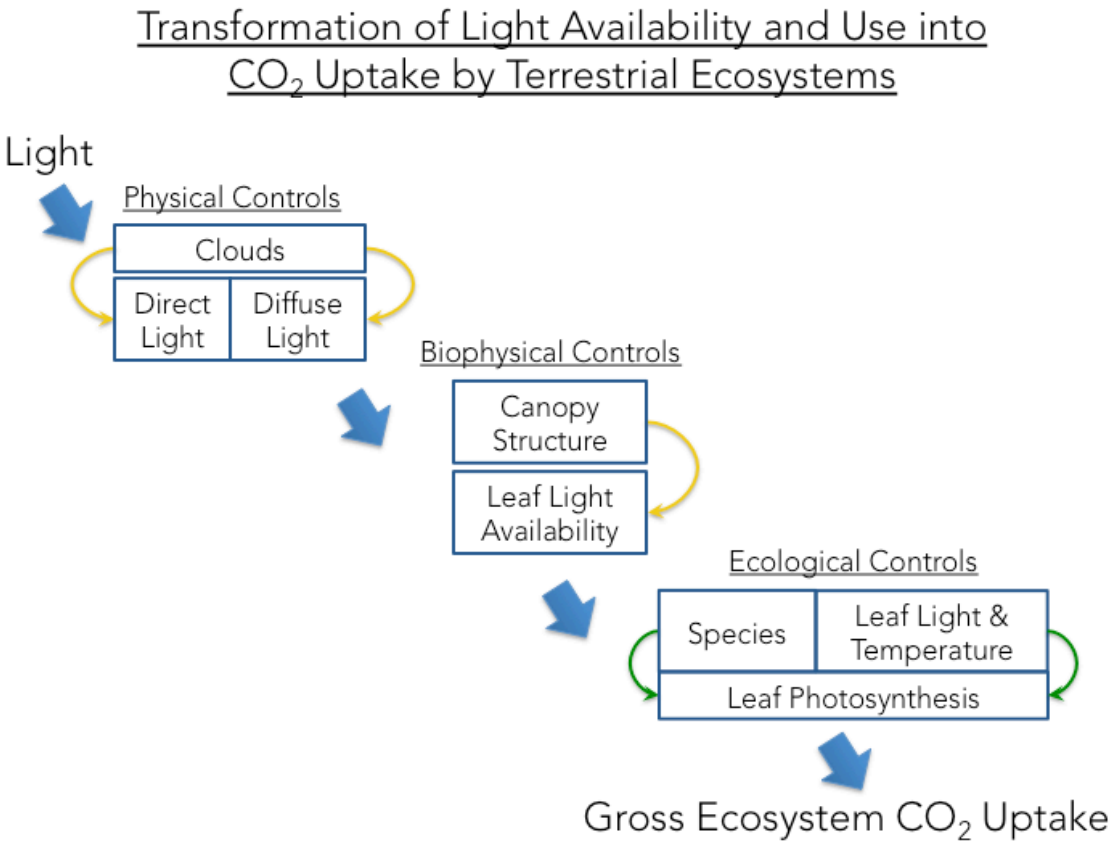

Figure 1.1: The effect of light (photosynthetically active radiation; 400-700 nm) on gross ecosystem CO_2 uptake (conceptually, the sum of leaf photosynthesis in all leaves within the plant canopy) is mediated through physical controls (i.e., clouds) on ecosystem light availability, biophysical controls (i.e., plant canopy structure) on leaf light availability within a canopy, and ecological controls (i.e., species composition, leaf light environment, and leaf temperature) on how light is used by plant canopies in photosynthesis.

1.2 Role of Light in Terrestrial Carbon Cycling

In terrestrial ecosystems, the importance of light is captured by plant adaptations and photosynthetic responses to changing light conditions. At the leaf level, photosynthesis increases with light until the leaf is light saturated and then decreases because absorbed light not used or dissipated by plants can damage leaves (Demmig-Adams and Adams III 1992). Because of the positive and negative effects of light on photosynthesis, plants have evolved the ability to produce leaves that are adapted to their light environment. In a plant canopy, light levels are highest at the top and decrease non-linearly with depth in the canopy according to equations in Monsi and Saeki (2005). As a result, leaves at the top of a plant canopy (i.e., sun leaves) are generally smaller in area and angled vertically to limit excess light absorption (McMillen and

McClendon 1979). In contrast, leaves in low light environments (i.e, shade leaves) have larger leaf area and are angled horizontally to maximize light capture. In addition, sun leaves generally have higher rates of photosynthesis at saturating light levels than do shade leaves (Bohning and Burnside 1956). These leaf-level processes and adaptations scale to the plant community, with light-demanding species dominating early stages in ecological succession and shade-tolerant species dominating in later successional stages (Bazzaz 1979). Shifts in species composition and leaf area distribution during succession or after moderate disturbances can maintain ecosystem productivity by limiting the decrease in canopy light absorption and increasing canopy light use efficiency (Gough et al. 2013).

1.3 Role of Diffuse Light in Ecosystem Carbon Cycling

The amount and type of light available for a plant canopy to use is modified by clouds in two ways. First, clouds absorb or reflect incoming solar radiation (Twomey 1991, Cess et al. 1995), which reduces the total amount of light that reaches the top of a plant canopy. Second, clouds change the type of light available by scattering direct solar radiation and producing diffuse light (Fritz 1954). One of the first theoretical models for light transmission discussed how light extinction coefficients within a hypothetical canopy could differ under direct and diffuse light (Anderson 1966). This conclusion was supported by a field study of grass canopies that measured steeper extinctions of light under clear skies than under overcast conditions (Sheehy and Chapas 1976). Thus, clouds have the potential to change gross ecosystem CO_2 uptake by increasing the amount of diffuse light available above plant canopies and, therefore, the distribution of light within canopies.

One of the first model simulations of leaf photosynthesis under different types of light demonstrated that diffuse light can increase CO_2 uptake in plants (Oker-Blom 1985). These simulations of a Scots pine shoot demonstrated that photosynthesis increased because more needles on the shoot intercepted radiation when more of the light was diffuse, rather than direct. This theory can be applied to the canopy-level, where on a clear day, leaves at the top of a canopy can intercept more light than leaves at the bottom (Figure 1.2a). If clouds are present in the atmosphere and produce diffuse light, more light can reach deeper through canopies, reducing shading and changing the distribution of light among leaves (Figure 1.2b). Under this scenario, an increase in light absorption by lower-canopy “shade” leaves under higher levels of

diffuse light is hypothesized to compensate for the decrease in absorption by upper-canopy "sun" leaves (Roderick et al. 2001).

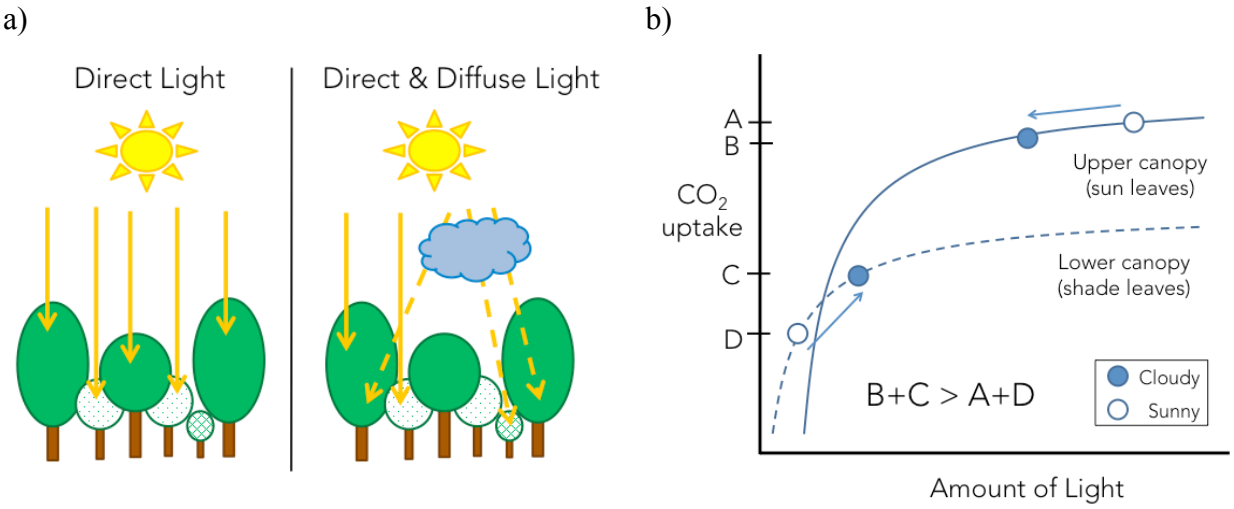

Figure 1.2: a) Diffuse light (dashed lines) reaches deeper into canopies and illuminates more shade leaves. b) Gross ecosystem CO_2 uptake is hypothesized to be higher under cloud-created diffuse light (B+C) than under direct light on clear days (A+D).

The conclusions from theoretical models of how diffuse light influences plant canopies are biased by how they simplify the variability in light and ecology that occurs in ecosystems. However, the development of the eddy covariance technique changed the study of ecosystem ecology by providing direct measurements of ecosystem fluxes—allowing the scientific community to gain insight into such variability. This technique is based on wind moving across the top of canopies and forming eddies that transfer gases between the ecosystem and the atmosphere. In the 1990s, the first towers were installed with infra-red gas analyzers to measure water vapor and CO_2, and sonic anemometers to measure wind speed and direction (Baldocchi 2003). The fluxes of CO_2 and water vapor between plant canopies and the atmosphere are then calculated over specified time intervals as the products of air density and the covariance between the vertical velocity of air and the mixing ratio of the gas (Baldocchi et al. 1988). Unlike previous methods of measuring gas exchange between plants and the atmosphere, the eddy covariance technique directly measures ecosystem-level CO_2 exchange (i.e, net ecosystem exchange; NEE) for long periods of time at relatively high temporal resolution (e.g., at 10 Hz, although often averaged at 30-minutes or 1-hour). Multiple statistical methods have been developed to partition NEE into gross primary production (GPP) and ecosystem respiration

(Desai et al. 2008). GPP is calculated as the combination of NEE and ecosystem respiration, where daytime ecosystem respiration is predominately based on a correlation between nighttime ecosystem respiration and a set of environmental variables, such as soil or air temperature (Desai et al. 2008). Because photorespiration cannot be measured at the ecosystem level, GPP from the eddy covariance method does not represent gross ecosystem CO_2 uptake, and is instead, gross ecosystem CO_2 uptake minus photorespiration (Wohlfahrt and Gu 2015). However, these GPP data still allow us to examine how changes in environmental conditions, including incoming direct and diffuse radiation, influence other processes in photosynthesis at the ecosystem level.

Studies using eddy covariance towers have tested the hypothesized positive effect of diffuse light on plant productivity in actual ecosystems. For example, eddy covariance data from a temperate beech forest and a boreal spruce forest showed that light use efficiency (LUE) was higher under cloudy conditions compared to clear skies (Hollinger et al. 1994, Fan et al. 1995). In these studies, cloud conditions were deduced in one of two ways. In Hollinger et al. (1994), overcast days were defined as days when diffuse light comprised 33-84% of the light above plant canopies. In Fan et al. (1995), diffuse light was not measured and overcast conditions were defined as times when the measured total light was less than 50% of the expected value for clear skies.

The impact of diffuse light on photosynthetic activity has also been examined at larger spatial scales using a variety of models. For example, Roderick et al. (2001) adjusted a LUE model so that the LUE parameter changed with the proportion of total light that is diffuse. When this model was scaled to the continental level, predictions of net primary production were within an order of magnitude of other studies. More recently, simulations from a global land surface model demonstrated that the global land carbon sink may have been ~25% higher because of increases in the proportion of diffuse light that occurred predominately from aerosol emissions during 1960-1999 (Mercado et al. 2009). These studies provide a compelling reason to incorporate the effect of diffuse light into Earth system models and couple them to changes in atmospheric drivers of diffuse light. However, modifying one portion of an Earth system model is difficult to do without causing errors in other components of the model. Thus, it is critical to rigorously examine whether the effect of diffuse light on gross ecosystem CO_2 uptake has a) a large impact relative to other drivers, b) occurs independently of other environmental conditions

that co-vary with diffuse light, c) is generalizable across ecosystems, and d) is empirically supported through direct mechanisms that mediate this effect.

1.4 Limitations in Current Understanding

Recent studies that combine larger eddy covariance datasets, derived data, and models have yielded conflicting results on how large and generalizable the effect of diffuse light on ecosystem productivity is. One of the first studies using eddy covariance measurements in multiple ecosystems and a set of LUE models concluded that forests, a prairie, and a wheat field used diffuse light more efficiency than they used direct light (Gu et al. 2002). In addition, ecosystem LUE of diffuse light varied across these ecosystems by up to a factor of two. Niyogi et al. (2004) found that when there were more light-scattering particles in the atmosphere, NEE into forests and croplands increased by different rates, but decreased in grasslands. However, LUE did not vary across 23 grasslands, croplands, and a forest under patchy clouds, defined as conditions when 40-80% of the total light was diffuse (Wang et al. 2008). These studies suggest that ecosystems vary in how they respond to diffuse light. Canopy simulations provide support for this by showing that light within a modeled canopy is redistributed as light conditions change (Knohl and Baldocchi 2008). However, it is unclear why responses should differ. One possibility is that these differences occur only between ecosystems with drastically different canopy structures, such as between a forest and a grassland, which could create a strong difference in how light is distributed within these two canopies. Another possibility is that species differ in physiological response to light environments enough to mediate ecosystem-specific responses to diffuse light in canopies from the same land cover type.

In addition, no consensus exists on the magnitude or direction of the effect of diffuse light on ecosystem productivity or how this is directly linked to atmospheric drivers of diffuse light. NEE from eddy covariance measurements was estimated to be up to 140% higher under cloudy conditions than under clear skies (Urban et al. 2007). However, analyses of field-based data and canopy model simulations suggest that increases in GPP are small, and may only occur when atmospheric conditions that produce diffuse light do not concurrently reduce total light availability (Alton 2008, Knohl and Baldocchi 2008, Oliphant et al. 2011). The inconsistency across modeling and field studies may stem from the different tools and experimental designs used.

There are three ways in which the methods used may distort our understanding of how diffuse light influences ecosystem productivity. First, conclusions from these studies would depend on the assumptions these models make about how light is partitioned between direct and diffuse light as it moves through the atmosphere. For example, the difference between ecosystem light use efficiencies for diffuse and direct light changed when using direct measurements instead of calculations of direct and diffuse light (Gu et al. 2002). Second, additional environmental factors, aside from light (i.e., air temperature and vapor pressure deficit), and ecological processes that influence photosynthesis also change under atmospheric conditions that increase diffuse light, and may confound existing estimates of the diffuse light effect (Gu et al. 1999, Gu et al. 2002). Understanding the role of air temperature and light in photosynthesis is particularly important because both influence the leaf's energy balance and leaf temperature (Gates 1968), which subsequently affect rates of leaf biochemical reactions (Bernacchi et al. 2012). Third, cloud conditions are primarily inferred from calculations or measurements of diffuse light without testing for a direct link (Hollinger et al. 1994, Rocha et al. 2004, Urban et al. 2012). These limitations must be addressed before evaluating whether inclusion of the interaction between diffuse light and photosynthesis in Earth system models can improve estimates of land-atmosphere fluxes of CO_2.

1.5 Summary of Dissertation Objectives

The overall objective of my dissertation is to begin addressing the limitations discussed above by empirically investigating mechanisms that alter the effects of light on gross ecosystem CO_2 uptake. By linking datasets and tools from atmospheric science, ecosystem ecology, and plant physiology, my dissertation links the transformation of light into organic carbon from the atmosphere, through the canopy, and finally, to the leaf for photosynthesis (Figure 1.1). My dissertation achieves this in the following chapters by addressing three questions:

- *How do clouds change the amount and type of light available for plant canopies to use in photosynthesis?* Theoretically, clouds can increase gross ecosystem CO_2 uptake by producing diffuse light. However, clouds can also counteract that effect by absorbing and reflecting solar radiation and reducing the total amount of light reaching plant canopies (Section 1.3). Despite the role that clouds play in radiative transfer, few studies have examined how clouds directly influence the amount of diffuse and direct light above plant canopies. Instead,

"cloudiness" is often defined based on the fraction of total incoming light that is diffuse as in Hollinger et al. (1994) and Rocha et al. (2004). This assumes a mechanistic link between clouds and diffuse light that may not be as strongly correlated as is assumed under current definitions. In addition, these studies compared changes in ecosystem productivity only under a few qualitative categories of cloudiness. This limits the capacity to predict how ecosystem productivity responds to changes across the spectrum of sky conditions.

In Chapter 2 (Cheng et al. in review-a), I address the limitations in our understanding of how clouds influence GPP in three ways. First, I empirically link clouds to above-canopy light environments using satellite-derived data on cloud properties and ground-based eddy covariance tower measurements of diffuse and direct light. Second, I quantify the direct relationship between cloudiness and diffuse light during the mid-day along a continuous measure of cloud optical thickness, which is an integrative measure of the scattering and absorbing properties of clouds and accounts for variations in cloud phase, thickness, and particle size and distribution. Third, I examine whether the response of GPP to diffuse light can be directly predicted by cloud optical thickness, data on which are available at the global scale. This allows me to test whether a relationship between clouds and GPP can be used to scale changes in light availability from the single site to the global-level. This chapter adds to our understanding of how light controls the magnitude of gross ecosystem CO_2 uptake by empirically examining a physical process that mediates the effect of the atmosphere on ecosystem light availability and GPP.

- *How does GPP respond to diffuse light and change with ecosystem canopy structure, independent of co-varying environmental variables?* Previous research shows inconsistent patterns in the way ecosystem productivity responds to diffuse light (Section 1.4). This inconsistency may be a consequence of using theoretical estimates of diffuse light in place of direct measurements (Gu et al. 2002). In addition, the impact of diffuse light on ecosystem productivity may be overestimated. This could occur because clouds not only alter the amount of diffuse light above plant canopies, but also change direct light levels, air temperature, and atmospheric vapor pressure deficit, all of which influence the rate of photosynthesis. As a result, it is unclear whether diffuse light itself increases ecosystem

productivity. This makes it difficult to evaluate whether adding this process into Earth system models would improve projections of land-atmosphere CO_2 fluxes.

In Chapter 3 (Cheng et al. 2015), I refine our understanding of how GPP responds to diffuse light by addressing the limits of the methods used in previous studies. First, I use eddy covariance measurements of diffuse light and GPP to examine how broadleaf deciduous forests, mixed forests, soy croplands, and maize croplands respond to diffuse light. Second, I determine whether diffuse light has a direct effect on GPP by removing the confounding effects of direct light, vapor pressure deficit, and air temperature, before calculating the response of GPP to increases in above-canopy diffuse light. Third, I determine whether GPP responds differently to diffuse light depending on the time of day. This identifies whether the relationship between diffuse light and GPP is constant during daylight hours, or if it depends on how the angle of incoming light interacts with the distribution of leaf area, gaps, and species within plant canopies (i.e., canopy structure). This chapter extends our understanding of how light influences GPP by using ecosystem-level measurements to test how biophysical features of plant canopies alter the effects of incoming light from the atmosphere.

- *How does the variation in species and light within plant canopies alter leaf-level photosynthesis?* In Chapters 2 and 3, I examine the physical factors of the atmosphere (i.e., clouds) and biophysical factors of canopies (i.e., canopy structure) that influence the distribution of solar radiation to leaves within canopies. At the leaf-level, the total amount of light drives the rate of photosynthesis. However, the light environment of individual leaves influences how leaf photosynthesis scales to the canopy (Section 1.2) through changes in leaf light availability and leaf temperature. In Earth system models, this process is based on three rate-limiting biochemical reactions in photosynthesis (Von Caemmerer 2000, Dietze 2014). Due to limited computational power and field-available data, models simplify how these rates respond to environmental and ecological change. These simplifications include using one of the rate limiting reactions, the maximum rate of CO_2 carboxylation ($V_{c,max}$), to calculate the other two reaction rates (the maximum rate of electron transport; J_{max} and triose phosphate utilization; *TPU*) as well as assuming that all species within the same model-designated plant functional type (PFT) have the same $V_{c,max}$. However, recent analyses using

plant traits or environmental conditions to estimate $V_{c,max}$ show that $V_{c,max}$ varies widely within a biome or PFT (Kattge et al. 2009, Verheijen et al. 2013, Ali et al. 2015). This implies that ecological variation within plant canopies may alter the photosynthetic potential of the whole canopy.

In Chapter 4 (Cheng et al. in review-b), I extend our understanding of how variation in species, leaf temperature, and leaf light environment within canopies alters the photosynthetic limitations of terrestrial ecosystems. I accomplish this by making net photosynthesis measurements at different CO_2 concentrations on leaves of mature, canopy-dominant trees and using plant physiological methods to derive values for the rate-limiting processes involved in both gross and net photosynthesis. Using these field-based data, I examine which rate-limiting reactions in photosynthesis vary with species and leaf light environment and whether they differ in their response to leaf temperature. In completing this analysis, I concurrently test Earth system model representations of photosynthetic limitations and how they scale them from leaf to canopy. This chapter adds to our understanding of the relationship between light and gross ecosystem CO_2 uptake by examining how ecological variation within canopies alters leaf-level light use and photosynthesis within a plant canopy.

Overall, this dissertation provides mechanistic explanations for how physical, biophysical, and biological characteristics of the atmosphere and plant canopies modify gross ecosystem CO_2 uptake by terrestrial ecosystems. It achieves this by 1) identifying a mechanism that links the physical transformation of light by clouds to above-canopy light availability, 2) empirically quantifying how plant canopies biophysically mediate the response of GPP to diffuse light, and 3) examining how within-canopy variation in species and light ecologically modify the rate-limiting reactions in leaf photosynthesis. Linking the effect of light on photosynthesis in this way from the atmosphere to leaf biochemistry provides a foundation for the scientific community to predict how future changes in light and plant canopy structure will alter gross ecosystem CO_2 uptake. Mechanistically linking processes in the atmosphere to those within the plant canopy also improves our understanding of how land-atmosphere interactions influence the land carbon sink. Finally, it also identifies which processes may improve Earth system model

projections of how the terrestrial carbon cycle and land-atmosphere interactions will respond to, and influence, feedbacks to climate.

References

Ali, A. A., C. Xu, A. Rogers, N. G. Mcdowell, B. E. Medlyn, R. A. Fisher, S. D. Wullschleger, P. B. Reich, J. A. Vrugt, W. L. Bauerle, L. S. Santiago, and C. J. Wilson. 2015. Global scale environmental control of plant photosynthetic capacity. Ecological Applications **25**:2349-2365.

Alton, P. B. 2008. Reduced carbon sequestration in terrestrial ecosystems under overcast skies compared to clear skies. Agricultural and Forest Meteorology **148**:1641-1653.

Anderson, M. C. 1966. Stand Structure and Light Penetration. II. A Theoretical Analysis. Journal of Applied Ecology **3**:41-54.

Bahn, M., M. Reichstein, J. S. Dukes, M. D. Smith, and N. G. Mcdowell. 2014. Climate–biosphere interactions in a more extreme world. New Phytologist **202**:356-359.

Baldocchi, D. D. 2003. Assessing the eddy covariance technique for evaluating carbon dioxide exchange rates of ecosystems: past, present and future. Global Change Biology **9**:479-492.

Baldocchi, D. D., B. B. Hincks, and T. P. Meyers. 1988. Measuring Biosphere-Atmosphere Exchanges of Biologically Related Gases with Micrometeorological Methods. Ecology **69**:1331-1340.

Bazzaz, F. A. 1979. The Physiological Ecology of Plant Succession. Annual Review of Ecology and Systematics **10**:351-371.

Bernacchi, C., A. Diaz-Espejo, and J. Flexas. 2012. Gas-exchange analysis: basics and problems.*in* J. Flexas, F. Loreto, and H. Medrano, editors. Terrestrial Photosynthesis in a Changing Environment: A Molecular, Physiological and Ecological Approach. Cambridge University Press.

Bohning, R. H., and C. A. Burnside. 1956. The Effect of Light Intensity on Rate of Apparent Photosynthesis in Leaves of Sun and Shade Plants. American Journal of Botany **43**:557-561.

Bonan, G. B. 2008. Forests and Climate Change: Forcings, Feedbacks, and the Climate Benefits of Forests. Science **320**:1444-1449.

Bonan, G. B. 2015. Ecological climatology: concepts and applications. Cambridge University Press.

Cess, R. D., M. H. Zhang, P. Minnis, L. Corsetti, E. G. Dutton, B. W. Forgan, D. P. Garber, W. L. Gates, J. J. Hack, E. F. Harrison, X. Jing, J. T. Kiehi, C. N. Long, J.-J. Morcrette, G. L. Potter, V. Ramanathan, B. Subasilar, C. H. Whitlock, D. F. Young, and Y. Zhou. 1995. Absorption of Solar Radiation by Clouds: Observations Versus Models. Science **267**:496-499.

Cheng, S. J., G. Bohrer, A. L. Steiner, D. Y. Hollinger, A. Suyker, R. P. Phillips, and K. J. Nadelhoffer. 2015. Variations in the influence of diffuse light on gross primary productivity in temperate ecosystems. Agricultural and Forest Meteorology **201**:98-110.

Cheng, S. J., A. L. Steiner, D. Y. Hollinger, G. Bohrer, and K. J. Nadelhoffer. in review-a. Using satellite-derived optical thickness to assess the influence of clouds on terrestrial carbon uptake. Journal of Geophysical Research: Biogeosciences.

Cheng, S. J., R. Q. Thomas, J. V. Wilkening, P. S. Curtis, T. D. Sharkey, and K. J. Nadelhoffer. in review-b. Photosynthesis from leaf to canopy: species and leaf light availability drive within-canopy variation in forest photosynthetic capacity. Journal of Geophysical Research: Biogeosciences.

Dai, A., and T. M. L. Wigley. 2000. Global patterns of ENSO-induced precipitation. Geophysical Research Letters **27**:1283-1286.

Demmig-Adams, B., and W. W. Adams Iii. 1992. Photoprotection and Other Responses of Plants to High Light Stress. Annual Review of Plant Physiology and Plant Molecular Biology **43**:599-626.

Desai, A. R., A. D. Richardson, A. M. Moffat, J. Kattge, D. Y. Hollinger, A. Barr, E. Falge, A. Noormets, D. Papale, M. Reichstein, and V. J. Stauch. 2008. Cross-site evaluation of eddy covariance GPP and RE decomposition techniques. Agricultural and Forest Meteorology **148**:821-838.

Dietze, M. 2014. Gaps in knowledge and data driving uncertainty in models of photosynthesis. Photosynthesis Research **119**:3-14.

Fan, S.-M., M. L. Goulden, J. W. Munger, B. C. Daube, P. S. Bakwin, S. C. Wofsy, J. S. Amthor, D. R. Fitzjarrald, K. E. Moore, and T. R. Moore. 1995. Environmental controls on the photosynthesis and respiration of a boreal lichen woodland: a growing season of whole-ecosystem exchange measurements by eddy correlation. Oecologia **102**:443-452.

Friedlingstein, P., M. Meinshausen, V. K. Arora, C. D. Jones, A. Anav, S. K. Liddicoat, and R. Knutti. 2014. Uncertainties in CMIP5 Climate Projections due to Carbon Cycle Feedbacks. Journal of Climate **27**:511-526.

Fritz, S. 1954. Scattering of solar energy by clouds of "large drops". Journal of Meteorology **11**:291-300.

Gates, D. M. 1968. Transpiration and Leaf Temperature. Annual Review of Plant Physiology **19**:211-238.

Gough, C. M., B. S. Hardiman, L. E. Nave, G. Bohrer, K. D. Maurer, C. S. Vogel, K. J. Nadelhoffer, and P. S. Curtis. 2013. Sustained carbon uptake and storage following moderate disturbance in a Great Lakes forest. Ecological Applications **23**:1202-1215.

Gu, L., D. Baldocchi, S. B. Verma, T. A. Black, T. Vesala, E. M. Falge, and P. R. Dowty. 2002. Advantages of diffuse radiation for terrestrial ecosystem productivity. Journal of Geophysical Research: Atmospheres **107**:ACL 2-1-ACL 2-23.

Gu, L., J. D. Fuentes, H. H. Shugart, R. M. Staebler, and T. A. Black. 1999. Responses of net ecosystem exchanges of carbon dioxide to changes in cloudiness: Results from two North American deciduous forests. Journal of Geophysical Research: Atmospheres **104**:31421-31434.

Halpert, M. S., and C. F. Ropelewski. 1992. Surface Temperature Patterns Associated with the Southern Oscillation. Journal of Climate **5**:577-593.

Hollinger, D. Y., F. M. Kelliher, J. N. Byers, J. E. Hunt, T. M. Mcseveny, and P. L. Weir. 1994. Carbon Dioxide Exchange between an Undisturbed Old-Growth Temperate Forest and the Atmosphere. Ecology **75**:134-150.

Hurrell, J. W. 1996. Influence of variations in extratropical wintertime teleconnections on northern hemisphere temperature. Geophysical Research Letters **23**:665-668.

Ipcc. 2013. Summary for Policymakers. In: Climate Change 2013: The Physical Science Basis. Contribution of Working Group I to the Fifth Assessment Report of the Intergovernmental Panel on Climate Change. Cambridge, United Kingdom and New York, NY, USA.

Kattge, J., W. Knorr, T. Raddatz, and C. Wirth. 2009. Quantifying photosynthetic capacity and its relationship to leaf nitrogen content for global-scale terrestrial biosphere models. Global Change Biology **15**:976-991.

Knohl, A., and D. D. Baldocchi. 2008. Effects of diffuse radiation on canopy gas exchange processes in a forest ecosystem. Journal of Geophysical Research: Biogeosciences **113**:G02023.

Kreft, H., and W. Jetz. 2007. Global patterns and determinants of vascular plant diversity. Proceedings of the National Academy of Sciences **104**:5925-5930.

Mcmillen, G. G., and J. H. Mcclendon. 1979. Leaf Angle: An Adaptive Feature of Sun and Shade Leaves. Botanical Gazette **140**:437-442.

Mercado, L. M., N. Bellouin, S. Sitch, O. Boucher, C. Huntingford, M. Wild, and P. M. Cox. 2009. Impact of changes in diffuse radiation on the global land carbon sink. Nature **458**:1014-1017.

Monsi, M., and T. Saeki. 2005. On the Factor Light in Plant Communities and its Importance for Matter Production. Ann Bot **95**:549-567.

Niyogi, D., H.-I. Chang, V. K. Saxena, T. Holt, K. Alapaty, F. Booker, F. Chen, K. J. Davis, B. Holben, T. Matsui, T. Meyers, W. C. Oechel, R. A. Pielke, R. Wells, K. Wilson, and Y. Xue. 2004. Direct observations of the effects of aerosol loading on net ecosystem CO_2 exchanges over different landscapes. Geophysical Research Letters **31**:L20506.

Oker-Blom, P. 1985. Photosynthesis of a scots pine shoot: simulation of the irradiance distribution and photosynthesis of a shoot in different radiation fields. Agricultural and Forest Meteorology **34**:31-40.

Oliphant, A. J., D. Dragoni, B. Deng, C. S. B. Grimmond, H. P. Schmid, and S. L. Scott. 2011. The role of sky conditions on gross primary production in a mixed deciduous forest. Agricultural and Forest Meteorology **151**:781-791.

Peñuelas, J., J. Sardans, M. Estiarte, R. Ogaya, J. Carnicer, M. Coll, A. Barbeta, A. Rivas-Ubach, J. Llusià, M. Garbulsky, I. Filella, and A. S. Jump. 2013. Evidence of current impact of climate change on life: a walk from genes to the biosphere. Global Change Biology **19**:2303-2338.

Richardson, A. D., T. F. Keenan, M. Migliavacca, Y. Ryu, O. Sonnentag, and M. Toomey. 2013. Climate change, phenology, and phenological control of vegetation feedbacks to the climate system. Agricultural and Forest Meteorology **169**:156-173.

Rocha, A. V., H.-B. Su, C. S. Vogel, H. P. Schmid, and P. S. Curtis. 2004. Photosynthetic and Water Use Efficiency Responses to Diffuse Radiation by an Aspen-Dominated Northern Hardwood Forest. Forest Science **50**:793-801.

Roderick, M. L., G. D. Farquhar, S. L. Berry, and I. R. Noble. 2001. On the direct effect of clouds and atmospheric particles on the productivity and structure of vegetation. Oecologia **129**:21-30.

Ropelewski, C. F., and M. S. Halpert. 1987. Global and Regional Scale Precipitation Patterns Associated with the El Niño/Southern Oscillation. Monthly Weather Review **115**:1606-1626.

Sheehy, J. E., and L. C. Chapas. 1976. The Measurement and Distribution of Irradiance in Clear and Overcast Conditions in Four Temperate Forage Grass Canopies. Journal of Applied Ecology **13**:831-840.

Twomey, S. 1991. Symposium on Global Climatic Effects of Aerosols Aerosols, clouds and radiation. Atmospheric Environment. Part A. General Topics **25**:2435-2442.

Urban, O., D. Janouš, M. Acosta, R. Czerný, I. Marková, M. Navrátil, M. Pavelka, R. Pokorný, M. Šprtová, R. U. I. Zhang, V. Špunda, J. Grace, and M. V. Marek. 2007. Ecophysiological controls over the net ecosystem exchange of mountain spruce stand.

Comparison of the response in direct vs. diffuse solar radiation. Global Change Biology **13**:157-168.
Urban, O., K. Klem, A. Ač, K. Havránková, P. Holišová, M. Navrátil, M. Zitová, K. Kozlová, R. Pokorný, M. Šprtová, I. Tomášková, V. Špunda, and J. Grace. 2012. Impact of clear and cloudy sky conditions on the vertical distribution of photosynthetic CO_2 uptake within a spruce canopy. Functional Ecology **26**:46-55.
Verheijen, L. M., V. Brovkin, R. Aerts, G. Bönisch, J. H. C. Cornelissen, J. Kattge, P. B. Reich, I. J. Wright, and P. M. Van Bodegom. 2013. Impacts of trait variation through observed trait–climate relationships on performance of an Earth system model: a conceptual analysis. Biogeosciences **10**:5497-5515.
Von Caemmerer, S. 2000. Biochemical models of leaf photosynthesis. Csiro publishing.
Wang, K., R. E. Dickinson, and S. Liang. 2008. Observational evidence on the effects of clouds and aerosols on net ecosystem exchange and evapotranspiration. Geophysical Research Letters **35**:L10401.
Westoby, M., and I. J. Wright. 2006. Land-plant ecology on the basis of functional traits. Trends in Ecology & Evolution **21**:261-268.
Wohlfahrt, G., and L. H. Gu. 2015. The many meanings of gross photosynthesis and their implication for photosynthesis research from leaf to globe. Plant Cell and Environment **38**:2500-2507.

Chapter 2

Using Satellite-Derived Optical Thickness to Assess the Influence of Clouds on Terrestrial Carbon Uptake [1]

Abstract

Clouds scatter direct solar radiation, generating diffuse radiation and altering the ratio of direct to diffuse light. If diffuse light increases plant canopy CO_2 uptake, clouds may indirectly regulate climate by altering the terrestrial carbon cycle. However, past research primarily uses proxies or qualitative categories of clouds to connect the effect of diffuse light on CO_2 uptake to sky conditions. We mechanistically link and quantify effects of cloud optical thickness (τ_c) to surface light and plant canopy CO_2 uptake by comparing satellite retrievals of τ_c to ground-based measurements of diffuse and total photosynthetically active radiation (PAR; 400-700 nm) and gross primary production (GPP) in forests and croplands. Overall, total PAR decreased with τ_c, while diffuse PAR increased until an average τ_c of 6.8 and decreased with larger τ_c. When diffuse PAR increased with τ_c, 7-24% of variation in diffuse PAR was explained by τ_c. Light use efficiency (LUE) in this range increased 0.001-0.002 μmol m^{-2} s^{-1} GPP per μmol m^{-2} s^{-1} total PAR. Although τ_c explained 10-20% of the variation in LUE, there was no significant relationship between τ_c and GPP ($p > 0.05$) when diffuse PAR increased. We conclude that diffuse PAR increases under a narrow range of optically thin clouds and the dominant effect of clouds is to reduce total plant-available PAR. This decrease in total PAR offsets the increase in LUE under increasing diffuse PAR, providing evidence that changes within this range of low cloud optical thickness are unlikely to alter the magnitude of terrestrial CO_2 fluxes.

[1] To be published by S.J. Cheng, A.L. Steiner, D.Y. Hollinger, G. Bohrer, K.J. Nadelhoffer. In review at the *Journal of Geophysical Research: Biogeochemistry*.

2.1 Introduction

Clouds alter the Earth's energy balance in multiple ways, including through the greenhouse effect and changes in planetary albedo (Arking 1991, Stephens 2005). Calculating the net effect of clouds on climate in Earth system models remains an important challenge (Boucher et al. 2013, Bony et al. 2015). Much of the research addressing this has focused on understanding the radiative effects of clouds (Andrews et al. 2012, Lauer and Hamilton 2013). However, clouds can also influence Earth's climate through the carbon cycle by changing the amount and type of light available for plants to use in photosynthesis (Jenkins et al. 2007). Similar to modeling clouds, difficulties in modeling the carbon cycle lead to projections of CO_2 fluxes into terrestrial ecosystems that carry large uncertainty. The most recent Earth system model intercomparison project estimates that terrestrial ecosystems can be either a source of or sink for carbon by 2100, with fluxes ranging from -6 to 9 Pg C yr^{-1} (Friedlingstein et al. 2014). One way to identify a potential source of uncertainty in land surface models while also improving understanding of how clouds impact climate, is to mechanistically link and quantify the effects of clouds on terrestrial CO_2 fluxes.

Clouds can influence the terrestrial carbon cycle by changing light availability in two ways. First, clouds can reduce the amount of light that reaches plant canopies by absorbing and reflecting solar radiation (Twomey 1991, Cess et al. 1995). Second, cloud droplets and ice crystals interact with incoming solar radiation to produce scattered, diffuse light (Hansen 1971, Davis and Marshak 2010). Regional climate model simulations demonstrate that model skill for estimating variability in summer temperatures improves only up to 3% when radiation is explicitly partitioned into direct and diffuse components (Davin and Seneviratne 2012). In addition, when more of the photosynthetically active radiation (PAR; 400-700 nm) above a light-saturated plant canopy is diffuse rather than direct, a greater percentage of PAR reaches more leaves within the canopy and increases canopy light-use efficiency (LUE) (Hollinger et al. 1994, Gu et al. 2002, Niyogi et al. 2004, Knohl and Baldocchi 2008, Still et al. 2009). Studies using modeled and measured diffuse PAR to predict ecosystem productivity infer that forest CO_2 uptake is greater under cloudy skies than under clear skies (Law et al. 2002, Rocha et al. 2004). However, a series of modeling studies collectively show that increases in LUE under diffuse light conditions may be too small to compensate for decreases in shortwave radiation on longer timescales (Alton et al. 2005, Alton 2008, Knohl and Baldocchi 2008). In contrast, additional

studies show that carbon uptake can be higher under diffuse light conditions, despite reductions in total PAR (Hollinger et al. 1994, Gu et al. 1999, Mercado et al. 2009).

Although studies have examined the effect of diffuse light on terrestrial carbon processing, few have directly linked this relationship to clouds. Most studies have examined the assumption that clouds alter plant canopy uptake using proxies for cloud cover, rather than measurements of cloud properties (Gu et al. 1999, Alton et al. 2005, Alton et al. 2007, Jenkins et al. 2007). For example, cloud conditions have been inferred from the ratio of surface radiation to extraterrestrial radiation at the top of the atmosphere calculated from the solar constant and Earth-Sun geometry (Liu and Jordan 1960). Similarly, Gu et al. (1999) quantified cloudiness using the ratio of total radiation at the surface under a given sky condition to a modeled clear sky radiation. However, these proxies are biased by the assumptions used to model and partition radiation (Kanniah et al. 2012). The use of direct observations of cloud cover would provide key empirical evidence of the impact of clouds on plant carbon uptake.

Of the studies using direct cloud observations, most use categorical descriptions of cloud cover (e.g., "cloud-free", "mixed", "cloudy") (Niyogi et al. 2004, Oliphant et al. 2011). This limits our ability to predict the effects of small changes in cloud optical thickness that have been observed over the last few decades (Marchand 2013, Free and Sun 2014). One study using ground-based measurements of diffuse light and cloud measurements found that surface diffuse light changes non-linearly over a narrow range of cloud optical thickness (0 to 5), with a peak in diffuse light at a cloud optical thickness of 2 (Min 2005). However, this analysis was done at a single site, making it difficult to determine whether the effect of cloud optical thickness on carbon uptake can be applied to broader spatial scales. One study used a satellite-retrieved measure of clouds (i.e., cloud fraction) from the International Satellite Cloud Climatology project (ISCCP) to show that satellite data over the Amazon can predict site-specific surface light conditions (Butt et al. 2010). However, this work did not connect cloud fraction to primary production or beyond the region.

In this study, we use satellite-derived cloud optical thickness from Moderate Resolution Imaging Spectroradiometer (MODIS) as a metric to mechanistically link and quantify the influence of clouds on surface diffuse light and canopy CO_2 uptake across multiple ecosystems. We use MODIS data because they are still collected, whereas ISCCP data are available only through 2009. We choose cloud optical thickness because it describes the cumulative depletion

of light through a cloud (Platnick et al. 2003). It also combines the influence of cloud presence, physical thickness, and phase (i.e., liquid, solid) on the amount of surface radiation that is reflected, transmitted, and absorbed by the atmosphere (Leontyeva and Stamnes 1994, Platnick et al. 2003, Kikuchi et al. 2006). Cloud optical thickness (τ_c) is a dimensionless factor defined as:

$$\tau_c = \int_0^d \beta(z)dz \quad (1)$$

where d is the height of the atmosphere and β is the cloud extinction coefficient, which is the sum of the scattering coefficient and absorption coefficient (Mayer et al. 1998). MODIS provides cloud τ_c at 1-km^2 resolution across the globe (Platnick et al. 2003).

To identify whether there is an empirical link among clouds, diffuse PAR, and ecosystem carbon uptake, we combine MODIS τ_c values with ground observations of surface total, direct, and diffuse PAR and gross primary production (GPP) collected from a set of sites in the AmeriFlux network. We also use these data to identify if there is a signal of τ_c in GPP. Results from our study provide insights into how biosphere-atmosphere interactions influence the Earth's climate in two important ways. First, we evaluate the use of satellite-derived τ_c to determine the relationship between diffuse light and canopy CO_2 uptake identified in previous studies. This allows us to quantify the effects of clouds on carbon uptake and to identify how changes in clouds may alter fluxes of CO_2 into terrestrial ecosystems. Second, we quantify this effect at multiple sites of contrasting temperate zone ecosystem types (i.e., broadleaf forest, mixed forest, cropland). By linking and quantifying the relationships among τ_c, surface PAR, and GPP, we provide insight into how changes in clouds may impact climate through the carbon cycle by altering radiation regimes in terrestrial ecosystems.

2.2 Methods

2.2.1 Site Selection and AmeriFlux Data

To examine the relationships between τ_c, surface PAR, and GPP, we used ground-based observations provided through the AmeriFlux program (http://ameriflux.lbl.gov/). AmeriFlux is a network of flux and meteorological towers in the United States (U.S.) that measures fluxes of water vapor and CO_2 between the land surface and the atmosphere using the eddy-covariance technique (Baldocchi 2003), along with site-level soil, vegetation, radiation, and meteorological conditions. The online AmeriFlux data we used are available online are standardized, reviewed, and quality controlled.

For the first part of our analysis, we analyzed the relationships between τ_c and both surface total and diffuse PAR. We chose AmeriFlux sites designated as unmanaged, temperate ecosystems, for which at least three years of CO_2 flux, total PAR, diffuse PAR, and MODIS data were available (2000-present) (Platnick et al. 2003). Eight sites (Table 2.1) met these criteria. For these sites, we used May through September diffuse PAR data from Level 2, with-gap files (processed and quality controlled) that have data available at 30-minute or 1-hour resolution to capture the primary Northern Hemisphere growing season. For Howland Forest, we included April data when this month was calculated as part of the site's peak growing season (see below for details).

Diffuse PAR was measured at Sherman Island with a custom-designed rotating shadow band radiometer. As the shadow band rotates around the photodiode in the radiometer, measurements of global (i.e., direct and diffuse) and diffuse light are recorded when the sensor is fully shaded and covered (Michalsky et al. 1988). At the remaining sites, diffuse PAR was measured with a model BF2, BF3, or BF5 sensor (Delta-T Devices, Ltd., Cambridge, UK).

For the second part of the analysis, we analyzed the relationship between τ_c and GPP, which is directly linked with light and, unlike net ecosystem exchange (NEE), does not include respiration. Of the eight sites with diffuse PAR measurements, only four had Level 2 NEE and with-gap GPP data. These sites represent mixed forest (Howland Forest), deciduous broadleaf forest (Morgan Monroe and UMBS), and cropland (Mead Irrigated Maize). At these sites, ecosystem respiration is modeled and then subtracted from observed NEE to calculate GPP.

Table 2.1: AmeriFlux site information and ecosystem characteristics

Site (SiteID)	Lat, Lon (°N, °W)	Years of Diffuse PAR Data	Canopy Height (m)	Vegetation Community	Management	LAI (m^2 m^{-2})	Average Cumulative May-Sept Precipitation (mm)	GPP	Average Peak Growing Season Start Date (DOY)	Growing Season Length in Days (Min, Max)
Howland Forest (US-Ho1)	45.204, 68.740	2006-2008	20[a]	Red spruce (*Picea rubens*) and Eastern hemlock (*Tsuga canadensis*) with balsam fir (*Abies balsamea)*, white pine (*Pinus strobus)*, white cedar (*Thuja occidentalis*), red maple (*Acer rubrum*), and paper birch (*Betula papyrifera*)[b].	None	~ 6[a]	358 (includes April)	Yes	141	106, 141
Mead (US-Ne1)	41.165, 96.476	2001-2012	2.9[c]	Maize (*Zea mays)*[d]	Center-pivot irrigation[d]	5.7[c]	630	Yes	184	31, 56
Morgan Monroe (US-MMS)	39.323, 86.413	2006-2013	27[e]	Sugar maple (*A. saccharum*), tulip poplar (*Liriodendron tulipifera*), sassafras (*Sassafras albidum*), white oak (*Quercus alba*), and black oak (*Q. nigra*)[e].	None	5[f]	495	Yes	142	41, 121
UMBS (US-UMB)	45.559, 84.713	2007-2012	22[g]	Bigtooth aspen (*Populus grandidentata*), red oak (*Q. rubra*), red maple (*A. rubrum*), and white pine (*P. strobus*) with trembling aspen (*P. tremuloides*), white birch (*B. papyrifera*), sugar maple (*A. saccharum*), red pine (*P. resinosa*), and American beech (*Fagus grandifolia*)[g].	None	~3.5[g]	355	Yes	164	51, 106
Bartlett (US-Bar)	44.064, 71.288	2004-2011	22[h]	American beech (*F. grandifolia*), sugar maple (*A. saccharum*), yellow birch (*Betula alleghaniensis*) with red maple (*A. rubrum*), paper birch (*B. papyrifera*), eastern hemlock (*T. canidensis*), eastern white pine (*P. strobus*), and red spruce (*Picea rubens*)[h.]	None	3.6[h]	589	No	--	--
Flagstaff (US-Fuf)	35.089, 111.762	2006-2010	18[i]	*Pinus ponderosa* (Ponderosa pine)[i]	None	2.3[i]	301	No	--	--

Sherman Island (US-Snd)	38.037, 121.753	2010-2013	--	Grasses, including pepperweed (*Lepidium latifolium*) and mouse barley (*Hordeum murinum L.)*[j]	None	0.68-0.81[j]	13	No	--	--
Vaira Ranch (US-Var)	38.406, 120.950	2006-2013	0.55[k] (Xu 2004)	Grasses, including purple false brome (*Brachypodium distachyon L.)*, smooth cat's ear (*Hypochaeris glabra L.*), lesser trefoil (*Trifolium dubium Sibth.*) rose clover (*Trifolium hirtum All.*), twinning snakelily (*Dichelostemma volubile A.*), and Big Heron bill (*Erodium botrys Cav*)[k]	Grazed[k]	<2[l]	35	No	--	--

[a]Scott et al. (2004), [b]Hollinger et al. (2004), [c]personal communication with site investigator, [d]Suyker and Verma (2008),[e]Dragoni et al. (2011), [f]Oliphant et al. (2011), [g]Gough et al. (2013), [h]Jenkins et al. (2007), [i]Dore et al. (2012), [j]Ma et al. (2012), [k]Xu and Baldocchi (2004), [l]Miller et al. (2007)

2.2.2 MODIS Cloud Optical Thickness (τ_c)

MODIS τ_c measurements are globally available at 1-km^2 resolution (Platnick et al. 2003). The MODIS instrument is a 36-band spectroradiometer measuring radiation between 0.415-14.235 μm from 705 km above Earth's surface aboard two satellites, Terra and Aqua (Platnick 2003). Terra moves in a descending orbit and crosses the equator at approximately 10:30 local time and Aqua moves in an ascending orbit with an overpass at the equator of approximately 13:30 local time (Qu 2006). MODIS has a 2,330 km swath width, which leads to global coverage approximately every 2 days (King 2003). Level 2 MODIS data are stored in 5-minute data granules typically containing 2,030 along-track pixels (Baum and Platnick 2006).

Daytime τ_c values over land are retrieved using look-up tables to find the combinations of τ_c and cloud droplet effective radius values that best match solar reflectance measurements from one visible band (0.645 μm) and two near-infrared (1.6, 2.13, and 3.75 μm) bands (Platnick 1997, Platnick 2003). Calculations are made assuming plane-parallel, homogenous clouds over a black surface with no atmosphere and use separate libraries for ice and liquid water clouds (Baum and Platnick 2006). Additional algorithms correct for the effects of surface albedo and atmospheric transmittance on reflectance measurements, such as Rayleigh scattering and trace gas and water vapor absorption (Platnick 2003, Platnick 1997).

An uncertainty value is also calculated for each τ_c that accounts for several types of errors. These include errors in the models and libraries used in the retrieval, changes to instrument calibration, and changes in the composition of the atmosphere above the cloud, such as aerosols and water vapor (Platnick 1997). Uncertainties in the retrieval process, such as for cloud cover, phase, particle size and shape, and homogeneity, bias estimates of τ_c, particularly for thin and thick clouds (Zeng et al. 2012). To minimize the effect of bias from retrieval uncertainties in our study, we limit our analysis to values of τ_c with uncertainty < 25%.

We used daytime, Level 2 Terra and Aqua cloud products (MOD06_L2, MYD06_L2) from Collection 5.1 from NASA's Level 1 and Atmosphere Archive and Distribution System (https://ladsweb.nascom.nasa.gov/index.html). The algorithms in this collection retrieve τ_c for pixels with a cloud mask designation of cloudy or probably cloudy (King et al. 2013). However, they do not process pixels that are identified as partly-cloudy (King et al. 2013), which are included in the most recent collection (Pincus et al. 2012). Our results therefore reflect the effect of overcast skies within a 3x3 km^2 area on surface light and GPP. Latitude and longitude

coordinates from MODIS Level 1 Geolocation product (MOD03) were used to find the closest pixel within 0.01° of each AmeriFlux site. We compared the influence of τ_c on diffuse PAR using τ_c at two spatial resolutions: (1) τ_c from the 1x1 km^2 pixel that includes the AmeriFlux site and (2) the mean τ_c from nine pixels covering a 3x3 km^2 area with the AmeriFlux site in the center pixel of the pixel array. We did not apply filters to the pixels surrounding the center pixel. Calculations of mean τ_c therefore include pixels surrounding the center pixel with missing data and any uncertainty level. At 1x1 km^2 resolution, all sites showed a similar non-linear response of diffuse PAR to τ_c, except for Flagstaff (Appendix A, Figure A1). However, when we used the average τ_c from a 3x3 km^2 area, the response at Flagstaff matched the other sites. The larger spatial resolution may better explain the response of diffuse PAR to τ_c because a broader spatial area captures the spatial heterogeneity that may affect the half-hour or hourly ground-based diffuse PAR measurements. For the remainder of this paper, τ_c refers to the average τ_c from a 3x3 km^2 area with the site at the center.

2.2.3 Peak Growing Season Calculations

For each site, we analyze GPP data for the most photosynthetically active time of year. To define this time period, we use changes in NEE to identify phenological changes in the plant canopy (Garrity et al. 2011). We calculate 5-day averages from daytime NEE (AmeriFlux Level 2 gap-filled data when available, otherwise Level 2 with-gap data) and define the first day of the peak growing season when the 5-day NEE average is within 90% of the year's fourth highest 5-day NEE average. We used the fourth-highest NEE average to account for extreme values due to anomalous weather. Next, we define the end of the peak-growing season as the last day when the 5-day NEE average is within 75% of the year's fourth-highest NEE average. We use different cutoffs for the beginning and end of the season because phenological changes in the canopy are quicker in the beginning of the season (e.g., leaf out) than they are at the end (e.g., senescence). Although this approach cannot detect the exact beginning and end of the peak-growing season, it provides a uniform method to define the period of time during which plants are at full seasonal growth and activity across our sites. In addition, only using data from the peak-growing season allows us to quantify the maximum effect that clouds and diffuse light have on GPP.

2.2.4 Data Analysis

After obtaining τ_c values retrieved from MODIS, we matched each τ_c timestamp to the closest AmeriFlux tower time. The τ_c retrievals at our sites occurred during midday (10:00-15:00) and fell within a small range of zenith angles (16-30°). We excluded data points with missing vapor pressure deficit (VPD), air temperature, diffuse PAR, and total PAR and only used total PAR values > 20 μmol m^{-2} s^{-1}, assuming that lower radiation levels indicate sensor errors or marginal weather conditions (e.g., rain events). Under clear skies, aerosols, ozone, and humidity also affect the partitioning of direct solar radiation into diffuse light (Bird and Riordan 1986). We do not specifically include the effect of aerosols on surface PAR or GPP in our analysis because: (1) aerosols have a relatively low optical depth compared to clouds (usually $\tau < 1.0$), (2) satellite-derived aerosol optical depth is not retrieved when clouds are present, which is the focus of this study, and (3) remote sites such as ours generally have low aerosol optical depths relative to areas closer to anthropogenic activity (Steiner et al., 2013).

Because clouds both transmit and absorb diffuse light, we expected diffuse light to increase and then decrease with τ_c. To identify the point of τ_c where the relationship between these two variables first changed from positive to negative (i.e., τ_c for maximum diffuse PAR), we used a smoothing spline function (R Core Team 2014). This identifies the range of τ_c when clouds increase diffuse light and are most likely to increase GPP. The region where diffuse PAR increases with τ_c met the statistical assumptions of linear regression analysis, which we used to quantify the relationship between cloud τ_c and surface light. We also analyzed the relationship between τ_c and diffuse PAR by month and found no large variation across the season. We used a spline function to assess the response of total PAR across the entire range of τ_c. For two of the sites (Flagstaff and Howland), the residuals from the linear models between total PAR and τ_c while diffuse PAR increased did not pass the Shapiro-Wilk test or visual inspection for normality. However, we kept these data untransformed to display the information in a consistent format as the other sites and for the diffuse PAR data.

We also used linear regression analysis to examine the relationship between τ_c and GPP across the entire range of available τ_c data, which met statistical assumptions of this analysis method. The residuals from linear models between LUE and τ_c below the peak τ_c were not normal at all sites, but applying a log transformation to LUE produced normal residuals. However, because the difference in R^2 did not increase more than 0.04, we report untransformed

LUE data in the following analysis. Regressions between τ_c and transformed LUE are shown in Appendix A, Figure A2. For LUE data above the τ_c for maximum diffuse PAR, all but one site met the assumptions for linear regression. We kept the data untransformed to keep all data in a consistent format.

2.3 Results and Discussion

2.3.1 τ_c and Diffuse PAR

Our analysis of τ_c from overcast pixels and surface light above plant canopies at eight AmeriFlux sites shows a non-linear relationship between τ_c and diffuse PAR (Figure 2.1). Across all sites, diffuse PAR increases with τ_c until an average value of 6.8, above which diffuse PAR decreases. There is some site-level variation in this value of τ_c, ranging from 5.2 at Flagstaff to 9.7 at Sherman Island (Figure 2.1). To our knowledge, only one study has used measurements of τ_c to examine cloud effects on surface diffuse PAR (Min 2005). That study used measurements from a multi-filter rotating shadowband radiometer at one location (Harvard Forest) during one growing season to demonstrate that diffuse PAR increases up to $\tau_c = 2$ and decreases thereafter. Using new data, including satellite retrievals of τ_c and direct measurements of diffuse PAR from tower-mounted sensors, we expand this analysis across both space and time. We find that the response of diffuse PAR to τ_c is consistent across sites, yet diffuse PAR peaks at greater τ_c values than previously reported by Min (2005). Our estimated values for the τ_c where diffuse PAR reaches its maximum may be larger because we used data from a solar zenith angle of 16-30°, whereas Min (2005) used data from across zenith angles.

Quantifying ranges across which diffuse PAR and τ_c increase together is important for understanding canopy GPP fluxes because total PAR decreases across the entire range of τ_c (Figure 2.2). Below the τ_c value at which diffuse PAR peaks, we found significant positive relationships between τ_c and diffuse PAR at all sites (Figure 2.3, $p < 0.05$) except Flagstaff. The variation in diffuse PAR that is explained by τ_c at these sites ranges from 7 to 24% (Figure 2.3). The increase in diffuse PAR across this range of optically thin clouds ranged from 30 μmol m^{-2} s^{-1} per unit τ_c at Sherman Island to 71 μmol m^{-2} s^{-1} per unit τ_c at Vaira Ranch. These results illustrate the variability in light extinction in the atmosphere that occurs across sites.

Limitations in the retrieval and measurement methods of cloud properties and surface light may explain some of the remaining variation in the relationship between τ_c and diffuse

PAR. For example, satellite retrieval methods and ground-based sensors cannot entirely capture the impact of vertical and horizontal cloud heterogeneity on surface light. Cloud particle size, phase, and shape alter scattering properties of clouds (e.g., single scattering albedo) (King 1987, Chou et al. 1998, Macke et al. 1998), which could cause clouds with the same τ_c to produce different amounts of diffuse light. The effect of cloud heterogeneity can also cause additional biases in satellite retrievals of τ_c by violating the MODIS algorithm assumption that clouds are homogenous (Dim et al. 2007, Zeng et al. 2012). This has been seen in cloud resolving simulations and radiation schemes that demonstrate that the parameterization of cloud overlap influences model estimates of surface radiation (Barker et al. 1999, Shonk et al. 2010). In addition, inaccurate algorithm selection of phase and cloud-scattering properties for inhomogeneous skies can bias retrievals of τ_c (Várnai and Marshak 2002, Koren et al. 2008, Pincus et al. 2012). Our use of the nine-pixel average of τ_c allows us to capture some of the horizontal inhomogeneity in clouds that would not be possible if we only used the τ_c from one pixel alone. The average minimum and maximum standard deviation of τ_c over a 3x3 km^2 area ranged from 0.11 to 4.36 (Table 2.2). This suggests the potential importance of spatial variability in cloud conditions (Table 2.2). Finally, some of the site-level variation may result from the difference in temporal resolutions in MODIS retrievals (near instantaneous; 5 minutes for a granule) and AmeriFlux data (30-min or 1-hour) or calibration and measurement errors in ground-based PAR sensors. Despite these limitations in τ_c retrieval assumptions and the differences in the spatial and temporal resolution between datasets, we detect a signal of cloud optical thickness in surface diffuse PAR measurements.

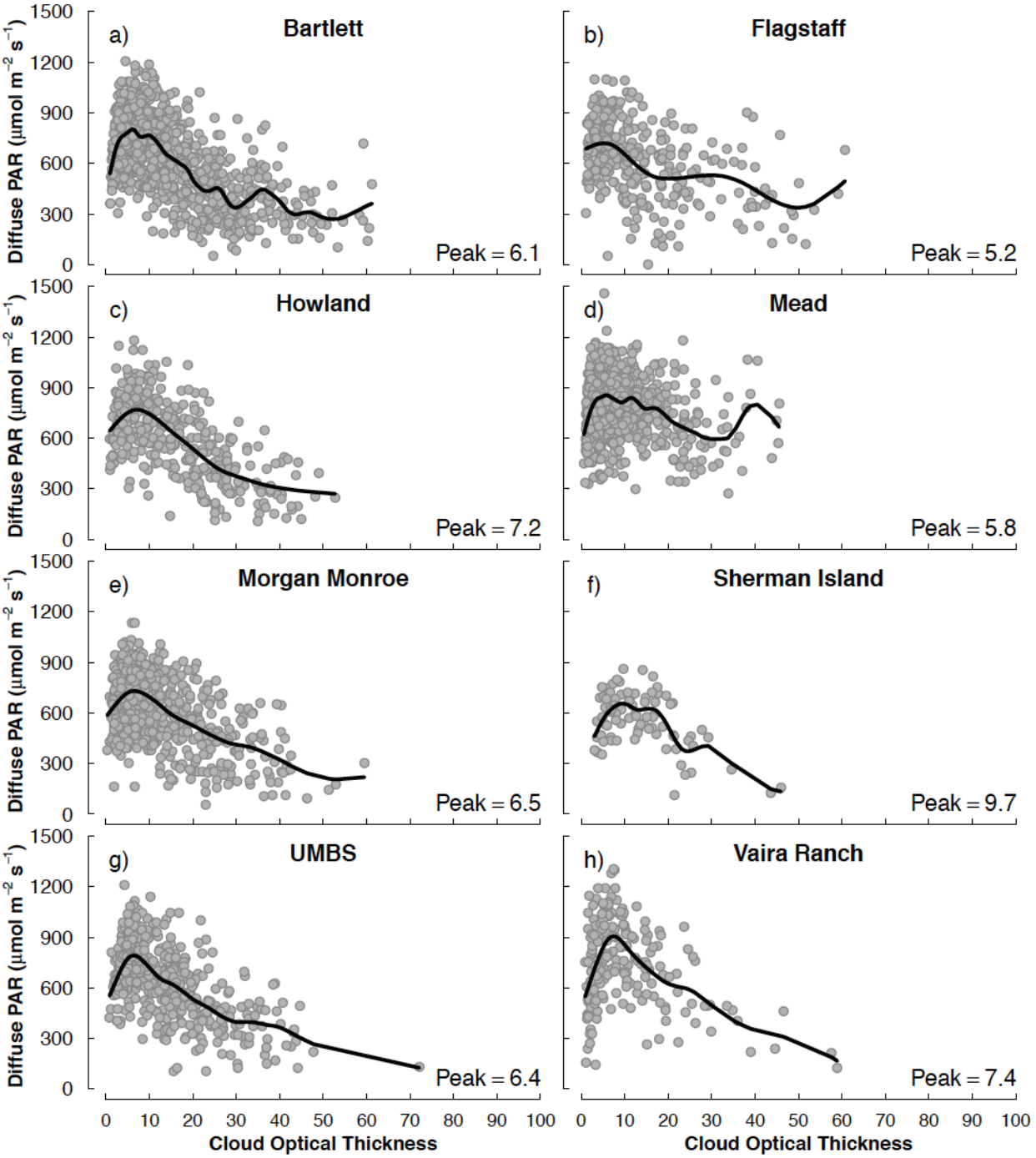

Figure 2.1: The response of AmeriFlux-tower measured diffuse photosynthetically active radiation (PAR; µmol m^{-2} s^{-1}) to 3x3 km^2 average cloud optical thickness (τ_c; unitless) with uncertainty < 25% retrieved from MODIS satellites. "Peak" refers to the highest value of τ_c associated with an increase in diffuse PAR. Data points include measurements from May through September from years with available data (see Table 2.1). For Howland Forest, April data are included when this month is calculated as part of the site's peak growing season. Plotted lines represent the general relationship between diffuse PAR and τ_c as estimated by a smoothing spline function.

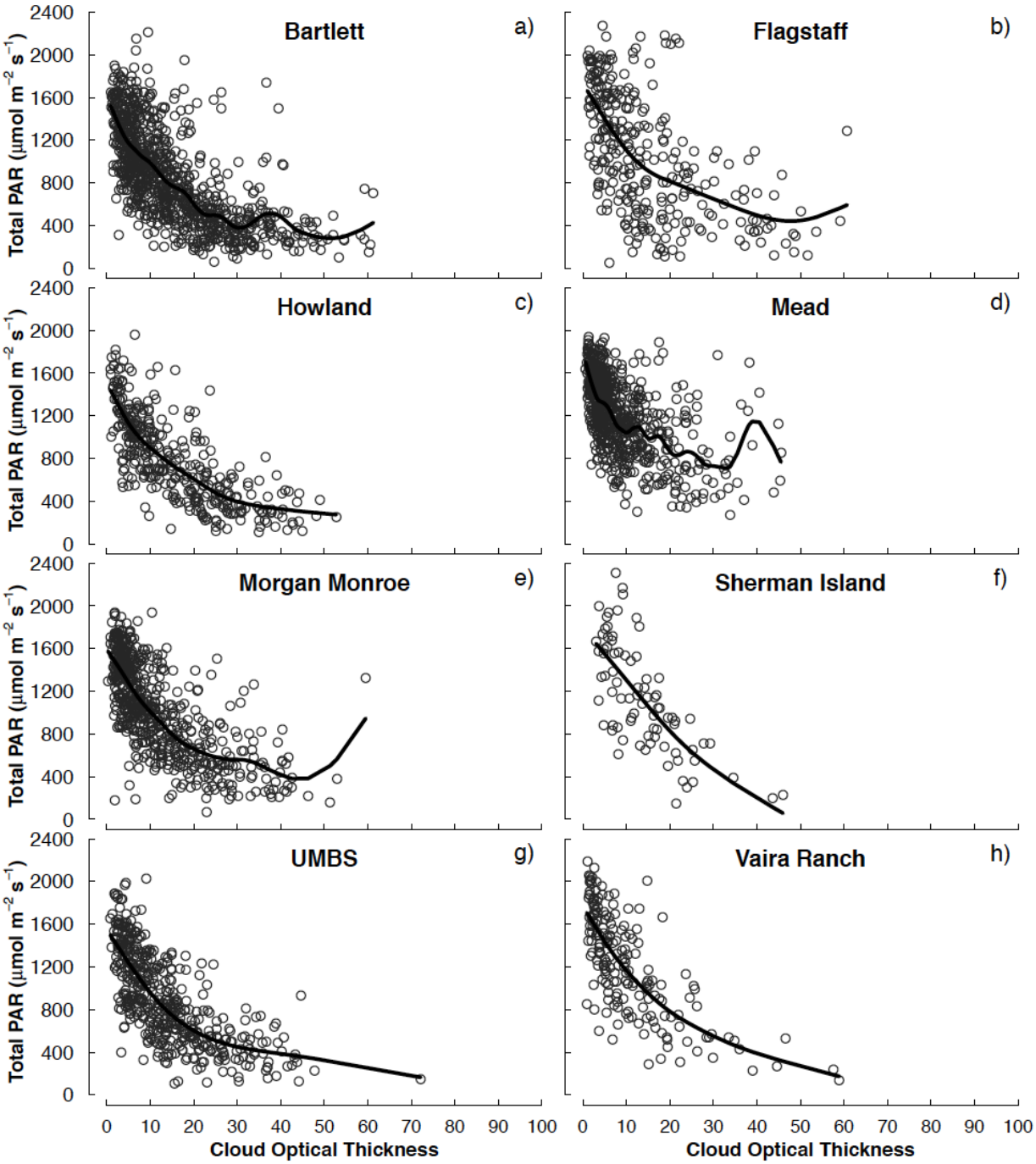

Figure 2.2: The response of AmeriFlux-tower measured total photosynthetically active radiation (PAR; µmol m^{-2} s^{-1}) to 3x3 km^2 average cloud optical thickness (τ_c; unitless) with uncertainty < 25% retrieved from MODIS satellites. Data points include measurements from May through September from years with available data (see Table 2.1). For Howland Forest, April data are included when this month is calculated as part of the site's peak growing season. Plotted lines represent the general relationship between total PAR and τ_c as estimated by a smoothing spline function.

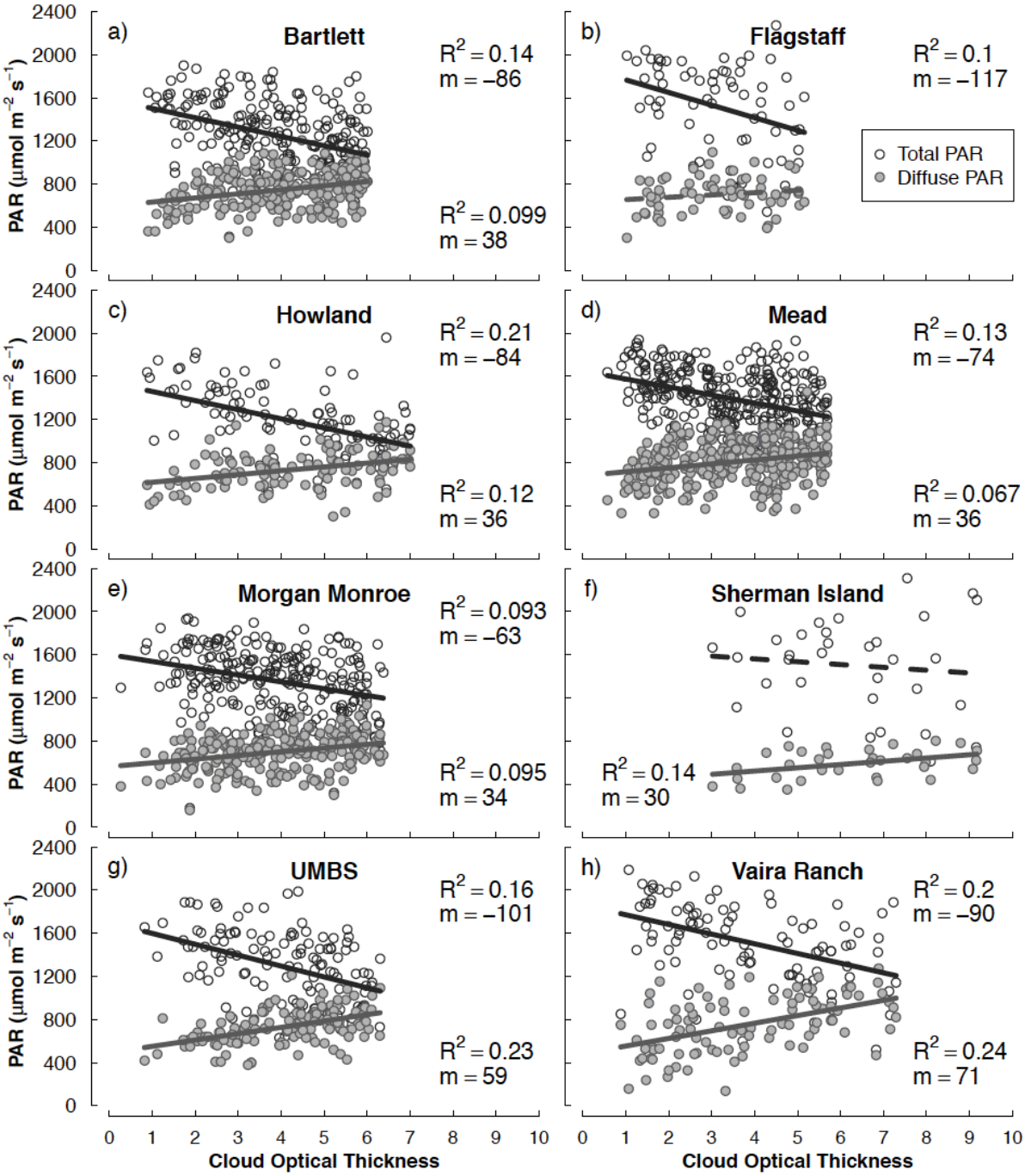

Figure 2.3: Relationship between diffuse and total photosynthetically active radiation (PAR; µmol m^{-2} s^{-1}) measured at AmeriFlux sites and 3x3 km^2 average cloud optical thickness (τ_c; unitless) retrieved from MODIS satellites. Data points include measurements from May through September from years with available data and for τ_c values lower than the peak of the diffuse PAR-τ_c curve (values listed in Figure 2.1). For Howland, April data are included when they are calculated as part of the site's peak growing season. R^2 and slopes (m) are listed for significant linear relationships with a $p < 0.05$.

Table 2.2: Standard deviation (SD) of τ_c for retrievals within a 3x3 km^2 area of each AmeriFlux site. Data include points with a 3x3 km^2 τ_c that is below the peak τ_c for diffuse PAR and during the sites' peak growing seasons.

Site	Mean SD of τ_c	Min SD	Max SD
Flagstaff	0.82	0.08	3.29
Sherman Island	1.73	0.48	3.79
UMBS	1.29	0.14	4.78
Bartlett	1.05	0.04	4.45
Mead	0.99	0.07	5.38
Howland	0.91	0.03	3.89
Vaira Ranch	0.92	0.00	4.21
Morgan Monroe	0.82	0.06	5.05

2.3.2 τ_c and Light Use Efficiency

For the four AmeriFlux sites with GPP measurements, we examined how τ_c changed the amount of GPP produced per unit of total PAR, which describes ecosystem-level LUE. To capture any negative or positive effects of clouds on ecosystem carbon processing, we analyzed how LUE changes when diffuse PAR increases separately from when diffuse PAR decreases with τ_c. The calculated values of τ_c for maximum diffuse PAR are shown in Figure 2.1 and explained in section 2.3.1.

When diffuse PAR increases with τ_c, LUE also increases with τ_c (Figure 2.4, $p < 0.01$). The increases in LUE in this region of τ_c are 71% at Howland, 22% at Mead, 62% at Morgan Monroe, and 60% at UMBS. Although the percent increases are large in the forests, the increase in LUE was only 0.001-0.002 μmol m^{-2} s^{-1} of GPP per μmol m^{-2} s^{-1} of total PAR. Our results are consistent with increases in LUE found on cloudy days compared to sunny days in a Sitka spruce forest (Dengel and Grace 2010) and with a 39% increase in LUE in a deciduous temperate forest under thin clouds compared to skies with aerosols (Min 2005). Another study reported increases in LUE ranging from 6-18% in a boreal needleleaf forest, 15-28% in a temperate broadleaf forest, and 30-33% in a tropical broadleaf forest depending on time of day (Alton et al. 2007). These rates may differ from ours because Alton et al. (2007) calculated LUE as the increase in GPP when diffuse fraction moves from below 0.5 to above 0.5, whereas we calculated LUE across a broader range of diffuse fraction for τ_c below the peak value for each site.

We found site-level variation in the strength of the relationship between τ_c and LUE below the τ_c for maximum diffuse PAR, with the strongest relationship observed at Howland Forest and Morgan Monroe ($R^2 = 0.20$) and the weakest relationship at Mead ($R^2 = 0.10$). This is

consistent with previous work demonstrating that diffuse PAR alone has no effect on GPP during the mid-day at Mead, but has a positive effect on GPP at the other three forest sites in this study (Cheng et al. 2015). LUE may be less strongly correlated with τ_c at Mead than at other sites because maize is a C_4 plant and thus, leaves are generally farther from light saturation than leaves in forests, which are C_3. Site-specific increases in LUE may be a result of the way plant canopy structure influences the distribution of light within the canopy (Cheng et al. 2015). The distribution of leaf area and the location of gaps in a plant canopy control light extinction and thus, how efficiently leaves absorb incoming PAR. Model simulations and field measurements demonstrate that different parts of the forest canopy contribute to total canopy photosynthesis when diffuse light changes (Knohl and Baldocchi 2008, Urban et al. 2012). Thus, canopy characteristics can interact with above-canopy meteorological conditions to create canopy microclimates that change the effect of clouds and diffuse PAR on ecosystem productivity.

Finally, LUE continues to increase past the τ_c for maximum diffuse PAR (Figure 2.4). LUE may increase with τ_c despite the reduction in diffuse and direct light because clouds can improve water and air temperature conditions for photosynthesis (Urban et al. 2007). However, the rate of increase in LUE under optically thick clouds is one order of magnitude smaller than compared to under optically thin clouds when diffuse PAR increases with τ_c. Overall, these results suggest that clouds can increase carbon processing in plant canopies through increases in diffuse PAR.

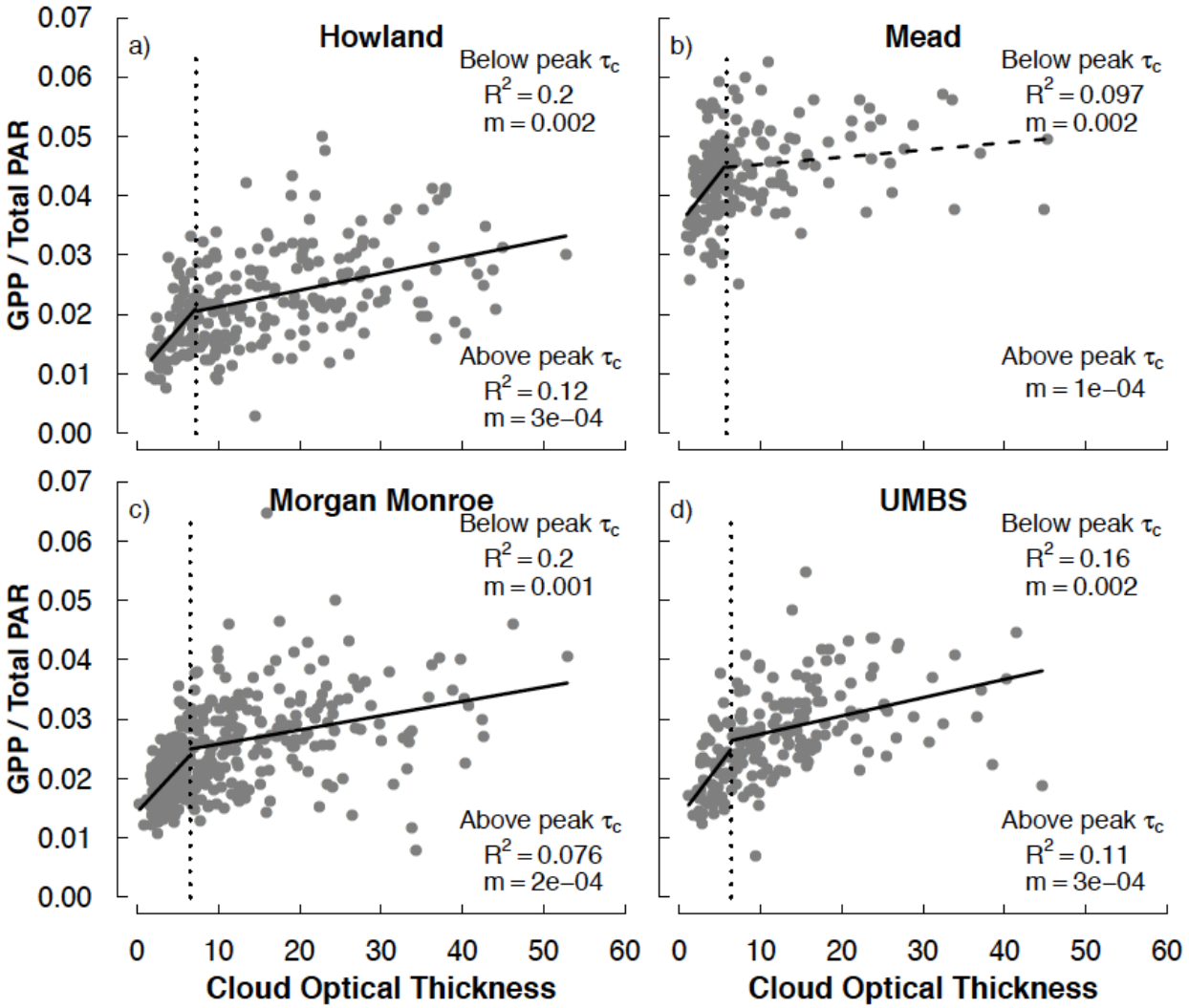

Figure 2.4: During the peak growing season (average start date and length listed in Table 2.1), light use efficiency (gross primary production per unit total PAR) increases with cloud optical thickness (τ_c) at a) Howland Forest, b) Mead, c) Morgan Monroe, and d) UMBS. The vertical dotted line represents the τ_c for maximum diffuse PAR at each site. Regression lines for below and above this peak τ_c are shown for relationships with $p < 0.01$. The peak-growing season only covers a portion of time from May through September, which are shown in Figures 2.1-2.3.

2.3.3 τ_c and GPP

Despite the positive relationship between optically thin clouds and LUE, we found no significant relationship between τ_c and canopy GPP at any of the sites while diffuse PAR increases ($p > 0.05$) (Figure 2.5). The lack of an observed relationship between GPP and low τ_c likely occurs because the decrease in direct PAR is greater than the increase in diffuse PAR at these sites (Figure 2.3 and Figure A3 in Appendix A). Although sites use light more efficiently under optically thin clouds, the increase in LUE is not large enough to compensate for the

decrease in direct PAR that occurs under optically thin clouds. In addition, we observed that GPP decreases as τ_c increases under optically thick clouds (Figure 2.5).

Previous studies have inferred the influence of clouds on ecosystem productivity using diffuse light as a proxy for cloud conditions. Some of these studies concluded that clouds do not increase total canopy productivity (Alton et al. 2005, Alton 2008, Knohl and Baldocchi 2008, Oliphant et al. 2011), while others have suggested that small changes in optically thin clouds will not increase canopy carbon uptake (Oliphant et al., 2011). By using satellite-derived τ_c, our results empirically demonstrate that optically thin clouds do not correlate with any changes in ecosystem productivity. The up to 5% decrease in cloud cover observed from satellites during 1984-2007 over the contiguous U.S. (Sun et al. 2015) is thus, unlikely to have affected the global carbon sink.

Given the lack of correlation between GPP and τ_c, our study suggests that the diffuse light effect may not be a significant driver of GPP at regional or global scales. Importantly, however, one limitation of our analysis is that we were only able to retrieve τ_c at mid-day when the effect of diffuse PAR on GPP is smallest in temperate ecosystems (Cheng et al. 2015). The effect of τ_c on GPP could be stronger at larger zenith angles or in ecosystems located at higher latitudes. However, the larger effect of diffuse light on GPP at larger zenith angles found in Cheng et al. (2015) could be independent of cloud conditions, given that diffuse PAR levels are higher at larger zenith angles (Earl et al. 2012). In addition, MODIS Collection 5.1 data only retrieve τ_c for pixels assigned as overcast (Otkin and Greenwald 2008). The response of GPP to clouds could be higher under partly cloudy skies if plants located under clear skies receive diffuse light from nearby clouds (Law et al. 2002). However, the effect of clouds on ecosystem carbon processing is smaller than what previously was concluded from studies using diffuse light data as a proxy for cloud cover.

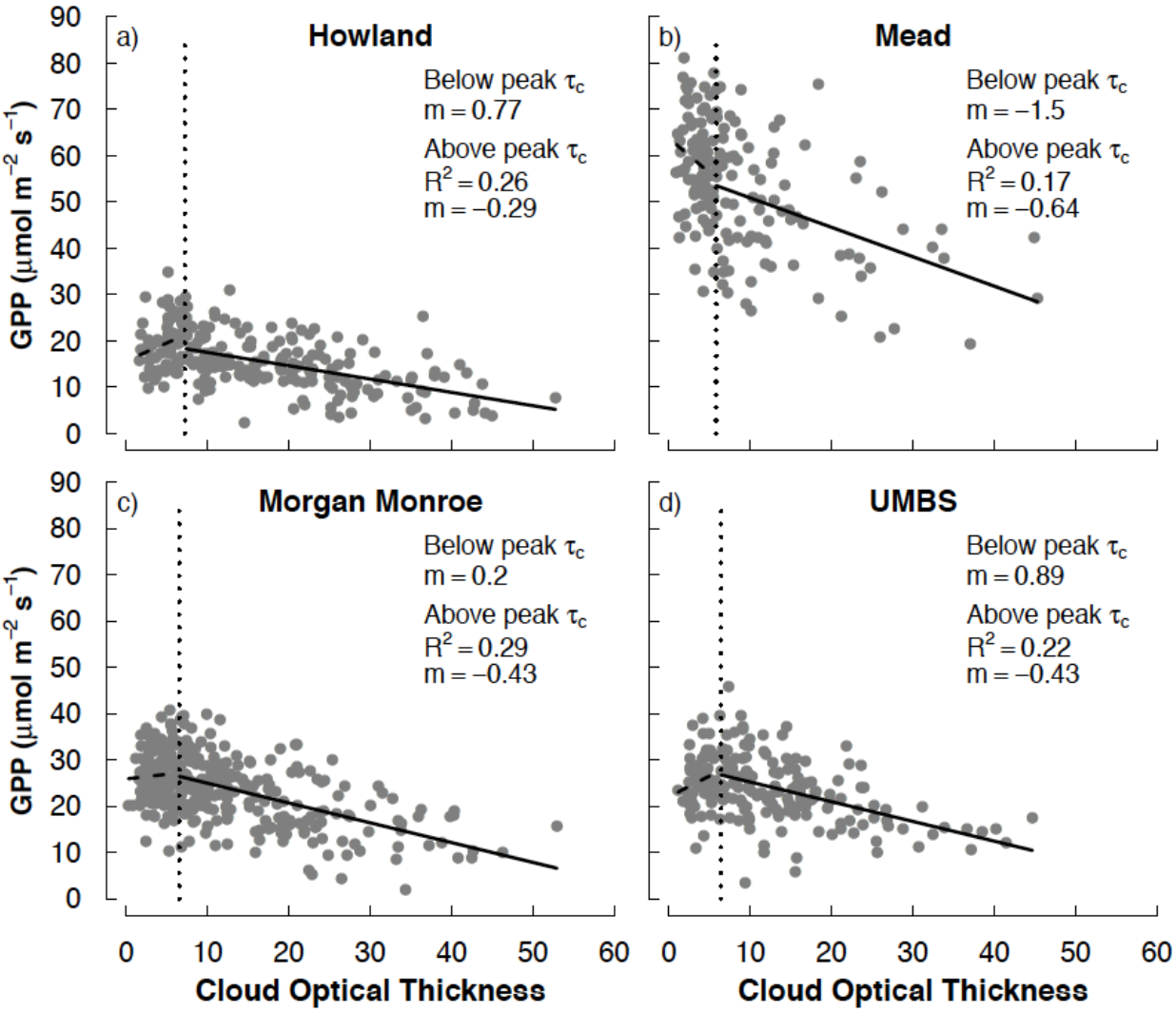

Figure 2.5: During the peak growing season, there is no relationship between cloud optical thickness (τ_c) and gross primary production (GPP) within the site-specific range of τ_c where diffuse photosynthetically active radiation (PAR) increases. Regression lines are drawn for relationships with $p > 0.05$. The vertical dotted line represents the peak τ_c for diffuse PAR at the site.

2.4 Conclusions

In this study, we quantify the effect of cloud conditions on surface light and ecosystem carbon uptake and determine the consistency of these relationships across ecosystems with different canopy structures. We evaluate the use of satellite retrievals of globally available τ_c to directly link the effect of clouds to the previously identified positive relationship between diffuse PAR and GPP. Our study expands on previous work by using direct measurements of diffuse

PAR and satellite-derived τ_c at several ecosystems instead of using proxies for diffuse light and categories of sky conditions.

We show that only optically thin clouds lead to increases in surface diffuse PAR, during which total PAR decreases. In addition, optically thick clouds decrease levels of total and diffuse PAR entering plant canopies. Specifically, we define a threshold value of $\tau_c = 6.8$ as the τ_c where diffuse PAR fluxes peak. Moreover, this value is relatively consistent across the ecosystems we studied. Across the range of τ_c where diffuse PAR increases, LUE in forest and maize canopies increases. However, the increases in LUE under optically thin clouds were too small to compensate for the decreased fluxes of direct surface light due to increasing optical thickness. As a result, τ_c has no discernable net influence on ecosystem GPP over the growing season. Despite finding no net effect of clouds on ecosystem GPP, our study provides observational evidence for the processes that link atmospheric light conditions to ecosystem carbon uptake. This allows for further examination of how connections between clouds and other drivers of LUE, such as water stress and nutrients, may influence ecosystem GPP. For example, if water stress or nutrient availability become stronger drivers of LUE than the effect of clouds on surface radiation, the relationship between clouds and LUE may be even weaker than we observed.

Overall, satellite measurements and eddy co-variance data show that satellite-derived τ_c can be used to estimate the range of cloud conditions that increases surface diffuse light. In addition, the use of satellite-derived τ_c allows us to move past inferences of cloud conditions from diffuse PAR. This comprehensive measure of scattering and absorbing properties of clouds allows us to empirically evaluate how clouds directly influence surface diffuse PAR and the terrestrial carbon cycle. Using this combination of observations, our results provide evidence that optically thin clouds do not increase ecosystem productivity. However, an increase in the frequency of optically thick clouds will likely reduce the amount of diffuse and total PAR available for plant canopies and decrease ecosystem GPP. These results suggest that the diffuse light effect from clouds is not as strong of a driver of regional or global ecosystem productivity in temperate ecosystems during the mid-day as previously suggested in other studies. We conclude that there is not a strong relationship between optically thin clouds and climate through diffuse light and the carbon cycle. However, the decreases in diffuse and direct light under optically thick clouds could remain an important effect on climate. By empirically linking and quantifying the relationships between τ_c, diffuse PAR, and GPP, we provide insight into how

changes in atmospheric conditions alter radiation regimes for terrestrial ecosystems to use for carbon uptake.

2.5 Acknowledgements and Data

We acknowledge and thank the following AmeriFlux sites for their data records: US-Ho1, US-Ne1, US-MMS, US-UMB, US-Bar, US-Fuf, US-Snd, US-Var. We also thank Dori Mermelstein and Stacey Kawecki for help with NCL scripts, the University of Michigan Center for Statistical Consulting and Research for statistical advisement, and Paul Hubanks and Gala Wind for responding to questions about MODIS data. We also appreciate the thoughtful comments from Bill Currie, Peter Curtis, Deborah Goldberg, and Gretchen Keppel-Aleks that helped strengthen the quality of this paper. Funding for SJC was provided in part by the University of Michigan Department of Ecology and Evolutionary Biology Brower Fellowship and the Michigan Space Grant Consortium. GB was funded in part by NSF 1521238. Funding for AmeriFlux data resources and for core site (US-Ho1, US-Ne1, US-UMB, US-MMS) data was provided by the U.S. Department of Energy's Office of Science. Data from US-Fuf were also funded by grants from the North American Carbon Program/USDA CREES NRI (2004-35111-15057, 2008-35101-19076) and Science Foundation Arizona (CAA 0-203-08) awarded to T. Kolb at Northern Arizona University. Additional support for US-Ho1 was provided by the USDA Forest Service Northern Research Station. The data we used in this paper can be found through the AmeriFlux Network (http://ameriflux.lbl.gov/) and NASA's Level 1 and Atmosphere Archive and Distribution System (https://ladsweb.nascom.nasa.gov/data/).

References

Alton, P. B. 2008. Reduced carbon sequestration in terrestrial ecosystems under overcast skies compared to clear skies. Agricultural and Forest Meteorology **148**:1641-1653.

Alton, P. B., P. North, J. Kaduk, and S. Los. 2005. Radiative transfer modeling of direct and diffuse sunlight in a Siberian pine forest. Journal of Geophysical Research: Atmospheres **110**:D23209.

Alton, P. B., P. R. North, and S. O. Los. 2007. The impact of diffuse sunlight on canopy light-use efficiency, gross photosynthetic product and net ecosystem exchange in three forest biomes. Global Change Biology **13**:776-787.

Andrews, T., J. Gregory, P. Forster, and M. Webb. 2012. Cloud Adjustment and its Role in CO_2 Radiative Forcing and Climate Sensitivity: A Review. Surveys in Geophysics **33**:619-635.

Arking, A. 1991. The Radiative Effects of Clouds and their Impact on Climate. Bulletin of the American Meteorological Society **72**:795-813.

Baldocchi, D. D. 2003. Assessing the eddy covariance technique for evaluating carbon dioxide exchange rates of ecosystems: past, present and future. Global Change Biology **9**:479-492.

Barker, H. W., G. L. Stephens, and Q. Fu. 1999. The sensitivity of domain-averaged solar fluxes to assumptions about cloud geometry. Quarterly Journal of the Royal Meteorological Society **125**:2127-2152.

Baum, B., and S. Platnick. 2006. Introduction to MODIS Cloud Products. Pages 74-91 *in* J. Qu, W. Gao, M. Kafatos, R. Murphy, and V. Salomonson, editors. Earth Science Satellite Remote Sensing. Springer Berlin Heidelberg.

Bird, R. E., and C. Riordan. 1986. Simple Solar Spectral Model for Direct and Diffuse Irradiance on Horizontal and Tilted Planes at the Earth's Surface for Cloudless Atmospheres. Journal of Climate and Applied Meteorology **25**:87-97.

Bony, S., B. Stevens, D. M. W. Frierson, C. Jakob, M. Kageyama, R. Pincus, T. G. Shepherd, S. C. Sherwood, A. P. Siebesma, A. H. Sobel, M. Watanabe, and M. J. Webb. 2015. Clouds, circulation and climate sensitivity. Nature Geosci **8**:261-268.

Boucher, O., D. Randall, P. Artaxo, C. Bretherton, G. Feingold, P. Forster, V. M. Kerminen, Y. Kondo, H. Liao, U. Lohmann, P. Rasch, S. K. Satheesh, S. Sherwood, B. Stevens, and X. Y. Zhang. 2013. Clouds and Aerosols.*in* T. F. Stocker, D. Qin, G.-K. Plattner, M. Tignor, S. K. Allen, J. Boschung, A. Nauels, Y. Xia, V. Bex, and P. M. Midgley, editors. Climate Change 2013: The Physical Science Basis. Contribution of Working Group I to the Fifth Assessment Report of the Intergovernmental Panel on Climate Change. Cambridge University Press, Cambridge, United Kingdom and New York, NY, USA.

Butt, N., M. New, Y. Malhi, A. C. L. Da Costa, P. Oliveira, and J. E. Silva-Espejo. 2010. Diffuse radiation and cloud fraction relationships in two contrasting Amazonian rainforest sites. Agricultural and Forest Meteorology **150**:361-368.

Cess, R. D., M. H. Zhang, P. Minnis, L. Corsetti, E. G. Dutton, B. W. Forgan, D. P. Garber, W. L. Gates, J. J. Hack, E. F. Harrison, X. Jing, J. T. Kiehi, C. N. Long, J.-J. Morcrette, G. L. Potter, V. Ramanathan, B. Subasilar, C. H. Whitlock, D. F. Young, and Y. Zhou. 1995. Absorption of Solar Radiation by Clouds: Observations Versus Models. Science **267**:496-499.

Cheng, S. J., G. Bohrer, A. L. Steiner, D. Y. Hollinger, A. Suyker, R. P. Phillips, and K. J. Nadelhoffer. 2015. Variations in the influence of diffuse light on gross primary productivity in temperate ecosystems. Agricultural and Forest Meteorology **201**:98-110.

Chou, M.-D., M. J. Suarez, C.-H. Ho, M. M.-H. Yan, and K.-T. Lee. 1998. Parameterizations for Cloud Overlapping and Shortwave Single-Scattering Properties for Use in General Circulation and Cloud Ensemble Models. Journal of Climate **11**:202-214.

Davin, E. L., and S. I. Seneviratne. 2012. Role of land surface processes and diffuse/direct radiation partitioning in simulating the European climate. Biogeosciences **9**:1695-1707.

Davis, A. B., and A. Marshak. 2010. Solar radiation transport in the cloudy atmosphere: a 3D perspective on observations and climate impacts. Reports on Progress in Physics **73**:026801.

Dengel, S., and J. Grace. 2010. Carbon dioxide exchange and canopy conductance of two coniferous forests under various sky conditions. Oecologia **164**:797-808.

Dim, J. R., T. Takamura, I. Okada, T. Y. Nakajima, and H. Takenaka. 2007. Influence of inhomogeneous cloud fields on optical properties retrieved from satellite observations. Journal of Geophysical Research: Atmospheres **112**:D13202.

Dore, S., M. Montes-Helu, S. C. Hart, B. A. Hungate, G. W. Koch, J. B. Moon, A. J. Finkral, and T. E. Kolb. 2012. Recovery of ponderosa pine ecosystem carbon and water fluxes from thinning and stand-replacing fire. Global Change Biology **18**:3171-3185.

Dragoni, D., H. P. Schmid, C. A. Wayson, H. Potter, C. S. B. Grimmond, and J. C. Randolph. 2011. Evidence of increased net ecosystem productivity associated with a longer vegetated season in a deciduous forest in south-central Indiana, USA. Global Change Biology **17**:886-897.

Earl, H., C. J. Bernacchi, and H. Medrano. 2012. Crop photosynthesis. Page 510 *in* J. Flexas, F. Loreto, and H. Medrano, editors. Terrestrial Photosynthesis in a Changing Environment. Cambridge University Press.

Free, M., and B. Sun. 2014. Trends in U.S. Total Cloud Cover from a Homogeneity-Adjusted Dataset. Journal of Climate **27**:4959-4969.

Friedlingstein, P., M. Meinshausen, V. K. Arora, C. D. Jones, A. Anav, S. K. Liddicoat, and R. Knutti. 2014. Uncertainties in CMIP5 Climate Projections due to Carbon Cycle Feedbacks. Journal of Climate **27**:511-526.

Garrity, S. R., G. Bohrer, K. D. Maurer, K. L. Mueller, C. S. Vogel, and P. S. Curtis. 2011. A comparison of multiple phenology data sources for estimating seasonal transitions in deciduous forest carbon exchange. Agricultural and Forest Meteorology **151**:1741-1752.

Gough, C. M., B. S. Hardiman, L. E. Nave, G. Bohrer, K. D. Maurer, C. S. Vogel, K. J. Nadelhoffer, and P. S. Curtis. 2013. Sustained carbon uptake and storage following moderate disturbance in a Great Lakes forest. Ecological Applications **23**:1202-1215.

Gu, L., D. Baldocchi, S. B. Verma, T. A. Black, T. Vesala, E. M. Falge, and P. R. Dowty. 2002. Advantages of diffuse radiation for terrestrial ecosystem productivity. Journal of Geophysical Research: Atmospheres **107**:ACL 2-1-ACL 2-23.

Gu, L., J. D. Fuentes, H. H. Shugart, R. M. Staebler, and T. A. Black. 1999. Responses of net ecosystem exchanges of carbon dioxide to changes in cloudiness: Results from two North American deciduous forests. Journal of Geophysical Research: Atmospheres **104**:31421-31434.

Hansen, J. E. 1971. Multiple Scattering of Polarized Light in Planetary Atmospheres Part II. Sunlight Reflected by Terrestrial Water Clouds. Journal of the Atmospheric Sciences **28**:1400-1426.

Hollinger, D. Y., J. Aber, B. Dail, E. A. Davidson, S. M. Goltz, H. Hughes, M. Y. Leclerc, J. T. Lee, A. D. Richardson, C. Rodrigues, N. A. Scott, D. Achuatavarier, and J. Walsh. 2004. Spatial and temporal variability in forest–atmosphere CO_2 exchange. Global Change Biology **10**:1689-1706.

Hollinger, D. Y., F. M. Kelliher, J. N. Byers, J. E. Hunt, T. M. Mcseveny, and P. L. Weir. 1994. Carbon Dioxide Exchange between an Undisturbed Old-Growth Temperate Forest and the Atmosphere. Ecology **75**:134-150.

Jenkins, J. P., A. D. Richardson, B. H. Braswell, S. V. Ollinger, D. Y. Hollinger, and M. L. Smith. 2007. Refining light-use efficiency calculations for a deciduous forest canopy using simultaneous tower-based carbon flux and radiometric measurements. Agricultural and Forest Meteorology **143**:64-79.

Kanniah, K. D., J. Beringer, P. North, and L. Hutley. 2012. Control of atmospheric particles on diffuse radiation and terrestrial plant productivity: A review. Progress in Physical Geography **36**:209-237.

Kikuchi, N., T. Nakajima, H. Kumagai, H. Kuroiwa, A. Kamei, R. Nakamura, and T. Y. Nakajima. 2006. Cloud optical thickness and effective particle radius derived from transmitted solar radiation measurements: Comparison with cloud radar observations. Journal of Geophysical Research-Atmospheres **111**.

King, M. D. 1987. Determination of the Scaled Optical Thickness of Clouds from Reflected Solar Radiation Measurements. Journal of the Atmospheric Sciences **44**:1734-1751.

King, M. D., S. Platnick, W. P. Menzel, S. A. Ackerman, and P. A. Hubanks. 2013. Spatial and Temporal Distribution of Clouds Observed by MODIS Onboard the Terra and Aqua Satellites. Ieee Transactions on Geoscience and Remote Sensing **51**:3826-3852.

Knohl, A., and D. D. Baldocchi. 2008. Effects of diffuse radiation on canopy gas exchange processes in a forest ecosystem. Journal of Geophysical Research: Biogeosciences **113**:G02023.

Koren, I., L. Oreopoulos, G. Feingold, L. A. Remer, and O. Altaratz. 2008. How small is a small cloud? Atmos. Chem. Phys. **8**:3855-3864.

Lauer, A., and K. Hamilton. 2013. Simulating Clouds with Global Climate Models: A Comparison of CMIP5 Results with CMIP3 and Satellite Data. Journal of Climate **26**:3823-3845.

Law, B. E., E. Falge, L. Gu, D. D. Baldocchi, P. Bakwin, P. Berbigier, K. Davis, A. J. Dolman, M. Falk, J. D. Fuentes, A. Goldstein, A. Granier, A. Grelle, D. Hollinger, I. A. Janssens, P. Jarvis, N. O. Jensen, G. Katul, Y. Mahli, G. Matteucci, T. Meyers, R. Monson, W. Munger, W. Oechel, R. Olson, K. Pilegaard, K. T. Paw U, H. Thorgeirsson, R. Valentini, S. Verma, T. Vesala, K. Wilson, and S. Wofsy. 2002. Environmental controls over carbon dioxide and water vapor exchange of terrestrial vegetation. Agricultural and Forest Meteorology **113**:97-120.

Leontyeva, E., and K. Stamnes. 1994. Estimations of Cloud Optical Thickness from Ground-Based Measurements of Incoming Solar Radiation in the Arctic. Journal of Climate **7**:566-578.

Liu, B. Y. H., and R. C. Jordan. 1960. The interrelationship and characteristic distribution of direct, diffuse and total solar radiation. Solar Energy **4**:1-19.

Ma, S., D. D. Baldocchi, J. A. Hatala, M. Detto, and J. Curiel Yuste. 2012. Are rain-induced ecosystem respiration pulses enhanced by legacies of antecedent photodegradation in semi-arid environments? Agricultural and Forest Meteorology **154–155**:203-213.

Macke, A., P. N. Francis, G. M. Mcfarquhar, and S. Kinne. 1998. The Role of Ice Particle Shapes and Size Distributions in the Single Scattering Properties of Cirrus Clouds. Journal of the Atmospheric Sciences **55**:2874-2883.

Marchand, R. 2013. Trends in ISCCP, MISR, and MODIS cloud-top-height and optical-depth histograms. Journal of Geophysical Research: Atmospheres **118**:1941-1949.

Mayer, B., A. Kylling, S. Madronich, and G. Seckmeyer. 1998. Enhanced absorption of UV radiation due to multiple scattering in clouds: Experimental evidence and theoretical explanation. Journal of Geophysical Research: Atmospheres **103**:31241-31254.

Mercado, L. M., N. Bellouin, S. Sitch, O. Boucher, C. Huntingford, M. Wild, and P. M. Cox. 2009. Impact of changes in diffuse radiation on the global land carbon sink. Nature **458**:1014-1017.

Michalsky, J. J., R. Perez, R. Stewart, B. A. Lebaron, and L. Harrison. 1988. Design and development of a rotating shadowband radiometer solar radiation/daylight network. Solar Energy **41**:577-581.

Miller, G. R., D. D. Baldocchi, B. E. Law, and T. Meyers. 2007. An analysis of soil moisture dynamics using multi-year data from a network of micrometeorological observation sites. Advances in Water Resources **30**:1065-1081.

Min, Q. 2005. Impacts of aerosols and clouds on forest-atmosphere carbon exchange. Journal of Geophysical Research: Atmospheres **110**:D06203.

Niyogi, D., H.-I. Chang, V. K. Saxena, T. Holt, K. Alapaty, F. Booker, F. Chen, K. J. Davis, B. Holben, T. Matsui, T. Meyers, W. C. Oechel, R. A. Pielke, R. Wells, K. Wilson, and Y. Xue. 2004. Direct observations of the effects of aerosol loading on net ecosystem CO_2 exchanges over different landscapes. Geophysical Research Letters **31**:L20506.

Oliphant, A. J., D. Dragoni, B. Deng, C. S. B. Grimmond, H. P. Schmid, and S. L. Scott. 2011. The role of sky conditions on gross primary production in a mixed deciduous forest. Agricultural and Forest Meteorology **151**:781-791.

Otkin, J. A., and T. J. Greenwald. 2008. Comparison of WRF Model-Simulated and MODIS-Derived Cloud Data. Monthly Weather Review **136**:1957-1970.

Pincus, R., S. Platnick, S. A. Ackerman, R. S. Hemler, and R. J. Patrick Hofmann. 2012. Reconciling Simulated and Observed Views of Clouds: MODIS, ISCCP, and the Limits of Instrument Simulators. Journal of Climate **25**:4699-4720.

Platnick, S., M. D. King, S. A. Ackerman, W. P. Menzel, B. A. Baum, J. C. Riedi, and R. A. Frey. 2003. The MODIS cloud products: Algorithms and examples from Terra. Ieee Transactions on Geoscience and Remote Sensing **41**:459-473.

Qu, J. J. 2006. Earth Science Satellite Remote Sensing Vol. 2: Data, Computational Processing, and Tools. Springer Berlin Heidelberg, Berlin, Heidelberg.

R Core Team. 2014. R: A language and environment for statistical computing. R Foundation for Statistical Computing, Vienna, Austria.

Rocha, A. V., H.-B. Su, C. S. Vogel, H. P. Schmid, and P. S. Curtis. 2004. Photosynthetic and Water Use Efficiency Responses to Diffuse Radiation by an Aspen-Dominated Northern Hardwood Forest. Forest Science **50**:793-801.

Scott, N. A., C. A. Rodrigues, H. Hughes, J. T. Lee, E. A. Davidson, D. B. Dail, P. Malerba, and D. Y. Hollinger. 2004. Changes in Carbon Storage and Net Carbon Exchange One Year

After an Initial Shelterwood Harvest at Howland Forest, ME. Environmental Management **33**:S9-S22.
Shonk, J. K. P., R. J. Hogan, J. M. Edwards, and G. G. Mace. 2010. Effect of improving representation of horizontal and vertical cloud structure on the Earth's global radiation budget. Part I: Review and parametrization. Quarterly Journal of the Royal Meteorological Society **136**:1191-1204.
Stephens, G. L. 2005. Cloud Feedbacks in the Climate System: A Critical Review. Journal of Climate **18**:237-273.
Still, C. J., W. J. Riley, S. C. Biraud, D. C. Noone, N. H. Buenning, J. T. Randerson, M. S. Torn, J. Welker, J. W. C. White, R. Vachon, G. D. Farquhar, and J. A. Berry. 2009. Influence of clouds and diffuse radiation on ecosystem-atmosphere CO_2 and $CO^{18}O$ exchanges. Journal of Geophysical Research: Biogeosciences **114**:G01018.
Sun, B., M. Free, H. L. Yoo, M. J. Foster, A. Heidinger, and K.-G. Karlsson. 2015. Variability and Trends in U.S. Cloud Cover: ISCCP, PATMOS-x, and CLARA-A1 Compared to Homogeneity-Adjusted Weather Observations. Journal of Climate **28**:4373-4389.
Suyker, A. E., and S. B. Verma. 2008. Interannual water vapor and energy exchange in an irrigated maize-based agroecosystem. Agricultural and Forest Meteorology **148**:417-427.
Twomey, S. 1991. Symposium on Global Climatic Effects of Aerosols Aerosols, clouds and radiation. Atmospheric Environment. Part A. General Topics **25**:2435-2442.
Urban, O., D. Janouš, M. Acosta, R. Czerný, I. Marková, M. Navrátil, M. Pavelka, R. Pokorný, M. Šprtová, R. U. I. Zhang, V. Špunda, J. Grace, and M. V. Marek. 2007. Ecophysiological controls over the net ecosystem exchange of mountain spruce stand. Comparison of the response in direct vs. diffuse solar radiation. Global Change Biology **13**:157-168.
Urban, O., K. Klem, A. Ač, K. Havránková, P. Holišová, M. Navrátil, M. Zitová, K. Kozlová, R. Pokorný, M. Šprtová, I. Tomášková, V. Špunda, and J. Grace. 2012. Impact of clear and cloudy sky conditions on the vertical distribution of photosynthetic CO_2 uptake within a spruce canopy. Functional Ecology **26**:46-55.
Várnai, T., and A. Marshak. 2002. Observations of Three-Dimensional Radiative Effects that Influence MODIS Cloud Optical Thickness Retrievals. Journal of the Atmospheric Sciences **59**:1607-1618.
Xu, L., and D. D. Baldocchi. 2004. Seasonal variation in carbon dioxide exchange over a Mediterranean annual grassland in California. Agricultural and Forest Meteorology **123**:79-96.
Zeng, S., C. Cornet, F. Parol, J. Riedi, and F. Thieuleux. 2012. A better understanding of cloud optical thickness derived from the passive sensors MODIS/AQUA and POLDER/PARASOL in the A-Train constellation. Atmos. Chem. Phys. **12**:11245-11259.

Chapter 3

Variations in the Influence of Diffuse Light on Gross Primary Productivity in Temperate Ecosystems [2]

Abstract

The carbon storage potential of terrestrial ecosystems depends in part on how atmospheric conditions influence the type and amount of surface radiation available for photosynthesis. Diffuse light, resulting from interactions between incident solar radiation and atmospheric aerosols and clouds, has been postulated to increase carbon uptake in terrestrial ecosystems. However, the magnitude of the diffuse light effect is unclear because existing studies use different methods to derive above-canopy diffuse light conditions. We used site-based, above-canopy measurements of diffuse light and gross primary productivity (GPP) from ten temperate ecosystems (including mixed conifer forests, deciduous broadleaf forests, and croplands) to quantify the GPP variation explained by diffuse photosynthetically active radiation (PAR) and to calculate increases in GPP as a function of diffuse light. Our analyses show that diffuse PAR explained up to 41% of variation in GPP in croplands and up to 17% in forests, independent of direct light levels. Carbon enhancement rates in response to diffuse PAR (calculated after accounting for vapor pressure deficit and air temperature) were also higher in croplands (0.011-0.050 μmol CO_2 per μmol photons of diffuse PAR) than in forests (0.003-0.018 μmol CO_2 per μmol photons of diffuse PAR). The amount of variation in GPP and carbon enhancement rate both differed with solar zenith angle and across sites for the same plant functional type. At crop sites, diffuse PAR had the strongest influence and the largest carbon enhancement rate during early mornings and late afternoons when zenith angles were large, with greater enhancement in the afternoons. In forests, diffuse PAR had the strongest influence at

[2]Published as S.J. Cheng, G. Bohrer, A.L. Steiner, D.Y. Hollinger, A. Suyker, R.P. Phillips, K.J. Nadelhoffer (2015) in *Agricultural and Forest Meteorology*, 201:98-110. doi:10.1016/j.agrformet.2014.11.002.

small zenith angles, but the largest carbon enhancement rate at large zenith angles, with a trend in ecosystem-specific responses. These results highlight the influence of zenith angle and the role of plant community composition in modifying diffuse light enhancement in terrestrial ecosystems, which will be important in scaling this effect from individual sites to the globe.

3.1 Introduction

Forests are estimated to remove up to 27% of human-emitted CO_2 annually (2.6 ± 0.8 Gt C yr^{-1}), with temperate forests responsible for about half of this uptake globally (Sarmiento et al. 2010, Le Quéré et al. 2013). It is uncertain how this amount of carbon uptake will change in the future because forest carbon processes are affected by complex interactions driven by changes in climate and natural- and human-caused shifts in plant species composition and canopy structure. Isolating and quantifying the impacts of individual drivers of land-atmosphere CO_2 exchange could improve these calculations of the future terrestrial carbon sink.

One important factor influencing photosynthesis and hence forest CO_2 uptake is light availability. Rates of leaf-level CO_2 uptake increase with solar radiation until leaves are light saturated (Mercado et al. 2009). This implies that forest CO_2 uptake is greater on sunny days when leaves are fully exposed to direct light. However, increases in diffuse light, which is produced when clouds and aerosols interact with and scatter incoming solar radiation, may be even more beneficial than equal increases in direct light. At the ecosystem level, key processes related to photosynthesis, including gross primary productivity (GPP), net ecosystem exchange (NEE), and light-use efficiency (LUE), can increase in magnitude when the proportion of light entering a forest canopy is more diffuse (Hollinger et al. 1994, Gu et al. 1999, Jenkins et al. 2007, Oliphant et al. 2011, Zhang et al. 2011, Urban et al. 2012). In addition, global simulations from 1960-1999 indicate that increases in the proportion of diffuse light reaching plant canopy surfaces may have amplified the global land carbon sink by 24% (Mercado et al. 2009).

Several mechanisms have been proposed to explain how diffuse light increases ecosystem CO_2 uptake and LUE. First, diffuse light can penetrate deeper into a forest canopy and reach lower canopy leaves that would normally be light-limited on clear days when light is mostly direct (Hollinger et al. 1994, Oliphant et al. 2011). Second, the same amount of light is distributed across more leaves when diffuse light is dominant, which can minimize light saturation and photo-inhibition of upper canopy leaves and increase canopy LUE or photosynthesis (Gu et al. 2002, Knohl and Baldocchi 2008). Third, diffuse light can create conditions favorable for photosynthesis by reducing water and heat stress on plants (Steiner and Chameides 2005, Urban et al. 2012). Finally, a fourth hypothesis suggests that diffuse light has a higher ratio of blue to red light, which may stimulate photochemical reactions and stomatal opening (Urban et al. 2012).

There is no consensus regarding the magnitude of effect that diffuse light has on ecosystem carbon processing. Studies using derived values of diffuse light suggest that LUE is higher when most incident light is diffuse and can result in maximum carbon uptake under moderate cloud cover (Gu et al. 2002, Rocha et al. 2004, Min and Wang 2008). However, studies using a three-dimensional canopy model and a land surface scheme predict that diffuse radiation will not lead to significant increases in carbon uptake on cloudy days as compared to clear days because of reductions in total shortwave radiation (Alton et al. 2005, Alton et al. 2007). If clouds decrease surface radiation enough to lower total canopy photosynthetic activity, this could offset any potential GPP gain resulting from increased LUE under diffuse light conditions (Alton 2008).

Several studies using measurements of diffuse light support the hypothesis that LUE is higher under diffuse light, consistent with studies using derived diffuse light data (Jenkins et al. 2007, Dengel and Grace 2010). In addition, total carbon uptake can be greater under cloudy, diffuse light conditions compared to clear skies in three forest types (Hollinger et al. 1994, Law et al. 2002). Aerosol-produced diffuse light also leads to an increase in the magnitude of NEE in forests and croplands (Niyogi et al. 2004). Additional observation-based analyses indicate that diffuse light increases carbon uptake when compared to the same level of direct light, but also when total light levels decrease (Hollinger et al. 1994, Urban et al. 2007, Urban et al. 2012).

The magnitude of the diffuse light effect on terrestrial carbon uptake may depend on ecosystem type or canopy structural characteristics. A regional modeling study suggests that diffuse light can increase net primary productivity (NPP) in mixed and broadleaf forests, but has a negligible effect on croplands (Matsui et al. 2008). Another study using derived diffuse light data suggests that LUE increases with diffuse light, and that differences among ecosystems are potentially dependent on vegetation canopy structure (Zhang et al. 2011). The influences of ecosystem type and vegetation structure are also supported by an observation-based study showing that under diffuse light, CO_2 flux into a grassland decreased, but increased by different amounts in croplands depending on the species of crop planted (Niyogi et al. 2004). However, another study using derived diffuse light data found no difference in the effect of patchy clouds on LUE among 23 grassland, prairie, cropland, and forest ecosystems in the Southern Great Plains (Wang et al. 2008). Inconsistencies among these studies may be due to differences in the methods and models used to obtain diffuse light or sky conditions and assess their impacts on

ecosystem carbon processing (Gu et al. 2003).

Climate modelers have begun incorporating the influence of diffuse light on ecosystem carbon uptake into land surface schemes as more details of canopy structure are added to models (Dai et al. 2004, Bonan et al. 2012, Davin and Seneviratne 2012). Our study provides insight into the importance of diffuse light on ecosystem carbon processing for improving projections of the terrestrial carbon sink. We seek here to 1) quantify how much variation in ecosystem GPP is explained by diffuse light, independent of direct radiation levels, 2) compare the influence of diffuse light on GPP among temperate ecosystems differing in canopy structure and species composition, and 3) determine the strength of diffuse light enhancement of GPP while accounting for its correlation with zenith angle, vapor pressure deficit (VPD), and air temperature. Unlike many previous studies (Gu et al. 1999, Alton 2008, Min and Wang 2008, Butt et al. 2010, Zhang et al. 2010), we drive our analyses only with direct field measurements of diffuse light, rather than with derived values from radiation partitioning models, which may be biased by incorrect representations of clouds and aerosols. Finally, our paper highlights the changes in the diffuse light effect across the diurnal cycle and the role of time of day on the diffuse light enhancement in terrestrial ecosystems, which will be important in scaling this effect from individual sites to the globe.

3.2. Materials and Methods

3.2.1 Data Sources

All analyzed data were collected and processed by investigators participating in the AmeriFlux program (http://ameriflux.lbl.gov/), a network of meteorological towers in the United States (U.S.) that measures net fluxes of water vapor and CO_2 between the land surface and the atmosphere and corresponding meteorological, soil, and vegetation conditions (Baldocchi 2003). Data collection, analysis, and metadata are standardized, reviewed, and quality controlled by AmeriFlux for all sites. GPP is calculated by subtracting the modeled ecosystem respiration from observed NEE. Respiration is modeled empirically based on NEE observations during the night, when GPP is assumed to be zero. We focus our study on GPP instead of another measure of carbon processing because it describes ecosystem CO_2 uptake, is affected directly by radiation, and is the first step in processing atmospheric CO_2 into long-term storage in ecosystems.

3.2.2 Site Selection

We selected temperate AmeriFlux sites within the contiguous U.S. with at least three years of Level 2 (processed and quality controlled) NEE and GPP. Among these, we specifically selected sites that contain equipment to measure above-canopy total and diffuse photosynthetically active radiation (PAR, 400-700 nm) and report at least three years of diffuse PAR values to AmeriFlux. For the University of Michigan Biological Station (UMBS), we obtained updated total and diffuse PAR data from site coordinators that were not yet available on the AmeriFlux website at the time of our analyses. After separating sites with crop rotations by species, there were sufficient data for ten sites covering three ecosystem types, including mixed forest (Howland Logged, Howland N Fertilized, Howland Reference), deciduous broadleaf forest (Morgan Monroe and UMBS), and cropland (Mead Irrigated Maize, Mead Irrigated Rotation: Maize, Mead Irrigated Rotation: Soybean, Mead Rainfed Rotation: Maize, Mead Rainfed Rotation: Soybean). Site characteristics and data availability are listed in Table 3.1.

Table 3.1: AmeriFlux site information and ecosystem characteristics

Site (SiteID)	Lat, Lon (°)	Years of Data	Canopy Height (m)	Vegetation Community	Management	LAI (m^2 m^{-2})	Climatic Annual Precipitation (mm)	Mean Growing Season Temperature[a] (°C)	Mean Growing Season VPD[a] (kPa)
Howland Logged (US-Ho3)	45.207, -68.725	2006-2008	20[b]	Dominated by red spruce (*Picea rubens*) and eastern hemlock (*Tsuga canadensis*). Also contains balsam fir (*Abies balsamea)*, white pine (*Pinus strobus)*, white cedar (*Thuja occidentalis*), red maple (*Acer rubrum*), and paper birch (*Betula papyrifera*)[c].	Selected logging and harvest (2001)[b]	2.1 to ~4[e]	1000[b]	16.7	0.83
Howland Reference (US-Ho1)	45.204, -68.740	2006-2008			Minimal disturbance since 1900s[d]	~ 6[b]		17.6	0.87
Howland N Fertilized (US-Ho2)	45.209, -68.747	2006-2009			N addition (2001-2005)[d,e]	~ 6[b]		16.5	0.82
Mead Irrigated Maize (US-Ne1)	41.165, -96.476	2001-2012	2.9[f]	Maize (*Zea mays)*	Center-pivot irrigation[f]	5.7[e]	887[f]	27.0	1.33
Mead Irrigated Rotation: Maize (US-Ne2)	41.164, -96.470	2001, 2003, 2005, 2007, 2009-2012	2.9[e]	Maize (*Z. mays)*	Center-pivot irrigation[f]	5.3[e]		26.2	1.14
Mead Irrigated Rotation: Soybean (US-Ne2)		2002, 2004, 2006, 2008	1.0[e]	Soybean (*Glycine max)*		4.9[e]			
Mead Rainfed Rotation: Maize (US-Ne3)	41.179, -96.439	2001, 2003, 2005, 2007, 2009, 2011	2.6[e]	Maize (*Z. mays)*	Naturally rainfed[g]	4.2[e]		26.7	1.39
Mead Rainfed Rotation: Soybean (US-Ne3)		2002, 2004, 2006, 2008, 2010, 2012	0.9[e]	Soybean (*G. max)*		3.8[e]			

Morgan Monroe (US-MMS)	39.323, -86.413	2007-2010	27[h]	Dominated by sugar maple (*A. saccharum*), tulip poplar (*Liriodendron tulipifera*), sassafras (*Sassafras albidum*), white oak (*Quercus alba*), and black oak (*Q. nigra*)[h].	None	5[l]	1012[j]	24.3	1.12
UMBS (US-UMB)	45.559, -84.713	2007-2011	22[k]	Dominated by bigtooth aspen (*Populus grandidentata*) with red oak (*Q. rubra*), red maple (*A. rubrum*), and white pine (*P. strobus*), as co-dominants. Also contains trembling aspen (*P. tremuloides*), white birch (*B. papyrifera*), sugar maple (*A. saccharum*), red pine (*P. resinosa*), and American beech (*Fagus grandifolia*).[k]	None	~3.5[k]	817[k]	21.2	1.05

[a]Values calculated from AmeriFlux data, [b]Scott et al. (2004), [c]Hollinger et al. (2004), [d]AmeriFlux website, [e]personal communication with site investigator, [f]Yan et al. (2012), [g]Verma et al. (2005), [h]Dragoni et al. (2011), [i]Oliphant et al. (2011), [j]Curtis et al. (2002), [k]Gough et al. (2013)

3.2.3 Definition of Analysis Period

To determine the maximum effect of diffuse light on GPP, we limited our period of analysis to the portion of the year when ecosystems are most productive. We used a carbon-flux phenology approach, where NEE is the defining variable for phenological transitions and the peak-growing season is the time period when NEE is at its maximum magnitude (Garrity et al. 2011). To do this, we first calculated 5-day NEE means for each site and year. Climate, vegetation composition, and inter-annual weather variability lead to phenological variation among sites (Richardson et al. 2013). Therefore, we adjusted our definition for the beginning and end of the peak-growing season to uniformly capture a representative portion of the NEE peak across sites and years. We defined the start of the growing season as the first day when the 5-day NEE average was within 90% of the year's fourth highest 5-day NEE average. The fourth-highest value was used to account for any extreme NEE values that may have occurred because of anomalous weather conditions. We set the end of season as the last day within 75% of the year's fourth-highest 5-day NEE average. The cutoff for the start of the peak-growing season is higher than the cutoff for the end of the season because canopy leaf-out and growth initiation typically occur quickly in seasonal sites, whereas canopy phenological changes are slower at the end of the season. While this approach cannot detect the exact beginning and end of the season, the criteria we used provide a uniform method for defining the period during which plants were at full seasonal growth and activity at our sites. We included only daytime values by excluding points with total PAR values < 20 μmol m^{-2} s^{-1}, assuming such low radiation levels are characteristic for nighttime.

3.2.4 Data Analysis

For each site, we combined all available peak-growing season daytime data and removed observations with negative measurements of diffuse PAR, direct PAR, or GPP, as these were likely sensor errors or marginal weather conditions (e.g., rain events). We also excluded data points with missing air temperature and VPD. We divided the remaining data into nine categorical groups based on solar zenith angle and the time of observation. We chose to bin by zenith angle to account for the effect of the sun's position on the amount of direct and diffuse PAR above a canopy, differences in radiation penetration through the canopy, and changes in plant hydraulics throughout the day. Zenith angle was calculated as the following:

$$\cos \varphi = \sin \phi \sin \delta + \cos \phi \cos \delta \cos [15(t - t_0)] \quad (2)$$

where φ is the zenith angle, ϕ is the latitude, δ is the solar declination angle, t is time, and t_0 is the time of solar noon (Campbell and Norman 1998). Given the latitudes of the sites, we defined mornings to begin at zenith angles between 76-100°, noon to occur at the minimum calculated zenith angles of 16-30°, and the end of daylight to occur around 76-100°.

The effect of diffuse PAR on GPP may depend on total light conditions. For example, little scattering occurs under clear skies, which results in low diffuse and high direct PAR levels. As a result, small increases in diffuse PAR are unlikely to have a strong impact on canopy photosynthesis due to large amounts of direct PAR available for photosynthesis. If direct PAR levels are low, however, such as on cloudy days or during the morning and evening, the increase in diffuse PAR will have a larger effect because canopy leaves are below light-saturation. To calculate direct PAR, we subtracted the observed diffuse PAR from the observed total PAR. Because GPP and PAR are known to have a strong relationship that can be empirically described by a rectangular hyperbola, we used the non-linear regression function in the R program (R Core Team 2014) to fit the following relationship:

$$GPP_{fitted} = (\alpha \gamma PAR_{dir}) / (\gamma + \alpha PAR_{dir}) \quad (3)$$

where GPP_{fitted} is the value of GPP predicted by total PAR using a rectangular hyperbola model (Eq. 3), α is the canopy quantum efficiency, γ is the canopy photosynthetic potential, and PAR_{dir} is direct PAR (Gu et al. 2002). The α and γ are the fitted parameters and are solved iteratively. We used the initial conditions of 0.044 μmol CO_2 per μmol photons and 23.7 μmol CO_2 m^{-2} s^{-1} for α and γ, respectively (Ruimy et al. 1995). The resulting empirical relationships for each site are presented in Appendix B.

To remove the confounding effect of direct PAR, we first calculated the residuals between observed GPP and GPP_{fitted}. We then compared those residuals against diffuse PAR for ten sites and nine zenith angle bins. For each zenith angle category, we estimated the variation in GPP residuals that can be explained by diffuse PAR alone using the following simple linear regression:

$$GPP_r = GPP - GPP_{fitted} = \beta_0 + \beta_1 PAR_{diff} + \varepsilon \quad (4)$$

and a combination of diffuse PAR, VPD, and air temperature using the following multiple linear regression:

$$GPP_r = GPP - GPP_{fitted} = \beta_0 + \beta_1 PAR_{diff} + \beta_2 VPD + \beta_3 T_a + \varepsilon \quad (5)$$

where GPP_r represents the residuals between the observed GPP and GPP_{fitted} and PAR_{diff} is diffuse PAR. T_a is air temperature measured at the eddy covariance tower and β_0, β_1, β_2 and β_3 are the fitted parameters estimating the model intercept and the linear slopes of the effects of diffuse PAR ,VPD, and air temperature at each solar zenith bin, respectively. The ε is the error term.

ANOVA comparisons between the simple (diffuse PAR only) and multiple linear regressions (including VPD and air temperature) showed that the multiple linear regression model (Eq. 5) was significantly better ($p < 0.05$) than the simple regression model, with the exception of nine site/bin combinations. We did not include interactions in the multiple linear regression because ANOVA tests indicated that the interaction terms did not improve the model consistently, and improvements to the residual sum of squares averaged only 3.5% in cases where interaction terms were significant. We also accounted for multiple testing over solar zenith angle bins and different sites by using the Bonferroni correction to calculate a new critical p-value. Light-response curves could not be fit to all scenarios, reducing the final number of comparisons to 83. Thus, for the simple and multiple linear regression comparisons, we consider a relationship significant if $p < 6.02 \times 10^{-4}$ (= 0.05/83).

3.3. Results

3.3.1 Relationship between diffuse PAR and GPP

We found significant positive relationships between diffuse PAR and GPP_r throughout the day, except in a few cases where diffuse PAR was not a significant predictor of GPP_r (Figure 3.1, Figure 3.2, black bars). Exceptions to these relationships occurred mainly at the Mead crop sites during mid-day and to a lesser extent at the UMBS forest during early mornings and late afternoons (Figure 3.2, black bars). In addition, a rectangular hyperbola could not be fit to the direct PAR and GPP data in the afternoon at large zenith angles at the Mead sites and Morgan Monroe (Appendix B, Table B1). Overall, the linear fits between diffuse PAR and GPP_r indicate that across sites and zenith angles, diffuse PAR explains 3-22% of variation in GPP_r in the morning and 3-41% of variation in GPP_r in the afternoon (Figure 3.2, black bars).

The amount of variance in GPP_r attributable to diffuse PAR varied considerably between forests and crop sites (Figure 3.2, black bars). At the deciduous broadleaf and mixed conifer forests, diffuse PAR accounts for more of the variance in GPP_r at the smallest zenith angle bins

(mid-day) and less at larger zenith angles in the early mornings and late afternoons (Figure 3.2a-e, black bars). However, the opposite pattern occurs at the Mead crop sites, where more of the variance in GPP_r is associated with diffuse PAR at larger zenith angles (Figure 3.2f-j, black bars). Diffuse PAR accounted for the largest portion of GPP_r variance at crop sites during afternoon zenith angles of 61-75°, corresponding to approximately 17:00-18:00 standard time.

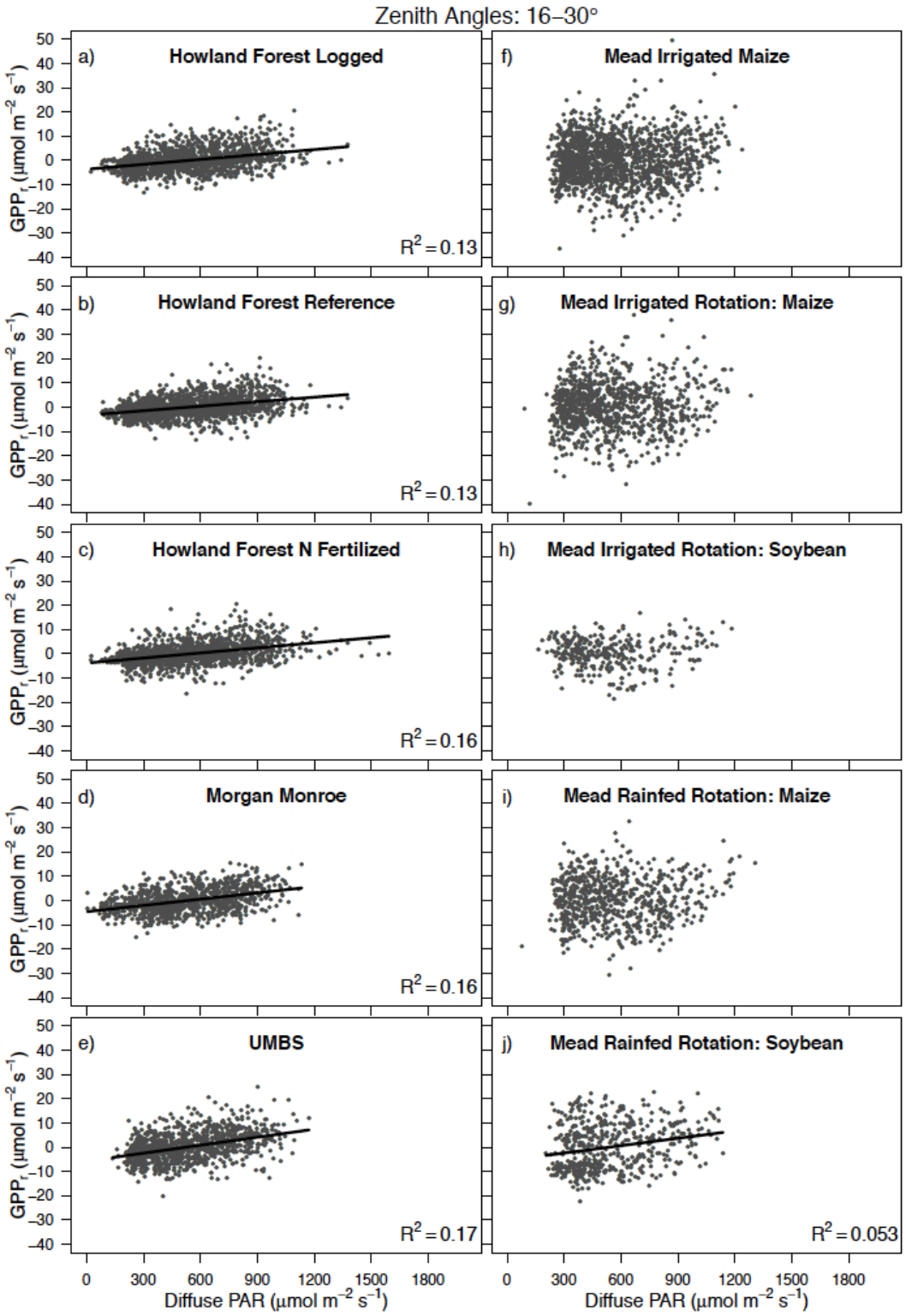

Figure 3.1: Simple linear regressions (Eq. 4) between diffuse PAR and GPP_r for observations around 10:00 – 14:00 standard time (zenith angles from 16-30°, other zenith angle bins not shown). Regression lines are only plotted for models with $p < 6.02 \times 10^{-4}$ (Bonferroni-corrected critical value).

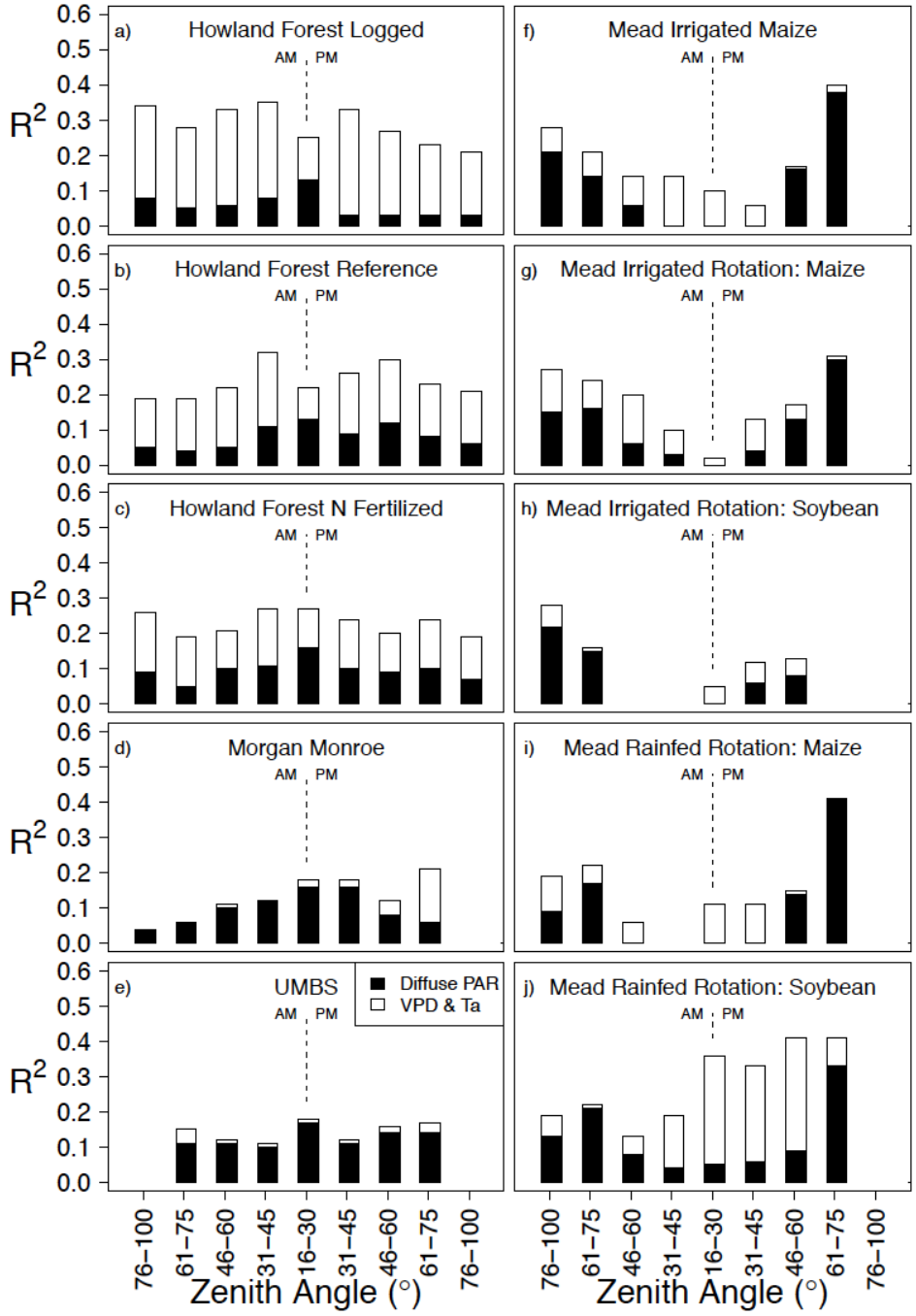

Figure 3.2: Proportions of variation in GPP_r explained by environmental variables. Solid bars represent R^2 values from simple linear regressions that include only the effect of diffuse PAR (Eq. 4). The total height of the bars (solid and white together) represents the R^2 from multiple linear regressions that include effects of air temperature (T_a) and vapor pressure deficit (VPD) with diffuse PAR (Eq. 5). Only R^2 values with $p < 6.02 \times 10^{-4}$ (Bonferroni-corrected critical value) are plotted. The minimum calculated zenith angle for these sites was ~16°.

3.3.2 Diffuse PAR cross-correlation with VPD and air temperature

Concomitant with changes in the partitioning of PAR into direct and diffuse streams, clouds and aerosols change surface VPD and air temperature. These two environmental factors influence stomatal conductance and photosynthesis, and thus affect rates of ecosystem GPP. When including the effects of these two variables on GPP_r with diffuse PAR (Eq. 5), the amount of variation in GPP_r explained increases up to an additional 31% during mornings and up to 32% during afternoons (Figure 3.2, white bars). This increase with VPD and air temperature is greatest across the most zenith angles at the Howland sites, where the multiple linear regression increases explanatory power of GPP_r by an additional 9-27% and 11-30% in the mornings and afternoons, respectively. VPD and air temperature also account for a relatively larger fraction of the variation of Mead Rainfed Rotation: Soybean GPP_r during the mid-day. Although we expected an increase in explanatory power with more variables in the regression, the increase in the explanation of GPP_r with the addition of these correlated environmental variables is small for the deciduous forests (Morgan Monroe and UMBS). This suggests that the effect of diffuse PAR at the deciduous forests is due to changes in light availability and not from indirect effects driven by the cross-correlation between diffuse PAR and other environmental conditions. Overall, the multiple linear regressions indicate that diffuse PAR is a significant predictor of GPP_r (except for the sites and zenith angle bins noted in Table 3.2). In addition, VPD and air temperature could not account for significant amounts of GPP_r variation under some conditions (Table 3.2).

Table 3.2: Parameter estimate values from relationships between GPP_r and diffuse PAR, vapor pressure deficit (VPD), and air temperature (T_a). All β_i estimate values (Eq. 4) have $p < 6.02 \times 10^{-4}$ (Bonferroni-corrected critical value), except for those designated as NS.

Site	β_i	Zenith Angle (°)								
		AM					PM			
		76-100	61-75	46-60	31-45	16-30	31-45	46-60	61-75	76-100
Howland Logged	Diffuse PAR	0.014	0.007	0.004	0.004	0.005	0.003	0.004	0.008	0.009
	VPD	-3.629	-2.627	-2.234	-3.847	-3.271	-3.205	-2.605	-2.339	-1.307
	T_a	0.183	0.343	0.427	0.546	0.352	0.495	0.383	0.296	0.172
Howland Reference	Diffuse PAR	0.010	0.005	0.004	0.005	0.005	0.005	0.008	0.010	0.011
	VPD	-2.004	NS	-1.914	-3.290	-2.728	-2.768	-2.309	-1.715	-1.208
	T_a	0.125	0.266	0.358	0.432	0.260	0.311	0.237	0.152	0.131
Howland N Fertilized	Diffuse PAR	0.014	0.007	0.006	0.005	0.006	0.006	0.007	0.012	0.014
	VPD	-2.625	NS	-1.876	-3.266	-3.204	-2.735	-2.052	-2.072	-1.330
	T_a	0.150	0.270	0.287	0.380	0.252	0.254	0.156	0.145	0.143
Morgan Monroe	Diffuse PAR	NS	0.010	0.011	0.010	0.008	0.009	0.008	0.008	NS
	VPD	NS	NS	NS	NS	-1.611	-1.734	-1.917	-2.479	NS
	T_a	NS	NS	NS	NS	NS	NS	NS	0.224	NS
UMBS	Diffuse PAR	NS	0.018	0.015	0.010	0.011	0.009	0.012	0.018	NS
	VPD	NS	4.218	3.078	NS	NS	NS	NS	-1.156	NS
	T_a	NS	NS	NS	-0.298	NS	NS	NS	NS	NS
Mead Irrigated Maize	Diffuse PAR	0.021	0.022	0.013	NS	NS	NS	0.024	0.050	NS
	VPD	NS	NS	NS	NS	-5.650	-3.061	NS	-1.252	NS
	T_a	0.304	0.445	0.811	1.315	1.215	0.660	NS	0.245	NS
Mead Irrigated Rotation: Maize	Diffuse PAR	0.019	0.021	0.012	0.011	NS	NS	0.027	0.042	NS
	VPD	NS	NS	NS	NS	NS	NS	NS	NS	NS
	T_a	0.332	NS	1.115	0.950	NS	1.135	NS	NS	NS
Mead Irrigated Rotation: Soybean	Diffuse PAR	0.017	0.015	NS	NS	NS	NS	0.011	NS	NS
	VPD	NS	NS	NS	NS	NS	NS	NS	NS	NS
	T_a	0.213	NS	NS	NS	0.598	0.534	NS	NS	NS
Mead Rainfed Rotation: Maize	Diffuse PAR	0.011	0.021	NS	NS	NS	NS	0.021	0.045	NS
	VPD	NS	NS	NS	NS	-6.365	-4.205	NS	NS	NS
	T_a	0.281	NS	NS	NS	NS	NS	NS	NS	NS

Mead Rainfed Rotation: Soybean	Diffuse PAR	0.014	0.021	NS	NS	NS	NS	NS	0.028	NS
	VPD	-3.148	NS	-5.123	-8.292	-8.021	-6.898	-5.035	-1.971	NS
	T_a	0.277	NS	NS	0.812	0.524	0.582	0.479	NS	NS

3.3.3 *Magnitude of the effects of diffuse PAR on GPP_r*

Howland Forest Reference, Morgan Monroe, and UMBS have not undergone any experimental manipulation (e.g., selective logging, N addition). At these sites, the sign of the significant parameter estimates indicate that in mornings and afternoons, GPP_r increased with diffuse PAR (Table 3.2). The predicted increases in GPP_r in the morning were calculated to be 0.004-0.010, 0.008-0.011, and 0.010-0.018 µmol CO_2 per µmol photons of diffuse PAR at Howland Forest Reference, Morgan Monroe, and UMBS, respectively (Figure 3.3). In the afternoon, the increases in GPP_r were similar in magnitude, and ranged from 0.005-0.011, 0.008-0.009, and 0.009-0.018 µmol CO_2 per µmol photons of diffuse PAR at Howland Forest Reference, Morgan Monroe, and UMBS, respectively (Figure 3.3).

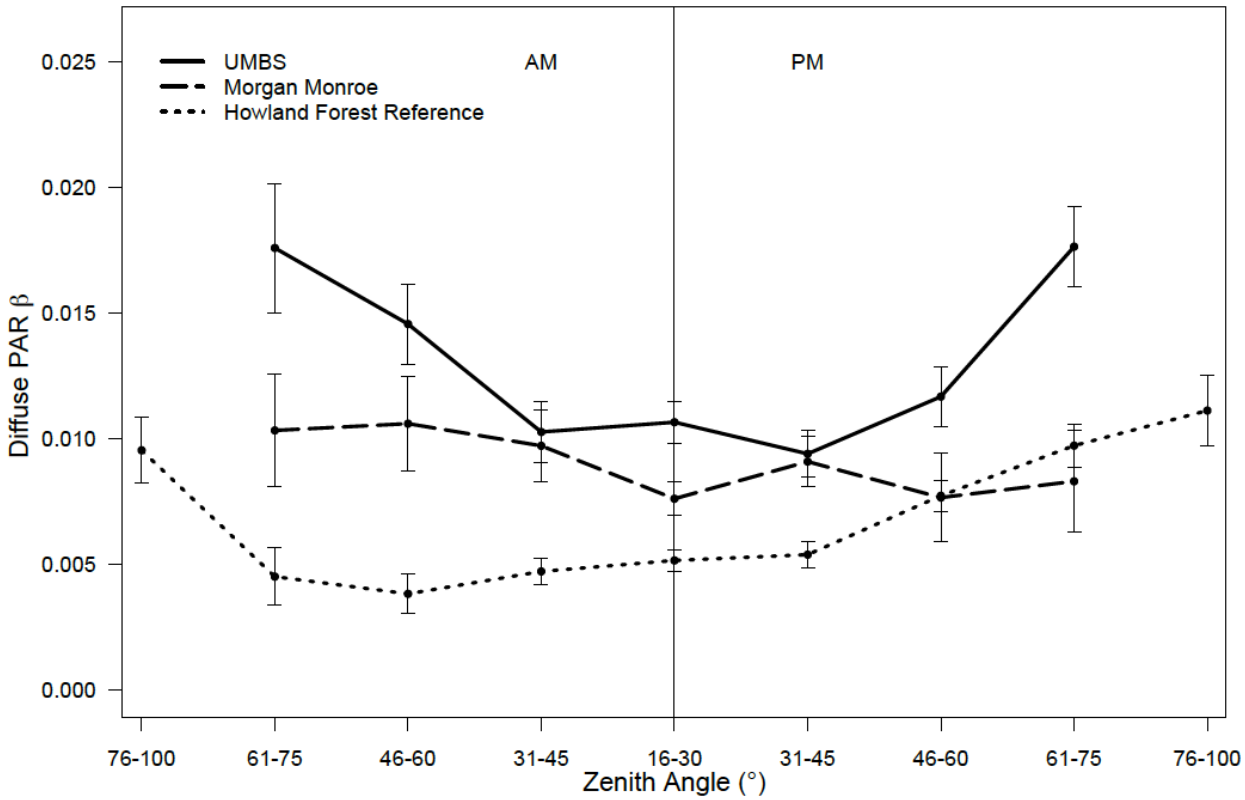

Figure 3.3: Diurnal patterns in diffuse PAR β estimates for unmanaged forests across zenith angles from a multiple linear regression that includes VPD and air temperature as covariates (Eq. 5). Error bars indicate one standard error. Only β estimates with $p < 6.02 \times 10^{-4}$ (Bonferroni-corrected critical value) are plotted.

The effect of diffuse PAR on rates of GPP_r varied among forest sites. UMBS had the largest increases in GPP_r with increases in diffuse PAR, and Howland Forest Reference had the

smallest increases in GPP_r. In addition, the calculated increases in GPP_r with diffuse PAR appear to depend on zenith angle at two of the sites. At UMBS, the influence of diffuse PAR on GPP_r is greatest in the early morning and late afternoon (zenith angles 61-75°) and decreases at mid-day (zenith angles 16-45°). At Howland Forest Reference, the response to zenith angle differs and the influence of diffuse PAR on GPP_r generally increases as the day continues and is highest in the late afternoon (zenith angles 76-100°). However, at Morgan Monroe, the influence of diffuse PAR on GPP_r did not vary with zenith angle. When we compare across these ecosystems, deciduous forests (UMBS, Morgan Monroe) appear to differ from the mixed conifer forest, particularly in the morning, with differences diminishing in the afternoon.

At Howland Forest, one site underwent selective logging while a second site was fertilized with 18 kg N/ha on a 21-hectare plot centered around the eddy covariance tower in five to six applications per growing season from 2001-2005 (David Dail, personal communication, 2013). Analysis of data at these manipulated sites indicates that the magnitude of increase in GPP_r with diffuse PAR was similar to that of the un-manipulated Howland forest (Figure 3.4). Differences among forest treatments are not apparent in the morning. In the afternoon, however, we observe a trend where diffuse PAR leads to the biggest GPP_r increase in the forest fertilized with N and the smallest change in GPP_r in the forest that has been selectively logged.

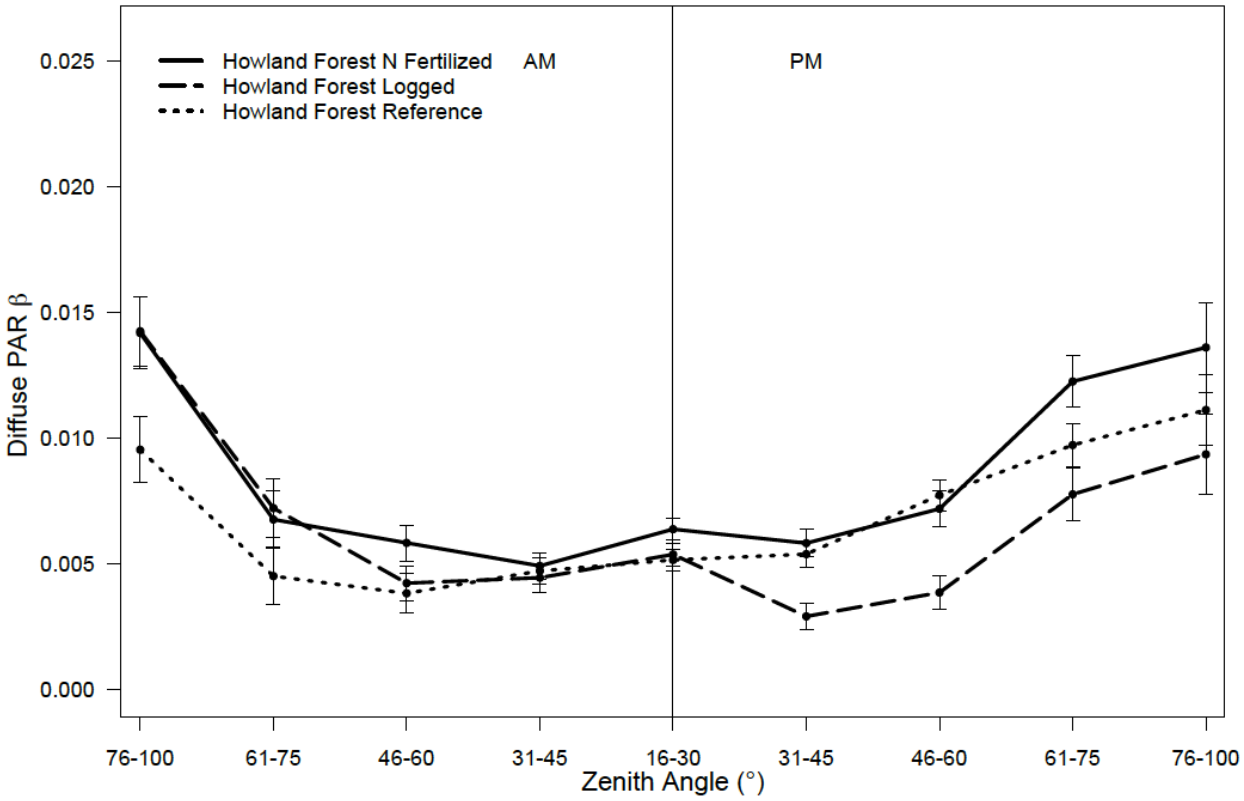

Figure 3.4: Diurnal patterns in diffuse PAR β estimate values for Howland Forest sites across zenith angles from a multiple linear regression that includes VPD and air temperature as covariates (Eq. 5). Error bars indicate one standard error. Only values with $p < 6.02 \times 10^{-4}$ (Bonferroni-corrected critical value) are plotted.

At the Mead Irrigated Rotation and Mead Rainfed Rotation sites, soybean and maize are planted in different years, allowing us to examine variations in the effect of diffuse PAR on GPP_r between crop types (Figure 3.5). The increases in GPP_r for maize were calculated to be 0.011-0.022 µmol CO_2 per µmol photons in the morning and 0.021-0.050 µmol CO_2 per µmol photons in the afternoon. For soybean, the increases in GPP_r in the morning were 0.014-0.021 µmol CO_2 per µmol photons and in the afternoon were 0.011-0.028 µmol CO_2 per µmol photons. Diffuse PAR led to increases in GPP_r at large zenith angles, but had no effect on GPP_r at small zenith angles for both crop species (values are only plotted in Figure 3.5 if they are significant). In addition, we observed no difference in the magnitude of the effect of diffuse PAR on GPP_r between soybean and maize in the morning. However, we did observe a greater effect of diffuse PAR on GPP_r for maize than soybean in the afternoon for zenith angles 46-75°. Irrigation did not appear to influence the magnitude of the diffuse PAR effect on GPP_r.

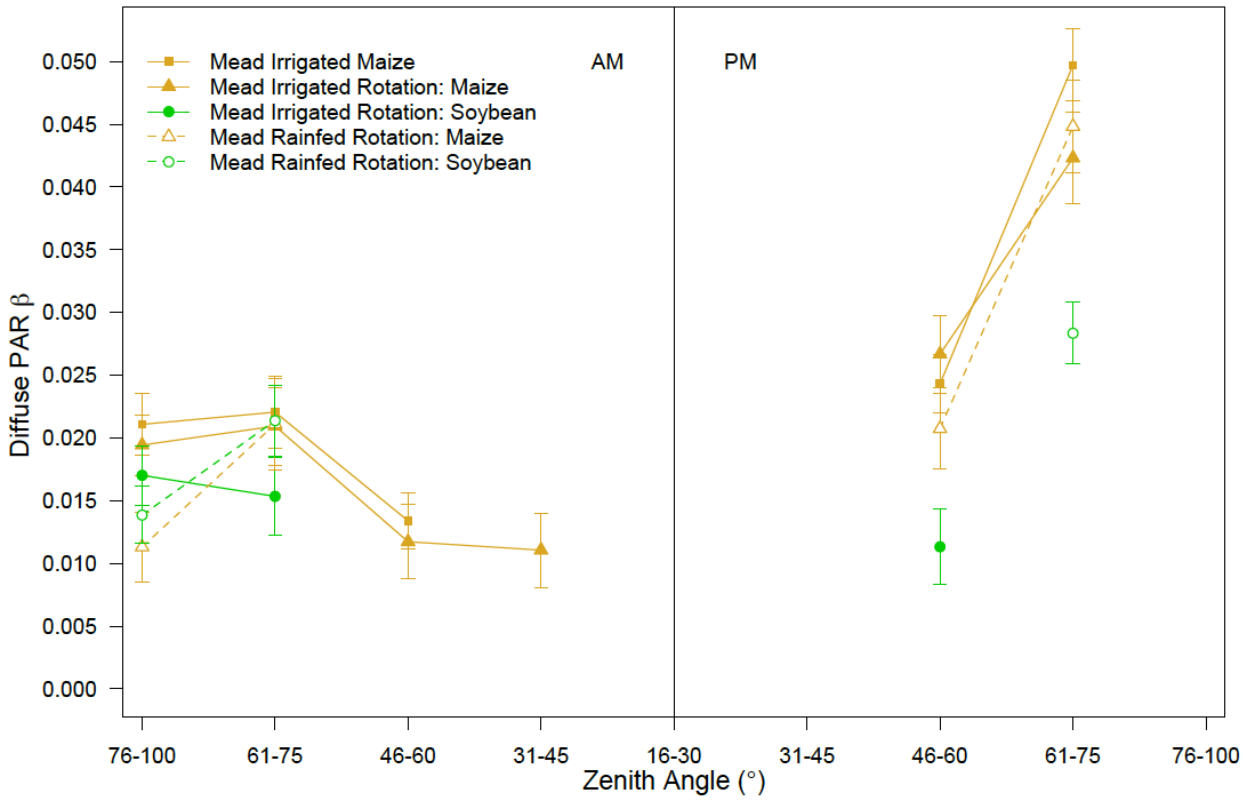

Figure 3.5: Diurnal patterns in diffuse PAR β estimate values for Mead crop sites across zenith angles from a multiple linear regression that includes VPD and air temperature as covariates (Eq. 5). Error bars indicate one standard error. Only β values with $p < 6.02 \times 10^{-4}$ (Bonferroni-corrected critical value) are plotted.

3.4. Discussion

Diffuse light influences Earth's climate by changing the amount and character of light available for photosynthesis, and thus, indirectly controls atmospheric CO_2 (Mercado et al. 2009). Depending on future anthropogenic emissions and their effects on atmospheric aerosols and clouds, the influence of diffuse light on the terrestrial carbon sink may increase. A more quantitative and mechanistic understanding of the link between diffuse light and land carbon uptake in different ecosystems would allow us to model how changes in diffuse light influence atmospheric and terrestrial carbon stocks, particularly as land-use change (e.g., deforestation, afforestation, and conversion of natural systems to cropland) continues (Arora and Boer 2010).

Past research has identified a positive correlation between diffuse light and ecosystem carbon uptake. However, this result may be due to a cross-correlation with total light availability, where diffuse light could more strongly influence photosynthesis when total light levels are low on overcast days as compared to high light levels on clear days (Gu et al. 1999, Zhang et al.

2010, Oliphant et al. 2011). The method we use in this paper addresses this confounding factor by removing the effect of direct light on ecosystem carbon uptake before calculating the rate of additional carbon uptake from diffuse light. Importantly, we tested for this potential independent effect using only direct field measurements of diffuse light, as opposed to deriving diffuse light levels with radiation partitioning models that make assumptions about aerosol and cloud conditions over terrestrial ecosystems. Our analysis of ten temperate ecosystems indicates that diffuse PAR correlates positively with GPP_r and this relationship is independent of direct PAR levels. Specifically, diffuse PAR independently explained up to 22% of the variation in GPP_r in mornings and up to 41% of the variation in GPP_r in afternoons.

Prior research shows that morning and afternoon responses to diffuse light can differ for the same zenith angles (Alton et al. 2005) and that in multiple ecosystems, rates of carbon enhancement vary across zenith angles (Zhang et al. 2010, Bai et al. 2012). However, to our knowledge, no other studies have investigated full diurnal patterns of diffuse light enhancement. We accomplished this by separating data according to zenith angle and time of day. Our results indicate that in forests, the proportion of variation in GPP_r explained by diffuse PAR (evaluated through R^2) is greatest at mid-day, and decreases as the sun moves closer to the horizon. The opposite pattern occurs at crop sites, where diffuse PAR did not predict GPP_r at small zenith angles (mid-day), but did correlate with variation in GPP_r at larger zenith angles (morning and afternoon). When we examined the magnitude of increase in GPP_r in response to diffuse PAR (β_1), the greatest increases were at larger zenith angles in crop sites (0.028 - 0.050 μmol CO_2 per μmol photons at 61-75° in the afternoon). In forests, however, diffuse PAR had the strongest influence (R^2) on GPP_r at small zenith angles when the sun is overhead (mid-day), but the largest carbon enhancement rate (β_1) at larger zenith angles (early mornings and late afternoons) when the sun is closer to the horizon.

In addition, some sites show a trend in an asymmetrical diurnal cycle of diffuse light enhancement, most notably in the crop sites. Although increases in GPP_r with diffuse PAR at forest sites appear to be similar in magnitude throughout the day, some of the zenith angle bins differed between the morning and afternoon. For example, the largest difference in carbon enhancement rates from a morning zenith angle bin to the same bin in the afternoon were 0.005 μmol CO_2 per μmol photons for mixed conifer forests, 0.003 μmol CO_2 per μmol photons for deciduous forests, 0.017 μmol CO_2 per μmol photons for soy, and 0.028 μmol CO_2 per μmol

photons for maize, though changes were usually within the standard error of the measurements. The response of GPP_r to diffuse light may differ in the morning and afternoon because environmental conditions influencing photosynthesis also vary during the day. For example, time lags between the effects of diurnal cycles of radiation and VPD on evapotranspiration (Zhang et al. 2014), stronger hydraulic stresses in the afternoon (Matheny et al. 2014), and morning and afternoon differences in leaf surface wetness that affect stomatal conductance (Misson et al. 2005) might explain the increased importance of diffuse light in the afternoon. These results can be used to evaluate ecosystem and global land surface models by testing if they capture the diurnal patterns we identified.

Our results indicate that there are ecosystem-specific responses of carbon uptake to diffuse light. The observed differences between crops and forests are consistent with (Niyogi et al. 2004) who used measured diffuse shortwave data to show that a crop site with a corn and soybean rotation was more sensitive to increases in aerosol-produced diffuse light than broadleaf and mixed conifer forests. Previous studies have hypothesized that differences in canopy structure among forests, grasslands, and croplands are responsible for differential responses of these ecosystems to diffuse light (Gu et al. 1999, Niyogi et al. 2004, Oliphant et al. 2011). However, they have not reported site-level canopy architectural measurements to test this potential modifier of land carbon uptake because they are difficult to collect and describe.

There are several hypotheses explaining why canopy structure may modify the effect of diffuse light on ecosystem carbon uptake. Canopy gaps, which interact with the angle of incident light, may influence how much light is distributed vertically through a canopy (Hutchison et al. 1980). For example, on clear days in a 30-m tall tulip poplar forest, the amount of radiation reaching the mid- and lower-parts of the canopy is lowest at large zenith angles (Hutchison et al. 1980). The authors attributed this to the low level of total radiation and reduced canopy gaps when the sun is near the horizon. Our analysis of UMBS gap fraction data derived from LAI-2000 measurements shows that as gap fraction decreases, carbon uptake with diffuse light increases (Figure 3.6). Because gap fraction here is the ratio of below-canopy PAR to above-canopy PAR, this indicates greater light extinction at larger zenith angles. Greater light extinction in the canopy may increase light scattering, which could expose more leaves to diffuse light. Thus, the response of GPP to diffuse light may be greater at larger zenith angles because of more complete canopy participation in photosynthesis. However, more gap fraction data and

canopy light profiles from across sites and collected with uniform methods are needed to test this idea, particularly in crop ecosystems. This would allow us to identify why crops and forests respond differently to diffuse PAR.

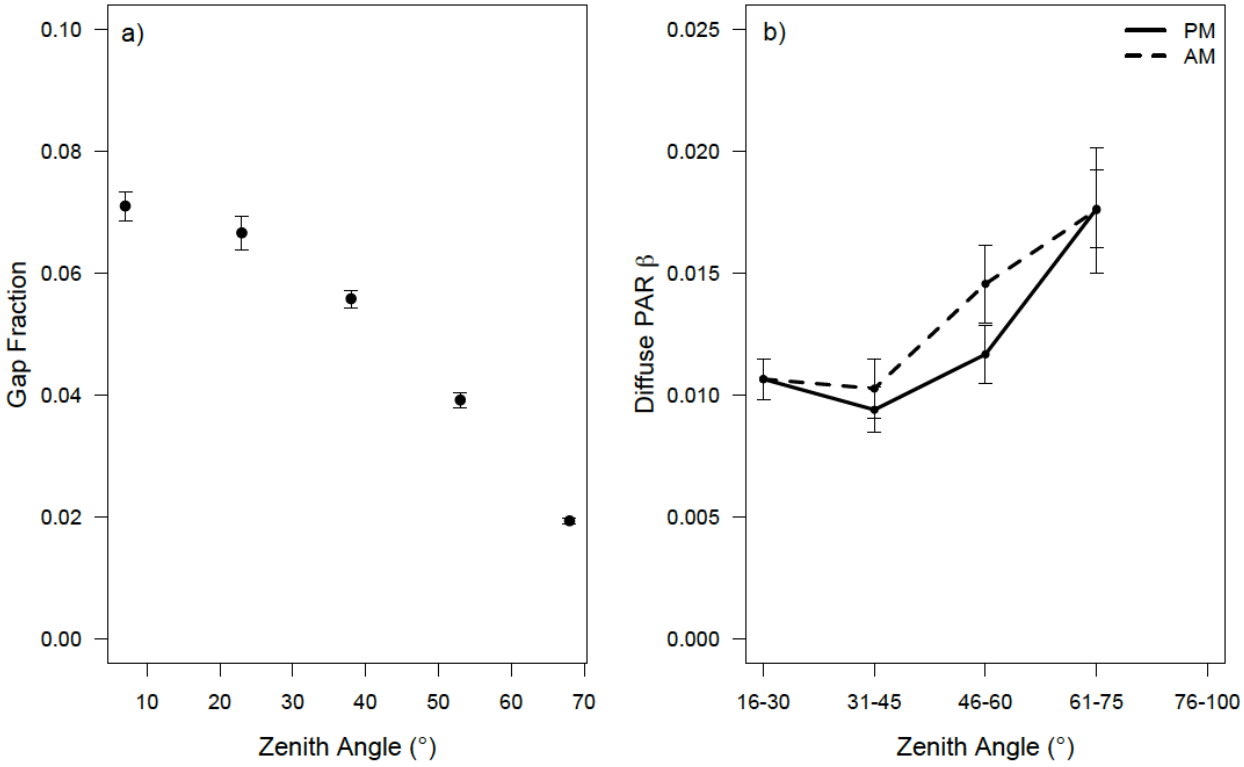

Figure 3.6. The relationship at UMBS (data from 2007-2011) between a) gap fraction and zenith angle and b) diffuse PAR β (carbon enhancement rate) and zenith angles (same data as shown in Figure 3.3). Error bars indicate one standard error.

Second, the distribution of photosynthetic tissues within a canopy depends on the plant community at each site and may contribute to observed differences between crops and forests. Forests have more stratified layers of vegetation and are much taller than crops. This means that leaf area index (LAI) in a forest is distributed over a larger volume than in crop sites. When the sun is overhead, forest canopies shade leaves at lower layers and diffuse light has a greater potential of reaching leaves near the bottom of the forest canopy as compared to direct light. Thus, the opportunity for diffuse light to reach more leaves in the canopy is greater when the sun is overhead (larger R^2). This explanation is supported by a study in a Norway spruce forest, which showed that needles deeper in the canopy contribute more to overall net ecosystem

production on cloudy days than on sunny days (Urban et al. 2012). However, the relative increases in GPP (β_1) may be smaller than those at crop sites because forest canopies are denser, which increases self-shading. On the other hand, crops are planted to minimize self-shading when the sun is overhead. In addition, β_1 may be higher at crop sites than at forests because multi-directional diffuse light at large zenith angles may reach deeper into crop canopies more effectively than direct light and increase light availability for crop stems, which are more photosynthetic than tree trunks.

Modeling studies have shown that species-dependent canopy characteristics, such as leaf clumping, LAI, and leaf inclination angle can affect the influence of diffuse PAR on carbon processing in ecosystems (Gu et al. 2002, Alton 2008, Knohl and Baldocchi 2008). This could be due to the penumbral effect, which occurs when the position and types of leaves (e.g., broadleaf and conifer) alter the amount and distribution of light to lower-level leaves (Denholm 1981, Way and Pearcy 2012). Although the arrangement of leaves in tall canopies with small leaves (e.g., forests) can increase shading of lower canopy leaves, it also increases the probability that leaves and branches scatter light, resulting in more distribution of light in the canopy. However, in shorter canopies with larger leaves (e.g., maize), there is less plant material that can scatter light and these sites may be more dependent on incident diffuse light. This may explain the higher carbon enhancement rates observed at crop sites compared to forests.

A few studies have measured how the distribution of light through plant canopies changes under diffuse light, but they are limited in their ability to test the influence of canopy structure on carbon enhancement from diffuse light because they have been conducted in a single ecosystem (Urban et al. 2012, Williams et al. 2014). Because site-level measurements of canopy structure are difficult to obtain, support for the mechanisms through which specific characteristics of canopy structure (e.g., leaf area distribution, leaf clumping) change ecosystem carbon uptake under diffuse light conditions has thus far depended on model assumptions (Alton et al. 2007, Knohl and Baldocchi 2008). To test whether canopy structural differences in height, canopy gaps, or leaf distribution within a canopy facilitate a diffuse light enhancement, a uniform method of collecting canopy structural data is needed. Methods are available for capturing some of this information, including light detection and ranging (LIDAR) remote sensing (Hardiman et al. 2013). However, no standardized method of collecting data has been applied among sites to allow for inter-site comparisons of canopy structure. Future research

should consider collecting data on canopy gaps, leaf distribution, and vertical light distribution to provide datasets that can be used to test whether gaps or leaf distribution within a canopy lead to an enhanced carbon uptake because of increased light distribution. Without this mechanistic connection, modelers cannot determine whether this missing biosphere-atmosphere connection results in a significant under- or over-prediction of the future terrestrial carbon sink. As scientists collect these canopy structural data, we suggest making these data publically available so they can be used to better interpret patterns seen using eddy covariance data.

We also observed differences in diffuse light effects among sites described as the same forest type (e.g., Morgan Monroe and UMBS). This argues for the consideration of site-specific responses to diffuse light because plant community composition of individual forest types (or ecosystems) determine unique canopy structures that can drive how strongly canopy gaps, leaf distribution, and penumbral qualities influence the effect of diffuse light on ecosystem carbon uptake. In particular, there were differences in afternoon carbon enhancement rates between the fertilized and formerly logged Howland Forest sites, which only differ in disturbance activity. Differences in nutrient availability for plants may explain why the N fertilized site correlated more strongly with diffuse light than the logged site. After two years of fertilization, foliage was one of the most N-enriched ecosystem pools (Dail et al. 2009). Increased soil N availability could lead to an increase in leaf N, which correlates with higher concentrations of Rubisco and chlorophyll (Evans 1989), implying an interaction between diffuse light and nutrient levels.

The effect of diffuse light on carbon uptake between maize and soybean also differed. This may be due to species differences in canopy structure as discussed above, but could also be due to the different photosynthetic pathways soy (C_3) and maize (C_4) use. Maize had a greater increase in carbon uptake with diffuse light than soy did, potentially because C_4 plants have a higher light saturation point (Greenwald et al. 2006). Because maize would be farther away from light saturation than soy, an increase in diffuse light (after accounting for cross-correlation with direct light) would bring maize closer to light saturation and thus, increase photosynthesis. In addition, C_4 plants are better adapted to warmer environments, which may cause environmental conditions, such as temperature and water availability, to change crop responses to diffuse light.

Finally, our results show that other environmental drivers that co-vary with diffuse PAR also contribute to GPP_r at some sites. In mixed conifer forests (e.g., the Howland sites), VPD, air temperature, and diffuse PAR together account for substantially more variation in GPP_r than

diffuse PAR itself does, implying a lesser role for radiation and a larger one for conditions that improve stomatal conductance under cloudy conditions at mixed conifer forests. In contrast, VPD and air temperature, within the ranges of values characteristic of measurement periods at the sites studied here, appear to have small effects on GPP_r in the broadleaf forests. This implies that the diffuse PAR effect at the broadleaf forests is due to the effect of scattered light itself. At the mixed conifer forests, the peak growing season temperature ranges from 16.5-17.6°C while the temperature is 21.2-24.3°C in the broadleaf forests. Comparing these site temperatures to the optimum temperature range of temperate deciduous trees (20-25°C) and evergreen coniferous trees (10-25°C), broadleaf forests are closer to their optimum temperature range (Larcher 2003). Considering that photosynthesis varies non-linearly with temperature, the same per unit change in temperature for a cooler site will lead to greater changes in GPP than in a warmer site. Increases in VPD in water-limited situations, on the other hand, should cause photosynthesis to drop because stomata will close to conserve water. However, VPD is actually lower in the mixed forests than in the deciduous broadleaf forests, implying that air temperature is a stronger driver of GPP than is VPD under our study's field conditions.

3.5. Conclusions

Field measurements show that diffuse PAR accounts for a substantial amount of variation in GPP once the quantity of direct PAR is removed. The observed changes in the diffuse PAR effect on GPP_r vary across zenith angles, ecosystem types, and plant functional groups, highlighting additional ways that ecosystem structural characteristics and the diurnal cycle influence ecosystem carbon cycling. In addition, observed site-level variation suggests that grouping forests together in regional or global models as the same plant functional type, without considering species composition or canopy structure, may lead to inaccuracies in assessing the impacts of radiation partitioning on modeled surface carbon fluxes.

To robustly extend these results, direct measurements of diffuse PAR and ecosystem flux data are needed from a wider range of ecosystems. Furthermore, research that can evaluate mechanisms (e.g, canopy gaps, leaf distribution, and species-specific characteristics) driving terrestrial carbon enhancement under diffuse light will remain stagnant without consistent field measurements of canopy structure at sites with diffuse light and eddy covariance measurements. The incorporation of standard methods for measuring canopy structure and within-canopy light

distribution and the availability of these data in common formats from across networks of eddy covariance towers (e.g., AmeriFlux, NEON) would enable the development of better predictive models of carbon exchange in relation to direct and diffuse solar radiation.

The interactions between diffuse light and ecosystem productivity may be of increasing importance as the community composition of our terrestrial ecosystems continues to change because of human land use change, natural ecological succession, and climate change. Thus, a more refined understanding of how diffuse PAR modifies atmosphere-land carbon cycling and subsequent representations of this relationship in models will likely advance our understanding of how human management of ecosystems will influence the land carbon sink as well as improve future calculations of atmospheric CO_2 concentrations for global climate projections.

3.6 Acknowledgments

We thank the FLUXNET community for their dedicated efforts in collecting and providing quality-controlled eddy covariance data for ecosystem research. We also thank the University of Michigan Center for Statistical Consultation and Research (Dr. Corey Powell and Dr. Kerby Shedden) for input on statistical techniques, Dr. Christoph Vogel for providing updated PAR data for UMBS, and Alex Fotis for early discussions and data organization for this paper. Support for SJC was provided in part by the University of Michigan Graham Sustainability Institute. Funding for data collection at UMBS was provided by the National Science Foundation grant DEB-0911461, the U.S. Department of Energy's (DOE) Office of Science Biological and Environmental Research (BER) project DE-SC0006708 and AmeriFlux National Core Flux Site award through Lawrence Berkeley National Laboratory contract #7096915, and National Oceanic and Atmospheric Administration grant NA11OAR4310190. Research at the Howland Forest is supported by the DOE's Office of Science BER. The Mead US-Ne1, US-Ne2, and US-Ne3 AmeriFlux sites were supported by the DOE Office of Science (BER; Grant Nos. DE-FG03-00ER62996, DE-FG02-03ER63639, and DE-EE0003149), DOE-EPSCoR (Grant No. DE-FG02-00ER45827), and NASA NACP (Grant No. NNX08AI75G). The Morgan Monroe team thanks the Indiana Department of Natural Resources for supporting and hosting the UM-MMS AmeriFlux site, and the U.S. DOE for funding operations through the Terrestrial Ecosystem Science program and the AmeriFlux Management Project.

References

Alton, P. B. 2008. Reduced carbon sequestration in terrestrial ecosystems under overcast skies compared to clear skies. Agricultural and Forest Meteorology **148**:1641-1653.

Alton, P. B., P. North, J. Kaduk, and S. Los. 2005. Radiative transfer modeling of direct and diffuse sunlight in a Siberian pine forest. Journal of Geophysical Research: Atmospheres **110**:D23209.

Alton, P. B., P. R. North, and S. O. Los. 2007. The impact of diffuse sunlight on canopy light-use efficiency, gross photosynthetic product and net ecosystem exchange in three forest biomes. Global Change Biology **13**:776-787.

Arora, V. K., and G. J. Boer. 2010. Uncertainties in the 20th century carbon budget associated with land use change. Global Change Biology **16**:3327-3348.

Bai, Y., J. Wang, B. Zhang, Z. Zhang, and J. Liang. 2012. Comparing the impact of cloudiness on carbon dioxide exchange in a grassland and a maize cropland in northwestern China. Ecological Research **27**:615-623.

Baldocchi, D. D. 2003. Assessing the eddy covariance technique for evaluating carbon dioxide exchange rates of ecosystems: past, present and future. Global Change Biology **9**:479-492.

Bonan, G. B., K. W. Oleson, R. A. Fisher, G. Lasslop, and M. Reichstein. 2012. Reconciling leaf physiological traits and canopy flux data: Use of the TRY and FLUXNET databases in the Community Land Model version 4. Journal of Geophysical Research: Biogeosciences **117**:G02026.

Butt, N., M. New, Y. Malhi, A. C. L. Da Costa, P. Oliveira, and J. E. Silva-Espejo. 2010. Diffuse radiation and cloud fraction relationships in two contrasting Amazonian rainforest sites. Agricultural and Forest Meteorology **150**:361-368.

Campbell, G. S., and J. M. Norman. 1998. An introduction to environmental biophysics. 2nd edition. Springer-Verlag, New York.

Curtis, P. S., P. J. Hanson, P. Bolstad, C. Barford, J. C. Randolph, H. P. Schmid, and K. B. Wilson. 2002. Biometric and eddy-covariance based estimates of annual carbon storage in five eastern North American deciduous forests. Agricultural and Forest Meteorology **113**:3-19.

Dai, Y., R. E. Dickinson, and Y.-P. Wang. 2004. A two-big-leaf model for canopy temperature, photosynthesis, and stomatal conductance. Journal of Climate **17**.

Dail, D. B., D. Hollinger, E. Davidson, I. Fernandez, H. Sievering, N. Scott, and E. Gaige. 2009. Distribution of nitrogen-15 tracers applied to the canopy of a mature spruce-hemlock stand, Howland, Maine, USA. Oecologia **160**:589-599.

Davin, E. L., and S. I. Seneviratne. 2012. Role of land surface processes and diffuse/direct radiation partitioning in simulating the European climate. Biogeosciences **9**:1695-1707.

Dengel, S., and J. Grace. 2010. Carbon dioxide exchange and canopy conductance of two coniferous forests under various sky conditions. Oecologia **164**:797-808.

Denholm, J. V. 1981. The influence of penumbra on canopy photosynthesis. 1. Theoretical considerations. Agricultural Meteorology **25**:145-166.

Dragoni, D., H. P. Schmid, C. A. Wayson, H. Potter, C. S. B. Grimmond, and J. C. Randolph. 2011. Evidence of increased net ecosystem productivity associated with a longer vegetated season in a deciduous forest in south-central Indiana, USA. Global Change Biology **17**:886-897.

Evans, J. R. 1989. Photosynthesis and nitrogen relationships in leaves of C_3 plants. Oecologia **78**:9-19.
Garrity, S. R., G. Bohrer, K. D. Maurer, K. L. Mueller, C. S. Vogel, and P. S. Curtis. 2011. A comparison of multiple phenology data sources for estimating seasonal transitions in deciduous forest carbon exchange. Agricultural and Forest Meteorology **151**:1741-1752.
Gough, C. M., B. S. Hardiman, L. E. Nave, G. Bohrer, K. D. Maurer, C. S. Vogel, K. J. Nadelhoffer, and P. S. Curtis. 2013. Sustained carbon uptake and storage following moderate disturbance in a Great Lakes forest. Ecological Applications **23**:1202-1215.
Greenwald, R., M. H. Bergin, J. Xu, D. Cohan, G. Hoogenboom, and W. L. Chameides. 2006. The influence of aerosols on crop production: A study using the CERES crop model. Agricultural Systems **89**:390-413.
Gu, L., D. Baldocchi, S. B. Verma, T. A. Black, T. Vesala, E. M. Falge, and P. R. Dowty. 2002. Advantages of diffuse radiation for terrestrial ecosystem productivity. Journal of Geophysical Research: Atmospheres **107**:ACL 2-1-ACL 2-23.
Gu, L., D. D. Baldocchi, S. C. Wofsy, J. W. Munger, J. J. Michalsky, S. P. Urbanski, and T. A. Boden. 2003. Response of a Deciduous Forest to the Mount Pinatubo Eruption: Enhanced Photosynthesis. Science **299**:2035-2038.
Gu, L., J. D. Fuentes, H. H. Shugart, R. M. Staebler, and T. A. Black. 1999. Responses of net ecosystem exchanges of carbon dioxide to changes in cloudiness: Results from two North American deciduous forests. Journal of Geophysical Research: Atmospheres **104**:31421-31434.
Hardiman, B. S., C. M. Gough, A. Halperin, K. L. Hofmeister, L. E. Nave, G. Bohrer, and P. S. Curtis. 2013. Maintaining high rates of carbon storage in old forests: A mechanism linking canopy structure to forest function. Forest Ecology and Management **298**:111-119.
Hollinger, D. Y., J. Aber, B. Dail, E. A. Davidson, S. M. Goltz, H. Hughes, M. Y. Leclerc, J. T. Lee, A. D. Richardson, C. Rodrigues, N. A. Scott, D. Achuatavarier, and J. Walsh. 2004. Spatial and temporal variability in forest–atmosphere CO_2 exchange. Global Change Biology **10**:1689-1706.
Hollinger, D. Y., F. M. Kelliher, J. N. Byers, J. E. Hunt, T. M. Mcseveny, and P. L. Weir. 1994. Carbon Dioxide Exchange between an Undisturbed Old-Growth Temperate Forest and the Atmosphere. Ecology **75**:134-150.
Hutchison, B. A., D. R. Matt, and R. T. Mcmillen. 1980. Effects of sky brightness distribution upon penetration of diffuse radiation through canopy gaps in a deciduous forest. Agricultural Meteorology **22**:137-147.
Jenkins, J. P., A. D. Richardson, B. H. Braswell, S. V. Ollinger, D. Y. Hollinger, and M. L. Smith. 2007. Refining light-use efficiency calculations for a deciduous forest canopy using simultaneous tower-based carbon flux and radiometric measurements. Agricultural and Forest Meteorology **143**:64-79.
Knohl, A., and D. D. Baldocchi. 2008. Effects of diffuse radiation on canopy gas exchange processes in a forest ecosystem. Journal of Geophysical Research: Biogeosciences **113**:G02023.
Larcher, W. 2003. Physiolgical Plant Ecology. 4th edition. Springer, Berlin.
Law, B. E., E. Falge, L. Gu, D. D. Baldocchi, P. Bakwin, P. Berbigier, K. Davis, A. J. Dolman, M. Falk, J. D. Fuentes, A. Goldstein, A. Granier, A. Grelle, D. Hollinger, I. A. Janssens, P. Jarvis, N. O. Jensen, G. Katul, Y. Mahli, G. Matteucci, T. Meyers, R. Monson, W. Munger, W. Oechel, R. Olson, K. Pilegaard, K. T. Paw U, H. Thorgeirsson, R. Valentini,

S. Verma, T. Vesala, K. Wilson, and S. Wofsy. 2002. Environmental controls over carbon dioxide and water vapor exchange of terrestrial vegetation. Agricultural and Forest Meteorology **113**:97-120.

Le Quéré, C., G. P. Peters, R. J. Andres, R. M. Andrew, T. A. Boden, P. Ciais, P. Friedlingstein, R. A. Houghton, G. Marland, R. Moriarty, S. Sitch, P. Tans, A. Arneth, A. Arvanitis, D. C. E. Bakker, L. Bopp, J. G. Canadell, L. P. Chini, S. C. Doney, A. Harper, I. Harris, J. I. House, A. K. Jain, S. D. Jones, E. Kato, R. F. Keeling, K. Klein Goldewijk, A. Körtzinger, C. Koven, N. Lefèvre, F. Maignan, A. Omar, T. Ono, G. H. Park, B. Pfeil, B. Poulter, M. R. Raupach, P. Regnier, C. Rödenbeck, S. Saito, J. Schwinger, J. Segschneider, B. D. Stocker, T. Takahashi, B. Tilbrook, S. Van Heuven, N. Viovy, R. Wanninkhof, A. Wiltshire, and S. Zaehle. 2013. Global carbon budget 2013. Earth Syst. Sci. Data Discuss. **6**:689-760.

Matheny, A. M., G. Bohrer, P. C. Stoy, I. T. Baker, A. T. Black, A. R. Desai, M. C. Dietze, C. M. Gough, V. Y. Ivanov, R. S. Jassal, K. A. Novick, K. V. R. Schäfer, and H. Verbeeck. 2014. Characterizing the diurnal patterns of errors in the prediction of evapotranspiration by several land-surface models: An NACP analysis. Journal of Geophysical Research: Biogeosciences **119**:2014JG002623.

Matsui, T., A. Beltrán-Przekurat, D. Niyogi, R. A. Pielke, and M. Coughenour. 2008. Aerosol light scattering effect on terrestrial plant productivity and energy fluxes over the eastern United States. Journal of Geophysical Research: Atmospheres **113**:D14S14.

Mercado, L. M., N. Bellouin, S. Sitch, O. Boucher, C. Huntingford, M. Wild, and P. M. Cox. 2009. Impact of changes in diffuse radiation on the global land carbon sink. Nature **458**:1014-1017.

Min, Q., and S. Wang. 2008. Clouds modulate terrestrial carbon uptake in a midlatitude hardwood forest. Geophysical Research Letters **35**:L02406.

Misson, L., M. Lunden, M. Mckay, and A. H. Goldstein. 2005. Atmospheric aerosol light scattering and surface wetness influence the diurnal pattern of net ecosystem exchange in a semi-arid ponderosa pine plantation. Agricultural and Forest Meteorology **129**:69-83.

Niyogi, D., H.-I. Chang, V. K. Saxena, T. Holt, K. Alapaty, F. Booker, F. Chen, K. J. Davis, B. Holben, T. Matsui, T. Meyers, W. C. Oechel, R. A. Pielke, R. Wells, K. Wilson, and Y. Xue. 2004. Direct observations of the effects of aerosol loading on net ecosystem CO_2 exchanges over different landscapes. Geophysical Research Letters **31**:L20506.

Oliphant, A. J., D. Dragoni, B. Deng, C. S. B. Grimmond, H. P. Schmid, and S. L. Scott. 2011. The role of sky conditions on gross primary production in a mixed deciduous forest. Agricultural and Forest Meteorology **151**:781-791.

R Core Team. 2014. R: A language and environment for statistical computing. R Foundation for Statistical Computing, Vienna, Austria.

Richardson, A. D., T. F. Keenan, M. Migliavacca, Y. Ryu, O. Sonnentag, and M. Toomey. 2013. Climate change, phenology, and phenological control of vegetation feedbacks to the climate system. Agricultural and Forest Meteorology **169**:156-173.

Rocha, A. V., H.-B. Su, C. S. Vogel, H. P. Schmid, and P. S. Curtis. 2004. Photosynthetic and Water Use Efficiency Responses to Diffuse Radiation by an Aspen-Dominated Northern Hardwood Forest. Forest Science **50**:793-801.

Ruimy, A., P. G. Jarvis, D. D. Baldocchi, and B. Saugier. 1995. CO_2 Fluxes over Plant Canopies and Solar Radiation: A Review. Pages 1-68 *in* M. Begon and A. H. Fitter, editors. Advances in Ecological Research. Academic Press.

Sarmiento, J. L., M. Gloor, N. Gruber, C. Beaulieu, A. R. Jacobson, S. E. Mikaloff Fletcher, S. Pacala, and K. Rodgers. 2010. Trends and regional distributions of land and ocean carbon sinks. Biogeosciences **7**:2351-2367.

Scott, N. A., C. A. Rodrigues, H. Hughes, J. T. Lee, E. A. Davidson, D. B. Dail, P. Malerba, and D. Y. Hollinger. 2004. Changes in Carbon Storage and Net Carbon Exchange One Year After an Initial Shelterwood Harvest at Howland Forest, ME. Environmental Management **33**:S9-S22.

Steiner, A. L., and W. L. Chameides. 2005. Aerosol-induced thermal effects increase modelled terrestrial photosynthesis and transpiration. Tellus B **57**:404-411.

Urban, O., D. Janouš, M. Acosta, R. Czerný, I. Marková, M. Navrátil, M. Pavelka, R. Pokorný, M. Šprtová, R. U. I. Zhang, V. Špunda, J. Grace, and M. V. Marek. 2007. Ecophysiological controls over the net ecosystem exchange of mountain spruce stand. Comparison of the response in direct vs. diffuse solar radiation. Global Change Biology **13**:157-168.

Urban, O., K. Klem, A. Ač, K. Havránková, P. Holišová, M. Navrátil, M. Zitová, K. Kozlová, R. Pokorný, M. Šprtová, I. Tomášková, V. Špunda, and J. Grace. 2012. Impact of clear and cloudy sky conditions on the vertical distribution of photosynthetic CO_2 uptake within a spruce canopy. Functional Ecology **26**:46-55.

Verma, S. B., A. Dobermann, K. G. Cassman, D. T. Walters, J. M. Knops, T. J. Arkebauer, A. E. Suyker, G. G. Burba, B. Amos, H. S. Yang, D. Ginting, K. G. Hubbard, A. A. Gitelson, and E. A. Walter-Shea. 2005. Annual carbon dioxide exchange in irrigated and rainfed maize-based agroecosystems. Agricultural and Forest Meteorology **131**:77-96.

Wang, K., R. E. Dickinson, and S. Liang. 2008. Observational evidence on the effects of clouds and aerosols on net ecosystem exchange and evapotranspiration. Geophysical Research Letters **35**:L10401.

Way, D. A., and R. W. Pearcy. 2012. Sunflecks in trees and forests: from photosynthetic physiology to global change biology. Tree Physiol **32**:1066-1081.

Williams, M., E. B. Rastetter, L. Van Der Pol, and G. R. Shaver. 2014. Arctic canopy photosynthetic efficiency enhanced under diffuse light, linked to a reduction in the fraction of the canopy in deep shade. New Phytologist **202**:1267-1276.

Yan, H., S. Q. Wang, D. Billesbach, W. Oechel, J. H. Zhang, T. Meyers, T. A. Martin, R. Matamala, D. Baldocchi, G. Bohrer, D. Dragoni, and R. Scott. 2012. Global estimation of evapotranspiration using a leaf area index-based surface energy and water balance model. Remote Sensing of Environment **124**:581-595.

Zhang, M., G.-R. Yu, J. Zhuang, R. Gentry, Y.-L. Fu, X.-M. Sun, L.-M. Zhang, X.-F. Wen, Q.-F. Wang, S.-J. Han, J.-H. Yan, Y.-P. Zhang, Y.-F. Wang, and Y.-N. Li. 2011. Effects of cloudiness change on net ecosystem exchange, light use efficiency, and water use efficiency in typical ecosystems of China. Agricultural and Forest Meteorology **151**:803-816.

Zhang, Q., S. Manzoni, G. Katul, A. Porporato, and D. Yang. 2014. The hysteretic evapotranspiration—Vapor pressure deficit relation. Journal of Geophysical Research: Biogeosciences **119**:125-140.

Zhang, Y., X. Y. Wen, and C. J. Jang. 2010. Simulating chemistry–aerosol–cloud–radiation–climate feedbacks over the continental U.S. using the online-coupled Weather Research Forecasting Model with chemistry (WRF/Chem). Atmospheric Environment **44**:3568-3582.

Chapter 4

Photosynthesis from Leaf to Canopy: Species and Leaf Light Availability Drive Within-Canopy Variation in Forest Photosynthetic Capacity [3]

Abstract

Plant canopies vary in physical structure, species composition, and in spatial distributions of environmental conditions that influence photosynthesis. The effects of canopy heterogeneity on the rate-limiting reactions in photosynthesis (i.e., photosynthetic capacity) may scale up to change canopy-level CO_2 uptake. To examine how leaf photosynthetic capacity varies within a plant canopy and among species grouped into the same plant functional type in Earth system models, we derived the rates of maximum carboxylation ($V_{c,max}$), electron transport (J), and triose phosphate utilization (TPU) from *in situ* measurements made on sun and shade leaves on adult, canopy-dominant trees of three temperate broadleaf species. We then compared model equations representing hypotheses about how species, leaf temperature, leaf nitrogen, and light availability (sun v. shade leaves) influence $V_{c,max}$, J, and TPU. Results showed that $V_{c,max}$ was best explained by a model that included leaf temperature and nitrogen per leaf area (N_{area}). The best model for J included leaf temperature, species, and leaf light environment. TPU was best explained by leaf light environment, with leaf temperature minimally improving the model's predictive power. The variations in J and TPU that occur with species or light environment suggest that species or leaf-type specific traits, in addition to N_{area}, are needed to explain patterns in J and TPU. We suggest that Earth system models test whether less-simplified parameterizations of these processes improves model estimates of land-atmosphere CO_2 fluxes. Our results thus provide future opportunities for models to quantify how canopy heterogeneity scales up to influence global terrestrial carbon uptake.

[2] To be published by S.J. Cheng, R.Q. Thomas, J.V. Wilkening, P.S. Curtis, T.D. Sharkey, K.J. Nadelhoffer. In review at the *Journal of Geophysical Research: Biogeosciences*.

4.1 Introduction

At the global scale, plants slow the increase of atmospheric CO_2 by storing the equivalent of approximately 25% of annual anthropogenic emissions in terrestrial ecosystems (Le Quéré et al. 2014). However, future rates of terrestrial CO_2 uptake depend on how interactions between climate and plant ecology alter rates of leaf photosynthesis. For example, when growing temperature increases, net photosynthesis in juvenile trees can increase or decrease, depending on whether the trees grow near the warm or cold edge of their species' range (Reich et al. 2015). Accurately predicting CO_2 uptake from the leaf to ecosystem level requires identifying how the biochemical mechanisms that control photosynthesis respond to environmental and ecological changes in plant canopies.

Leaf CO_2 assimilation is limited by three main photosynthetic sub-processes. The first is the maximum rate of carboxylation ($V_{c,max}$), which represents how quickly ribulose-1,5-bisphosphate carboxylase/oxygenase (Rubisco) catalyses the reaction between a saturated supply of ribulose-1,5-bisphosphate (RuBP) and CO_2 (Diaz-Espejo et al. 2012). The second rate-limiting reaction occurs when photosynthesis is constrained by RuBP regeneration, which depends partially on the maximum rate of electron transport (J_{max}) (Diaz-Espejo et al. 2012). Finally, triose phosphate utilization (*TPU*) releases phosphates for regenerating RuBP when the products of photosynthesis (i.e., triose phosphates) are converted to sugars and starches (Sharkey et al. 2007, Diaz-Espejo et al. 2012). Other factors influence $V_{c,max}$, J_{max}, and *TPU*, or a leaf's photosynthetic capacity, including leaf temperature (Walcroft et al. 1997, Hikosaka et al. 2007) and leaf allocation of nitrogen to photosynthetic machinery (Evans 1989, Harley and Baldocchi 1995, Reich et al. 1995). Often, the slowest rate of CO_2 uptake under these rate-limiting conditions is then used to estimate net leaf CO_2 assimilation (Von Caemmerer 2000, Sharkey et al. 2007).

Earth system models typically use either a subset or all three of these rate-limiting reactions to parameterize photosynthesis. This is primarily done by assigning a value of $V_{c,max}$ to each plant functional type (PFT) and adjusting $V_{c,max}$ based on a few leaf or canopy conditions, such as leaf nitrogen and leaf temperature (Oleson et al. 2013, Kim et al. 2015). Reviews of field studies demonstrate that the effects of leaf temperature on $V_{c,max}$ and J_{max} in seedlings can be somewhat generalized (Leuning 2002, Medlyn et al. 2002) and that PFTs have different $V_{c,max}$ values. For example, $V_{c,max}$ and J_{max} are higher in deciduous tree species (e.g., oaks and maples)

than in conifers (e.g. pines and spruces) (Wullschleger 1993). However, $V_{c,max}$ in deciduous seedlings ranges from 11-119 μmol m^{-2} s^{-1} and J_{max} ranges from 29-237 μmol m^{-2} s^{-1}, with leaf temperature only accounting for a portion of the variation in these values (Wullschleger 1993). Recent analyses using plant traits or environmental conditions to estimate $V_{c,max}$ also show that $V_{c,max}$ varies widely within a biome or PFT (Kattge et al. 2009, Verheijen et al. 2013, Ali et al. 2015). This suggests that parameterizing photosynthesis by PFT may exclude the impacts of species variations and distributions of light and leaf nitrogen in plant canopies (Ellsworth and Reich 1993, Canham et al. 1994, Frelich and Reich 1995) on canopy-level photosynthetic capacity.

Although there are environmental and ecological variations within forest canopies, field studies of adult trees lead to no consensus on whether $V_{c,max}$, J_{max}, and *TPU* at a leaf temperature of 25°C differ among species that are traditionally grouped into the same PFT. For example, $V_{c,max}$ and J_{max} do not differ between upper-canopy sun leaves of narrow-leafed ash (*Fraxinus angustifolia)* and English oak (*Quercus robur)* in a sub-Mediterranean forest plantation in Italy (Grassi et al. 2005). However, in a temperate, deciduous forest in the United States (Walker Branch, Tennessee), $V_{c,max}$ was higher in white oak (*Q. alba*) and chestnut oak (*Q. prinus*) than in sugar maple (*Acer saccharum)* and red maple (*A. rubrum)* (Wilson et al. 2000). Similarly, $V_{c,max}$ and J_{max} differed among five species sampled in a temperate, deciduous forest (Swiss Canopy Crane facility, Switzerland) undergoing CO_2 enrichment (Bader et al. 2010). Other forest sites also show species-specific responses in the rate-limiting reactions of photosynthesis. For example, in another temperate, deciduous forest (Harvard Forest, Massachusetts, United States), $V_{c,max}$ was higher in red oak (*Q. rubra)* than in paper birch (*Betula papyrifera*), but J_{max} did not differ between the two species, resulting in species-specific J_{max}:$V_{c,max}$ ratios (Dillen et al. 2012). These *in situ* measurements from multiple species of mature trees in the same forest are limited, which may contribute to the difficulty in generalizing photosynthetic capacity by species.

Leaf photosynthetic capacity in canopies also tends to exhibit vertical gradients that follow canopy environmental conditions. For example, leaves exposed to more light have higher $V_{c,max}$, J_{max}, and *TPU* than leaves with less light in several forests, including a Mediterranean evergreen oak woodland, a tropical rainforest, and temperate forests with different dominant species (Meir et al. 2002, Vaz et al. 2010). Previous studies also demonstrate that leaf nitrogen correlates with differences in $V_{c,max}$ and J_{max} between sun and shade leaves of European beech

(*Fagus sylvatica*), oaks, and maples (Harley and Baldocchi 1995, Wilson et al. 2000, Montpied et al. 2009, Cano et al. 2013). In addition, both species and canopy position influenced $V_{c,max}$ and J_{max} in red oak (*Q. rubra*), chestnut oak (*Q. prinus*), and red maple (*A. rubrum*) (Turnbull et al. 2002), while there were no differences in $V_{c,max}$ and J_{max} between sun and shade leaves in two of the five species sampled in a deciduous forest in Thuringia, Germany (Legner et al. 2014). Although most studies show consistent declines in $V_{c,max}$ and J_{max} from the top to the bottom of the canopy, less is known about the interactive effects that species and leaf environment have on $V_{c,max}$, J_{max}, and *TPU*.

Although a number of field studies have examined differences in $V_{c,max}$, J_{max}, and *TPU* among species or between sun and shade leaves, few have linked the combined effects of these variables to leaf nitrogen and leaf temperature (which simultaneously influence rates of photosynthesis) in mature trees of dominant, upper-canopy species in the same location. To examine how photosynthetic capacity varies within a forest canopy, we ask: (1) how do $V_{c,max}$, J, and *TPU* vary among species traditionally grouped into the same PFT, (2) how do these rates vary with leaf light environment (i.e., between sun and shade leaves), and (3) do the effects of leaf nitrogen and leaf temperature differ among species and between sun and shade leaves in the same forest canopy? In this study, we report values of J at light levels for saturating assimilation rates, as opposed to J_{max}, as is commonly reported. This practice is recommended by Buckley and Diaz-Espejo (2015) because saturating light is not the only condition that maximizes photosynthesis and because J at saturating light levels is often lower than actual J_{max} values.

We addressed our questions by making *in situ* net photosynthesis measurements on mature trees in a forest that is representative of the Great Lakes region. Most synthesis papers on the rates that biochemically limit photosynthesis rely heavily on studies of seedlings and saplings (Wullschleger 1993, Medlyn et al. 2002, Kattge et al. 2009). Our study adds to current understanding of photosynthetic capacity by providing measurements from an age cohort of trees that dominates the canopy and constitutes the majority of aboveground ecosystem productivity (Gough et al. 2013, Stuart-Haëntjens et al. 2015). In addition, sampling sun and shade leaves across a range of leaf temperatures on early and mid-successional tree species that are typically grouped into the same PFT allows us to test assumptions about model representations of forest photosynthesis.

We test which quantitative relationships among ecological and environmental conditions best explain variations in $V_{c,max}$, J, and TPU by evaluating contrasting model equations that isolate the influences of these conditions on leaf photosynthetic capacity. Our sampling and analysis methods improve understanding of forest carbon cycling in two important ways. First, modelers can use our data to evaluate and develop improved parameterizations of photosynthesis (Dietze 2014, Rogers et al. 2014) that capture the variation in photosynthetic capacity observed within a PFT (Verheijen et al. 2013). Second, by identifying differences in photosynthetic limitations within a forest canopy, we show how variations in leaf-level processes may control land-atmosphere CO_2 fluxes as species composition or canopy structure change due to natural processes or management practices.

4.2. Methods

4.2.1 Site Location

Our study site is in an approximately 90-year-old, temperate, mixed-broadleaf deciduous forest located at the University of Michigan Biological Station in northern, lower Michigan (45.55984°N, 84.71382°W). The average canopy height is 22 m and the mean leaf area index (LAI) is 3.5 (Gough et al. 2013). The upper canopy is composed of early successional bigtooth aspen (*Populus grandidentata*), trembling aspen (*P. tremuloides*), and paper birch, and to a lesser extent, contains mid-successional red maple and red oak. White pine (*Pinus strobus*) and American beech (*F. grandifolia*) are also of increasing abundance in the lower- to mid-canopy. Soils in this area are well drained, coarse-textured, Haplorthods of the Rubicon, Blue Lake, or Cheboygan series (Nave et al. 2011). The mean annual temperature at this site is 5.5°C (1942-2003) and the mean annual precipitation is 817 mm (Nave et al. 2011).

4.2.2 Tree Selection and Sampling

To estimate how $V_{c,max}$, J, and TPU vary in early successional and mid-successional tree species, we sampled three mature, canopy-dominant individuals each of bigtooth aspen, red maple, and red oak. The number of individuals sampled was limited by accessibility to branches from a canopy access vehicle (JLG M600JP™). Diameter-at-breast height (DBH) of individuals ranged from 19.2 to 44.6 cm.

For red maple and red oak, we sampled upper-canopy sun leaves (high light environment) and lower-canopy shade leaves (lower light environment). For bigtooth aspen, we only sampled sun leaves because bigtooth aspens have fairly uniform, bulbous crowns with few, if any, shade leaves. Sun-exposed branches of sampled individuals were located 12.0 to 17.4 m above the ground and shaded branches were 6.2 to 12.6 m above the ground.

4.2.3 Gas exchange measurements

We measured net photosynthesis across a range of CO_2 concentrations, also known as net assimilation versus intercellular CO_2 response curves (A/C_i curves), using a LI-COR 6400 portable photosynthesis system (LI-COR, Inc., Lincoln, NE, USA) fitted with a red/blue light source (6400-02B Red/Blue LED Light Source, LI-COR, Inc.). We sampled trees from 12 July to 16 August 2013 and from 9:00 to 14:30 EDT to avoid measurements during afternoon stomatal closure.

Before beginning an A/C_i curve, we acclimated each leaf in the cuvette at 400 ppm CO_2. We then increased CO_2 and recorded assimilation at stepwise decreases of CO_2 at the following concentrations: 2000, 1800, 1500, 1200, 800, 600, 400, 325, 250, 175, 100, and 50 ppm, similar to methods in Dungan et al. (2003) and Dreyer et al. (2001). Before each measurement, leaves acclimated to a new CO_2 concentration for three to five minutes. A full response curve took approximately one hour to complete. Each curve was measured at a photosynthetically active radiation (PAR) level of 2000 μmol m^{-2} s^{-1} for sun leaves and 1500 μmol m^{-2} s^{-1} for shade leaves. These values were selected based on light response curves previously collected at this site and represent light levels for saturating levels of leaf assimilation. We also maintained the sample relative humidity at 45 to 70% for optimal stomatal conductance.

We measured A/C_i curves at constant leaf temperature and each curve was measured at a different average leaf temperature that spanned: 23.0-29.5°C for red maple sun leaves (n=7), 24.0-29.8°C for red maple shade leaves (n=6), 24.8-30.1°C for red oak sun leaves (n=8), 22.9-29.8°C for red oak shade leaves (n=8), and 23.0-32.1°C for bigtooth aspen (n=7). The standard deviation of leaf temperature during an A/C_i curve ranged from 0.06-0.75°C. We controlled leaf temperature in the cuvette using the LI-COR 6400 temperature control feature and a reflective covering that allowed us to control how much sunlight could warm the outside of the leaf chamber during the measurement period.

4.2.4 Leaf Properties

After completing each curve, we collected the sampled leaf and measured leaf area, dry mass, and nitrogen (N) content. We measured the area of leaves using a LI-COR LI-3100 Area Meter and dried them at 60°C. Both leaf area and dry mass were measured without the petiole. To obtain N content, we ground samples using a ball mill and analyzed samples with a Costech Analytical CHN analyzer (Costech International, Valencia, California, USA).

4.2.5 A/C_i Curve Analysis

We derived $V_{c,max}$, J, and TPU using the method described in Sharkey et al. (2007). We examined each curve and assigned points below 20 Pa as Rubisco-limited and points above 30 Pa as RuBP regeneration-limited. Points between 20 to 30 Pa were assigned as either Rubisco- or RuBP-limited so the model would return the smallest sum of squares. Although not all leaves experience TPU limitation at high CO_2 concentrations (Harley et al. 1992), we estimated a minimum value of TPU by assigning the highest assimilation rate and any subsequent measurements at higher CO_2 concentrations as TPU-limited (Sharkey 2015). We saw evidence for TPU limitation in data from bigtooth aspen and red oak, but not in red maples. To account for curves with a decline in assimilation at high chloroplast CO_2 concentrations, we modified the method to allow for the lack of glycerate re-entry into the Calvin-Benson cycle Harley and Sharkey (1991) by using the equation:

$$A = TPU - R_d + \Theta v_O \quad (6)$$

where R_d is daytime respiration, Θ is the proportion of carbon that leaves the photo-respiratory cycle as serine or glycine, and v_O is the velocity of oxygenation. This allowed us to more accurately fit the TPU-limited points. We used the average leaf temperature during the measurement period for the curve as the input for leaf temperature, adjusted the atmospheric pressure to 91 kPa, and constrained calculations of mesophyll resistance to be between 0.5 and 2.0 μmol m^{-2} s^{-1} Pa^{-1}.

4.2.6 Data Analysis

We tested our hypotheses about how environmental and ecological characteristics influence rates of $V_{c,max}$, J, and TPU using maximum likelihood estimation and model selection techniques, as described below. We used maximum likelihood and model selection, rather than

an analysis of covariance, to fit and analyze non-linear models that reflect how variations in $V_{c,max}$, J, and TPU are often represented in photosynthesis models (De Pury and Farquhar 1997, Bernacchi et al. 2001). The key to maximum likelihood estimation and model selection is the development of contrasting equations (i.e., models) that isolate the influence of a factor on the dependent variable. For example, we can compare a model with one parameter relating nitrogen per leaf area (N_{area}) to $V_{c,max}$ to another that does the same, but also includes a unique parameter for each species. If the model with a unique parameter for each species is identified as the most parsimonious model, despite the additional parameters, then this indicates that species identity, in addition to species differences in N_{area}, is important for explaining patterns in $V_{c,max}$.

For $V_{c,max}$, we developed a set of 20 models that included one or more of the following variables in each equation: leaf temperature, N_{area}, leaf light environment (i.e., sun and shade leaves), and species identity (see Appendix C, Table C1]). For J and TPU, we used the same 20 models, but added two models that tested how well $V_{c,max}$ can estimate J and TPU, for a total of 22 models (see Appendix C, Tables C2 and C3). Each set of models for $V_{c,max}$, J, and TPU included equations that tested whether leaf temperature responses vary among species or between sun and shade leaves. We incorporated the effect of leaf temperature on $V_{c,max}$, J, and TPU into our models as an exponential relationship represented by a Q_{10} coefficient, which is the ratio between the reaction rates at two temperatures that are 10°C apart (Tjoelker et al. 2001). We calculated the Q_{10} coefficient with a base rate at 25°C because it is a leaf temperature commonly used in model parameterizations (Farquhar et al. 1980). Because photosynthesis can decrease at high leaf temperatures due to enzyme denaturation (Sage and Kubien 2007), we separately tested a temperature function where $V_{c,max}$, J, and TPU increased with temperature and then decreased after an optimum temperature. However, this functional form received less support than the Q_{10} temperature response function based on the model selection criteria described below. Thus, we only present results using the more parsimonious Q_{10} function.

For each model, we solved for the maximum likelihood estimate of each parameter using simulated annealing, which is an algorithm that searches for an approximation to the global optimum in a large solution space (Kirkpatrick 1984). Estimation was done using R version 3.1.1 (R Core Team 2014) and the R maximum likelihood package (Murphy 2014). For each model, we ran the simulated annealing process with 20,000 iterations and assumed a normal probability density function (PDF). We tested the assumption that residuals followed a normal

PDF using the Shapiro-Wilk test. Residuals for $V_{c,max}$ and J were normally distributed ($p > 0.05$), but the distribution of residuals for TPU did not have an obviously normal distribution ($p = 0.03$). We explored other continuous PDFs, including gamma, exponential, log-normal, and a normal distribution with a standard deviation that increases as a power function of the mean. Compared to these alternate PDFs, the normal distribution had the strongest support. Therefore, we present the TPU analysis using the normally distributed model uncertainty. In addition, the upper and lower support limits, or two-unit support interval, is calculated for each parameter and is analogous to the 95% confidence interval (CI) (Murphy 2014). The support interval is calculated as the range of values for each parameter that result in a two-unit or less reduction in the likelihood when all other parameters are held at their maximum likelihood estimated value.

Finally, we selected the most parsimonious model for explaining patterns in our data for $V_{c,max}$, J, and TPU using the Akaike Information Criterion corrected for small samples (AIC_c), which has been shown to be appropriate for model selection when many hypothesized models are evaluated (Aho et al. 2014). We considered models with a difference in AIC_c score < 2 units to be equally as likely (Burnham and Anderson 2002).

4.2.7 Derivation of J_{max}

Our study focused on the ecological and environmental controls on rates of electron transport at saturating light levels (J), and not on the maximum rate of electron transport (J_{max}). However, to compare J to J_{max}, we derived J_{max} from light response curves.

Light response curves were available for sun and shade leaves of the same individuals we used to measure A/C_i curves (n=6 for each group), but only during the year after we collected the A/C_i curves used in this study. For each leaf, net photosynthesis was measured at the following light levels: 10, 25, 50, 100, 250, 500, 750, 1000, and 1500 μmol m^{-2} s^{-1}, with an additional measurement at 2000 μmol m^{-2} s^{-1} for sun leaves. Measurements were taken at a CO_2 concentration of 400 ppm and the sample relative humidity was kept between 46% and 72%. Before a measurement was recorded, the leaf acclimated to a new light level for two to three minutes.

We used these light-reponse curves to derive J_{max} with the method described in Sharkey (2015) that uses the equations from Buckley and Diaz-Espejo (2015) to fit the initial slope of J versus light, the convexity parameter of a light response curve, and J_{max}. We did not use the

highest light levels in the analysis when there was evidence that something other than electron transport became limiting at high light. We used the average leaf temperature of the light response curve for the leaf temperature, 91 kPa for the atmospheric pressure, 21 kPa for the oxygen level, and 0.5 μmol m^{-2} s^{-1} as the day respiration as suggested by Sharkey (2015). For the stomatal conductance, we used 10% of the highest assimilation rate of the light response curve, as suggested by Caemmerer and Evans (1991).

4.3. Results

4.3.1 Photosynthesis measurements and parameter derivations

For red maple, red oak, and bigtooth aspen, photosynthesis increased with CO_2 and either plateaued or decreased at the highest CO_2 concentrations (Figure 4.1). Overall, bigtooth aspen had higher rates of net photosynthesis at the higher CO_2 concentrations than red maple or red oak. Some of the variation among A/C_i curves could result from differences in leaf temperature, leaf nitrogen, physiological variation among leaves and individual trees, or the interactions among these variables.

The A/C_i curves in Figure 4.1 were then used to derive values of V_{cmax}, J, and TPU using the Sharkey et al. (2007) method (n=36 curves). Across a leaf temperature range of 22.9 to 32.1°C and N_{area} range of 0.66 to 2.23 g m^{-2}, V_{cmax} ranged from 44 to 327 μmol m^{-2} s^{-1} (Figure 4.2), J ranged from 65 to 235 μmol m^{-2} s^{-1} (Figure 4.3), and TPU ranged from 3.2 to 11.7 μmol m^{-2} s^{-1} (Figure 4.4).

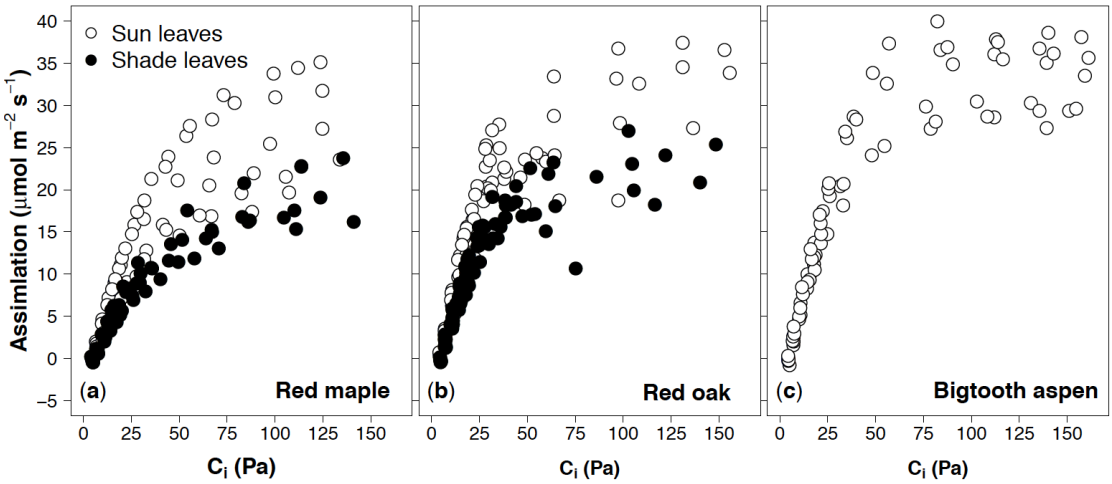

Figure 4.1: The response of assimilation (i.e., net photosynthesis) to increases in intercellular CO_2 (C_i) in sun and shade leaves. A/C_i curves were taken *in situ* on adult, canopy-dominant individuals of a) red maple, b) red oak, and c) bigtooth aspen in a temperate, deciduous forest. Points represent data used to derive values of the maximum rate of carboxylation ($V_{c,max}$), rate of electron transport (J), and rate of triose phosphate utilization (TPU).

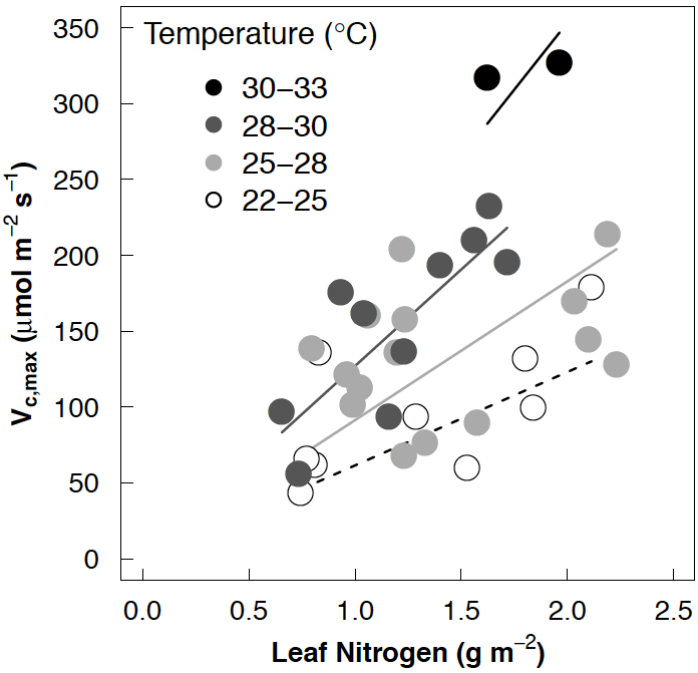

Figure 4.2: Derived values of the maximum rate of carboxylation ($V_{c,max}$) from A/C_i curves taken *in situ* on adult, canopy-dominant red maple, red oak, and bigtooth aspen trees. Points are separated according to variables (N_{area}, leaf temperature) included in the model with the most support for explaining patterns in $V_{c,max}$ (Model 4, Table 4.1), as indicated by the smallest Akaike information criterion adjusted for small sample sizes (AIC_c). Lines represent values of $V_{c,max}$ estimated from Model 4 using the midpoint of each leaf temperature range shown in the plot.

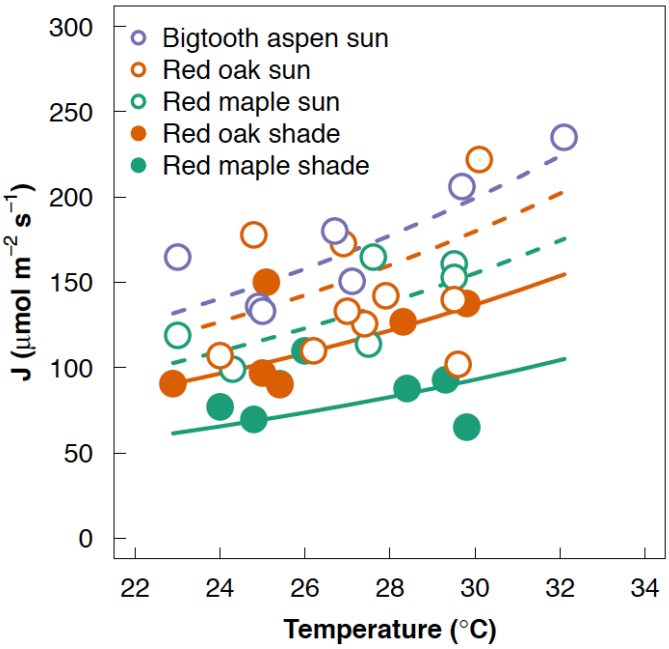

Figure 4.3: Derived values of the rate of electron transport (*J*) from A/C_i curves taken *in situ* on adult, canopy-dominant red maple, red oak, and bigtooth aspen trees. Points are separated according to variables (species, leaf light environment, leaf temperature) included in the model with the most support for explaining patterns in *J* (Model 11, Table 4.2), as indicated by the smallest Akaike information criterion adjusted for small sample sizes (AIC_c). Lines represent values of *J* estimated from Model 11.

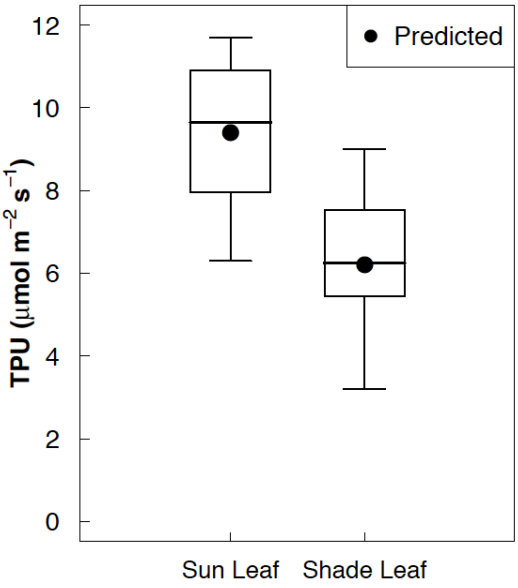

Figure 4.4: Boxplot of derived values for triose phosphate utilization (*TPU*) from A/C_i curves taken *in situ* on adult, canopy-dominant red maple, red oak, and bigtooth aspen trees. Points are separated according to the variable (leaf light environment) included in one of the two models with the most support for explaining patterns in *TPU* (Model 5, Table 4.3), as indicated by the smallest Akaike information criterion adjusted for small sample sizes (AIC_c). The box shows the 25th and 75th percentiles and the median. The whiskers outline the minimum and maximum values for *TPU* in sun and shade leaves. The dot represents *TPU* estimated for sun and shade leaves using Model 5.

4.3.2 Environmental and Ecological Influences on V_{cmax}

We compared 20 models to test for the influence of species, leaf light environment, leaf temperature, and N_{area} on $V_{c,max}$. Based on the AIC_c scores of the models we tested, the model that best explained $V_{c,max}$ included a Q_{10} leaf temperature response and N_{area} (Model 4 in Table 4.1; $R^2 = 0.64$). Increases in both leaf temperature and N_{area} led to increases in estimates of $V_{c,max}$ (Figure 4.2).

Using the mean N_{area} (1.35 g m^{-2}) of our sample population in our most parsimonious model, $V_{c,max}$ at a leaf temperature of 25°C was estimated to be 101.1 μmol m^{-2} s^{-1}. Results from our model selection also indicate that models explicitly incorporating differences among species or between sun and shade leaves that occur in addition to variations in N_{area} (e.g., Models 7, 10, and 12 in Table 4.1) do not better explain patterns in $V_{c,max}$. This does not imply that differences in $V_{c,max}$ do not exist among species or between sun and shade leaves. Instead, this suggests that variations in $V_{c,max}$ among species and between sun and shade leaves can be predicted by N_{area}

and that additional information on species or leaf light environment beyond N_{area} may not be needed for estimating $V_{c,max}$.

In addition, we found that including a separate leaf temperature response for each species or for sun and shade leaves did not improve $V_{c,max}$ predictions. This suggests that using the same leaf temperature function for the three species we sampled and for sun and shade leaves is sufficient for estimating $V_{c,max}$ at our field site. The Q_{10} coefficient for the best model explaining patterns in $V_{c,max}$, along with other parameter estimates for all the models we tested, can be found in Appendix C Table C1.

Table 4.1: Comparison of the 10 alternative models explaining patterns in the maximum rate of carboxylation ($V_{c,max}$) with the smallest Akaike information criterion adjusted for small sample sizes (AIC_c).

Model No.	Model Equation[a]	No. of Parameters	[b]ΔAIC_c	[c]R^2	[d]m
4	$V_{c,max} = V \times Q_{10}^{(T-25)/10} \times N_{area}$	3	0.00	0.64	0.82
10	$V_{c,max} = V[spp] \times Q_{10}^{(T-25)/10} \times N_{area}$	5	2.09	0.68	0.81
7	$V_{c,max} = V[loc] \times Q_{10}^{(T-25)/10} \times N_{area}$	4	2.14	0.65	0.78
20	$V_{c,max} = V \times Q_{10}[loc]^{(T-25)/10} \times N_{area}$	4	2.61	0.64	0.80
6	$V_{c,max} = V[loc] \times Q_{10}^{(T-25)/10}$	4	3.13	0.64	0.66
16	$V_{c,max} = V \times Q_{10}[spp]^{(T-25)/10} \times N_{area}$	5	4.62	0.65	0.82
19	$V_{c,max} = V \times Q_{10}[loc]^{(T-25)/10}$	4	5.18	0.62	0.63
11	$V_{c,max} = V[spp\_loc] \times Q_{10}^{(T-25)/10}$	7	5.44	0.70	0.69
12	$V_{c,max} = V[spp\_loc] \times Q_{10}^{(T-25)/10} \times N_{area}$	7	6.76	0.69	0.75
17	$V_{c,max} = V \times Q_{10}[spp\_loc]^{(T-25)/10}$	7	10.52	0.65	0.71

[a] "V" is the coefficient for each model equation. Model equations containing "spp" estimate parameters for each species, equations with "loc" estimate parameters for sun and shade leaves, and equations with "spp_loc" estimate parameters for species-specific canopy locations (i.e., red maple sun leaves, red maple shade leaves, bigtooth aspen sun leaves, red oak sun leaves, and red oak shade leaves). Q_{10} is the ratio between the reaction rates at two temperatures that are 10°C apart. N_{area} is leaf nitrogen per area in mg cm^{-2}.

[b] ΔAIC_c is the difference between the AIC_c score of a model and the one with the lowest AIC_c. ΔAIC_c scores for all 20 models are included in the Appendix C, Table C1.

[c] R^2 is the goodness-of-fit of the model.

[d] m is the slope of the linear relationship between the predicted and observed values for $V_{c,max}$.

4.3.3 Environmental and Ecological Influences on J

The model that best explained patterns in *J* differed from the best model for predicting $V_{c,max}$. This model, along with the most parsimonious model for $V_{c,max}$, included a Q_{10} temperature function. However, unlike the model that best explained the variation in $V_{c,max}$, the most parsimonious model for *J* includes separate species-specific coefficients for sun and shade leaves (Model 11 in Table 4.2; $R^2 = 0.72$). In addition, this model had more support than a model that estimated *J* as a proportion of $V_{c,max}$. Therefore, values of *J* are best explained by species identity and canopy location traits that are separate from the traits that control variation in $V_{c,max}$.

Overall, sun leaves had higher values of *J* than did shade leaves (Figure 4.3). Bigtooth aspen had the highest values of *J*, followed by red oak, and then by red maple (Figure 4.3). Using our best model for explaining patterns in our data for *J*, we estimated *J* at a leaf temperature of 25°C to be 148.9 μmol m^{-2} s^{-1} for bigtooth aspen, 134.4 μmol m^{-2} s^{-1} for red oak sun leaves, 116.0 μmol m^{-2} s^{-1} for red maple sun leaves, 102.2 μmol m^{-2} s^{-1} for red oak shade leaves, and 69.4 μmol m^{-2} s^{-1} for red maple shade leaves. The inclusion of separate coefficients for species and sun and shade leaves in the most parsimonious model for predicting *J* suggests that variations in N_{area} are insufficient for explaining the effect of species and leaf light environment (i.e., sun v. shade leaves) on this particular limitation to photosynthesis.

Similar to results for $V_{c,max}$, estimates of *J* were not improved with separate leaf temperature responses for each species or for sun and shade leaves. Estimates for the Q_{10} coefficient for the best model explaining patterns in *J*, along with other parameter estimates for all the models we tested, can be found in Appendix C, Table C2.

Table 4.2: Comparison of the 10 alternative models explaining patterns in the rate of electron transport (*J*) with the smallest Akaike information criterion adjusted for small sample sizes (AIC_c).

Model No.	Model Equation[a]	No. of Parameters	[b]ΔAIC_c	[c]R^2	[d]*m*
11	$J = C_J[spp\_loc] \times Q_{10}^{(T-25)/10}$	7	0.00	0.72	0.74
22	$J = C_J \times V_{c,max}$	2	6.45	0.50	0.86
6	$J = C_J[loc] \times Q_{10}^{(T-25)/10}$	4	6.84	0.56	0.57
19	$J = C_J \times Q_{10}[loc]^{(T-25)/10}$	4	13.85	0.47	0.47
10	$J = C_J[spp] \times Q_{10}^{(T-25)/10} \times N_{area}$	5	13.90	0.51	0.94
12	$J = C_J[spp\_loc] \times Q_{10}^{(T-25)/10} \times N_{area}$	7	14.34	0.58	0.87
9	$J = C_J[spp] \times Q_{10}^{(T-25)/10}$	5	15.21	0.49	0.51
13	$J = C_J[spp\_loc]$	6	15.76	0.52	0.52
5	$J = C_J[loc]$	3	17.83	0.36	0.36
17	$J = C_J \times Q_{10}[spp\_loc]^{(T-25)/10}$	7	18.09	0.53	0.59

[a] "C_J" is the coefficient for each model equation. Model equations containing "spp" estimate parameters for each species, equations with "loc" estimate parameters for sun and shade leaves, and equations with "spp_loc" estimate parameters for species-specific canopy locations (i.e., red maple sun leaves, red maple shade leaves, bigtooth aspen sun leaves, red oak sun leaves, and red oak shade leaves). Q_{10} is the ratio between the reaction rates at two temperatures that are 10°C apart. N_{area} is leaf nitrogen per area in mg cm^{-2}. $V_{c,max}$ is the maximum rate of carboxylation as derived from the A/C_i curves shown in Figure 4.1.

[b] ΔAIC_c is the difference between the AIC_c score of a model and the one with the lowest AIC_c. ΔAIC_c scores for all 22 models are included in Appendix C, Table C2.

[c] R^2 is the goodness-of-fit of the model.

[d] *m* is the slope of the linear relationship between the predicted and observed values for *J*.

4.3.4 Environmental and Ecological Influences on TPU

Our model selection analysis provided equivalent support ($\Delta AIC_c < 2$) for two models explaining patterns in *TPU*, both of which differ from the best models used to explain variations in $V_{c,max}$ and *J*. The first model includes separate coefficients for sun and shade leaves that take into the account the influence of leaf light environment on *TPU* (Model 5 in Table 4.3, R^2 = 0.44). The second model also includes separate coefficients for sun and shade leaves, but includes a Q_{10} temperature function (Model 6 in Table 4.3, R^2 = 0.46).

In both models, *TPU* values were higher in sun leaves than in shade leaves. Model 5 estimates *TPU* in sun leaves as 9.4 μmol m^{-2} s^{-1} (95% CI 8.7-10.1 μmol m^{-2} s^{-1}) and in shade leaves as 6.2 μmol m^{-2} s^{-1} (95% CI 5.3-7.1 μmol m^{-2} s^{-1}). Using Model 6, estimates of *TPU* are 9.1 μmol m^{-2} s^{-1} in sun leaves and 6.0 μmol m^{-2} s^{-1} in shade leaves at a leaf temperature of 25°C.

These results suggest that differences between sun and shade leaves, in addition to the vertical canopy gradient in N_{area}, influence values of *TPU*.

Similar to results for $V_{c,max}$ and *J*, the inclusion of separate leaf temperature response functions for each species or for sun and shade leaves did not improve explanation of patterns in *TPU* of the leaves we sampled. Additional information on the estimates for all 22 models used are included in Appendix C, Table C3.

Table 4.3: Comparison of the 10 alternative models explaining patterns in triose phosphate utilization (*TPU*) with the smallest Akaike information criterion adjusted for small sample sizes (AIC_c).

Model No.	Model Equation[a]	No. of Parameters	[b]ΔAIC_c	[c]R^2	[d]*m*
5	$TPU = C_{TPU}[loc]$	3	0.00	0.44	0.44
6	$TPU = C_{TPU}[loc] \times Q_{10}^{(T-25)/10}$	4	1.56	0.46	0.45
13	$TPU = C_{TPU}[spp\_loc]$	6	5.49	0.48	0.49
19	$TPU = C_{TPU} \times Q_{10}[loc]^{(T-25)/10}$	4	5.78	0.39	0.39
11	$TPU = C_{TPU}[spp\_loc] \times Q_{10}^{(T-25)/10}$	7	8.03	0.49	0.51
17	$TPU = C_{TPU} \times Q_{10}[spp\_loc]^{(T-25)/10}$	7	13.86	0.40	0.41
8	$TPU = C_{TPU}[spp]$	4	16.01	0.19	0.21
9	$TPU = C_{TPU}[spp] \times Q_{10}^{(T-25)/10}$	5	18.58	0.19	0.22
1	$TPU = C_{TPU}$	2	18.69	0.00	0.00
10	$TPU = C_{TPU}[spp] \times Q_{10}^{(T-25)/10} \times N_{area}$	5	20.60	0.15	0.71

[a] "C_{TPU}" is the coefficient for each model equation. Model equations containing "spp" estimate parameters for each species, equations with "loc" estimate parameters for sun and shade leaves, and equations with "spp_loc" estimate parameters for species-specific canopy locations (i.e., red maple sun leaves, red maple shade leaves, bigtooth aspen sun leaves, red oak sun leaves, and red oak shade leaves). Q_{10} is the ratio between the reaction rates at two temperatures that are 10°C apart. N_{area} is leaf nitrogen per area in mg cm^{-2}.

[b] ΔAIC_c is the difference between the AIC_c score of a model and the one with the lowest AIC_c. ΔAIC_c scores for all 22 models are included in Appendix C, Table C3.

[c] R^2 is the goodness-of-fit of the model.

[d] *m* is the slope of the linear relationship between the predicted and observed values for *TPU*.

4.3.5 Comparison of *J* and J_{max}

Although we measured A/C_i curves at saturating light levels for CO_2 assimilation, we report derivations of electron transport as values of *J* at light levels where assimilation saturates, and not as J_{max}. We report our data for electron transport in this way because a recent review

found that only 23% of 71 peer-reviewed papers provided enough detail to confirm that they did not report J as J_{max}, which can lead to underestimated values of J_{max} in Earth system models (Buckley and Diaz-Espejo 2015). To compare differences in J at saturating light levels and J_{max}, we calculated J_{max} at 25°C using methods in Sharkey (2015). To do this, we used light response curves measured on leaves from the same trees we sampled our A/Ci curves on, but taken a year after our A/Ci curves were collected (Table 4.4).

Our estimated values of J at leaf temperatures of 25°C from the most parsimonious model in our study (Table 4.2, Model 11) are lower than the values of J_{max} at 25°C that we calculated using methods in Sharkey (2015). In addition, we found that the species patterns in J and J_{max} differed. For example, among sun leaves, bigtooth aspen had the highest values for J, but the lowest values for J_{max} compared to red oak and red maple leaves. This may be because $J_{\max}$ is extrapolated from photosynthetic rates under light-limiting conditions while J is the rate when light is "saturating". This is similar to underestimating the maximum CO_2 assimilation rate when using data at low CO_2, where Rubisco activity determines the maximum rate, as opposed to using data when RuBP regeneration becomes limiting. The difference between species patterns in J and J_{max} could be due to variations in the relative capacity of different components of electron transport and their effects. Although it is not clear what causes J_{max} and J at saturating light levels to have different values, data on both J_{max} and J are useful for informing global models as long as it is clear which rate is reported (Buckley and Diaz-Espejo 2015).

Table 4.4: Rates of electron transport at 25°C using multiple estimation methods for sun and shade leaves of bigtooth aspen, red oak, and red maple.

Group of leaves	J at 25°C (μmol m^{-2} s^{-1})	J_{max} at 25°C (μmol m^{-2} s^{-1})
	MLE Model[a]	Sharkey et al. 2015[b]
Bigtooth aspen sun	149	220
Red oak sun	134	334
Red maple sun	116	398
Red oak shade	102	212
Red maple shade	69	181

[a] Derivations made using the parameters determined by maximum likelihood estimation from the most parsimonious model with $\Delta AIC_c = 0.00$ (Model 11, Table 4.2).

[b] Derivations made using methods in Sharkey (2015) with light response curves taken at the same field site one year later.

4.4. Discussion

$V_{c,max}$, J, and TPU limit rates of leaf assimilation and subsequently, canopy-level photosynthetic capacity and CO_2 uptake. We examined how these photosynthetic rate-limiting reactions vary with environmental and ecological conditions that differ vertically and horizontally within a forest canopy. This provides insight into the role of canopy heterogeneity in explaining the large ranges in photosynthetic capacity that exist within biomes or PFTs (Verheijen et al. 2013, Ali et al. 2015). To determine how photosynthetic capacity varies in a forest canopy, we derived $V_{c,max}$, J, and TPU from photosynthesis measurements taken from sun and shade leaves of mature, canopy-dominant species typically grouped into the same PFT. We then used maximum likelihood estimation and model selection techniques to test hypotheses about how leaf temperature, leaf nitrogen, species identity, and leaf light environment influence $V_{c,max}$, J, and TPU. This allowed us to identify which variables best estimate rates of photosynthetic capacity and to evaluate some methods used to parameterize photosynthesis in Earth system models.

Of the factors tested, leaf temperature and N_{area} explained most of the variation in $V_{c,max}$ within a forest canopy. The observed increase in $V_{c,max}$ across leaf temperatures from 22.9 to 32.1°C is consistent with the positive relationship that stomatal conductance and enzyme kinetics have with increasing temperatures below a certain threshold (Berry and Bjorkman 1980). In addition, the positive relationship we found between N_{area} and $V_{c,max}$ is consistent with the importance of plant-available nitrogen in photosynthesis. For example, plants allocate up to 30% of nitrogen to the synthesis and maintenance of Rubisco (Jensen 2000, Raven 2013), which is the limiting factor of leaf carboxylation rates. Previous studies have also found positive relationships between N_{area} and $V_{c,max}$ in trees from various species ranging from 0 to 30 years in age (Medlyn et al. 1999, Ripullone et al. 2003), which has led some Earth system models to adjust $V_{c,max}$ within or among PFTs based on leaf nitrogen (Oleson et al. 2013, Rogers 2014). Our results from mature, canopy-dominant trees support current model parameterizations of $V_{c,max}$ based on a leaf nitrogen gradient in the canopy.

We found that aside from leaf temperature, different biological variables were included in the models that explained the most variation in $V_{c,max}$ and J. For $V_{c,max}$, the most parsimonious model includes N_{area}, which varies with canopy height (or leaf light exposure) and species (Ellsworth and Reich 1993, Wright et al. 2004, Legner et al. 2014). However, including leaf light

environment and species in the most parsimonious model for $V_{c,max}$ does not improve the model's explanatory power, likely because species identity and canopy location co-vary with leaf nitrogen. However, the most parsimonious model for *J* did include species identity and leaf light environment, but did not include N_{area}. This suggests that differences among species and sun and shade leaves, in addition to N_{area}, are important in estimating *J*. Leaf light availability likely influences *J* because the regeneration of RuBP increases with the amount of light available for electron transport (Sharkey et al. 2007). Because light decreases from the top of the canopy to bottom, we expect *J* to be higher in sun leaves than shade leaves (Niinemets et al. 2015). We also hypothesize that species identity influences *J* if canopy allocation of leaf nitrogen per area in response to stress (e.g, wind, light) (Hollinger 1996, Kull and Niinemets 1998) or if leaf arrangement of chlorophyll, which affects light absorbance (Brugnoli and Björkman 1992), is species-specific. Our results provide ecosystem-specific data consistent with a recent global-level study that demonstrates that leaf nitrogen explains half as much of the variation in J_{max} as it does in $V_{c,max}$ (Ali et al. 2015).

Our results also show that $V_{c,max}$ increases faster than *J* does across a 10°C leaf temperature range (Q_{10} coefficient for $V_{c,max}$ = 3.7, 95% CI 3.0-4.5 and for *J* = 1.8, 95% CI 1.6-2.1, Appendix C, Tables C1 and C2). Because *J* and J_{max} are mutually dependent (Farquhar et al. 1980), factors influencing one rate are likely to influence the other. Therefore, our results on the response of *J* and $V_{c,max}$ to temperature support previous findings that J_{max}:$V_{c,max}$ at a leaf temperature of 25°C decreases with higher growth temperature (Kattge and Knorr 2007). Our results are also consistent with a greater sensitivity of $V_{c,max}$ than J_{max} to leaf temperature in Monterey pine (*Pinus radiata*) seedlings and Balsam poplar (*Populus balsamifera*) stem cuttings grown in pots (Walcroft et al. 1997, Silim et al. 2010). However, our model selection results (Model 11 v. Model 22 in Table 4.2) contradict current Earth system model estimates of J_{max} from $V_{c,max}$. Because we found that species traits, in addition to the ones influencing $V_{c,max}$ (i.e., leaf nitrogen), and leaf light environment best explained *J*, estimating J_{max} from $V_{c,max}$ might not accurately capture variations in J_{max} that occur in plant canopies. Although the J_{max}:$V_{c,max}$ ratios used in Earth system models are supported by meta-analyses of several plant species (Wullschleger 1993, Medlyn et al. 2002, Rogers et al. 2014), there are also field studies showing that this ratio differs between mature trees of red oak and paper birch (Dillen et al. 2012). Identifying which leaf traits, beyond those that we examined in this study, are different across

species may help identify potential improvements to the parameterizations of J and J_{max} in Earth system models.

Our analysis also shows that the variation in the minimum estimates of *TPU* in all three species was best explained by leaf light environment alone, with leaf temperature only minimally increasing model predictive power. The small response of *TPU* to leaf temperature (Q_{10} coefficient = 1.2, 95% CI 0.9-1.4, Appendix C, Table C3) is similar to results by Bauerle et al. (2007), who showed that *TPU* in red maple remained relatively unchanged to leaf temperature alterations. Vertical changes in light distribution may explain why *TPU* is higher for leaves at the top of the canopy than near the bottom. *TPU* limitation can also occur under extreme conditions, including long exposure periods to high light levels that are more commonly experienced by sun leaves (Sharkey 1985). Vertical gradients of water stress within forest canopies can affect stomatal conductance and drive differences observed between sun and shade leaves (Williams et al. 1996).

Similar to results for J, the model that estimated *TPU* from $V_{c,max}$ did not have the lowest AIC_c score. As such, estimating *TPU* from $V_{c,max}$ may not accurately capture photosynthetic capacity in plant canopies (Model 5 v. Model 22 in Appendix C, Table C3). We suggest that future modeling efforts compare canopy CO_2 uptake between simulations where J and *TPU* are calculated from $V_{c,max}$ and where they are calculated independently from $V_{c,max}$. This would identify whether incorporating additional details about species and leaf light environment in model parameterizations of photosynthesis improve calculations of canopy CO_2 uptake.

Our results highlight how changes in leaf-level photosynthesis could scale to the canopy-level and alter forest CO_2 uptake. Observations from a succession experiment near our field site indicates that the canopy becomes more structurally complex as red oak and red maple assume greater canopy dominance after aspen are removed (Gough et al. 2013). This shift from aspen to red oak and red maple implies that canopy-level J may decrease. Canopy-level J and *TPU* may also change if a shift in the distribution of leaves in the canopy alters light distribution and thus, the proportion of sun to shade leaves. A study by Meir et al. (2002) showed that light strongly correlates with $V_{c,max}$ in five different forest canopies spanning multiple biomes. However, changes in J and *TPU* would only affect forest CO_2 uptake and Earth system model estimates of CO_2 uptake if J and *TPU* are more limiting to photosynthesis than $V_{c,max}$ (Oleson et al. 2013, Rogers et al. 2014). Thus, model simulations could quantify how often changes in J and *TPU*

among species and between sun and shade leaves alter total canopy CO_2 uptake. In addition, the implications of our results on canopy CO_2 uptake should be used with the understanding that we only examined two later-successional species. The addition of multiple species with different crown architectures, such as European beech (*F. sylvatica*) and white pine, could increase light absorption in the canopy and increase forest productivity (Ishii and Asano 2010).

There are some limitations to this study that should be considered when using our results to understand how canopy CO_2 uptake may change on longer temporal or larger spatial scales and to inform model parameterizations of photosynthesis. First, our derived values of $V_{c,max}$, J, and TPU represent the effect of instantaneous changes in leaf temperature at one time during the growing season. Long-term estimates of canopy CO_2 uptake should consider how biochemical limitations to photosynthesis change across growing seasons (Grassi et al. 2005, Hikosaka et al. 2007, Dillen et al. 2012) and as plants acclimate to warmer growing conditions (Hikosaka et al. 2006, Bauerle et al. 2007, Smith and Dukes 2013). Model simulations with ED2, for example, show that for an oak-dominated forest, including seasonal variation in $V_{c,max}$ leads to a difference in gross primary productivity of 0.05 kg C m^{-2} $month^{-1}$ (Medvigy et al. 2013). Second, we were limited in how many leaves we could sample (n=36 across species, leaf light environment, and individuals) because of limited access to adult, canopy-dominant trees and because we did not want seasonal variation in photosynthetic capacity to influence our results. However, even with our sample size, we were able to identify drivers of photosynthetic capacity with respect to species differences and variation in leaf light environments. The patterns and model analyses here should be of value in scaling from leaf to canopy levels. Third, effects of increasing atmospheric CO_2 concentrations should be addressed in future studies, because studies show either no effect or a change in $V_{c,max}$ or J_{max} in canopy-dominant deciduous trees grown under elevated CO_2 (Ellsworth et al. 2004, Liberloo et al. 2007, Bader et al. 2010). Fourth, changes in plant resource use should be considered because plants can change nitrogen allocation to produce enzymes and proteins needed for photosynthesis. For example, leaves can allocate more nitrogen for chlorophyll synthesis when light levels are low (Liberloo et al. 2007). Finally, although our values for $V_{c,max}$, J, and TPU are based on field measurements in a forest canopy, they may differ if we had used another derivation method or made different assumptions about leaf physiology (Miao et al. 2009, Bernacchi et al. 2013, Sun et al. 2014). Despite these limitations, our results add *in situ* evidence to the limited amount of data that are available for understanding how

photosynthetic capacity in adult trees varies with leaf temperature, nitrogen, leaf light environment, and species identity in forest canopies.

4.5. Conclusions

Our study advances understanding of terrestrial carbon cycling from the leaf-to-canopy level in three ways. First, our *in situ* measurements from sun and shade leaves of upper-canopy trees show that forest canopy heterogeneity influences photosynthetic capacities of co-dominant species that are typically grouped into a single PFT in Earth system models. Second, our results indicate that *J* varies with species and leaf light environment and that *TPU* varies with leaf light environment. This provides insight into how leaf-level differences in physiology can scale up to change canopy-level CO_2 uptake, which will become increasingly important as climate change, land management, and ecological succession change forest canopy structure, species composition, and microclimate. Third, our data respond to climate model community requests for additional leaf-level measurements and photosynthesis response curves to scale and evaluate parameterizations of photosynthesis (Dietze 2014, Rogers et al. 2014) as plant traits are being incorporated into the development of new PFTs (Wullschleger et al. 2014, Verheijen et al. 2015). Our results also suggest testing the sensitivity of Earth system model estimates of canopy CO_2 uptake to variations in canopy species composition and leaf light environment and the separation of *J* and *TPU* calculations from $V_{c,max}$. This type of integration of field data with model development will allow us to better predict how canopy heterogeneity affects leaf-level photosynthetic capacity and scales up to drive carbon uptake across species, ecosystems, and the globe.

4.6. Acknowledgments

We would like to acknowledge a number of colleagues whose effort and time helped us complete this project. We thank Chris Vogel and Jim Le Moine for troubleshooting equipment problems, Ziru (James) Li for training on collection and analysis of A/C_i curves, Dave Karowe for providing feedback on our sampling scheme, Allison Steiner for discussions on this project and its broader implications to modeling, and Lora Murphy and Charles Canham for responding to questions about statistics. Support for JVW was provided by the University of Michigan Biological Station Research Experiences for Undergraduates Program (NSF Award # AGS-

1262634). Funding for SJC was provided in part by the Michigan Space Grant Consortium, University of Michigan Department of Ecology and Evolutionary Biology, and the University of Michigan Biological Station Marian and David Gates Graduate Student Fund. Partial salary support for TDS comes from Michigan State University AgBioResearch and for PSC from the U.S. Department of Energy's Climate and Environmental Sciences Division, Office of Science. The data used in this study will be available at the University of Michigan Biological Station Research Gateway (http://umbs.lsa.umich.edu/research/data). The programs used to derive $V_{c,max}$, J, J_{max}, and TPU are available as supplementary materials from Sharkey et al. (2007) (doi:10.1111/j.1365-3040.2007.01710.x) and Sharkey (2015) (doi:10.1111/pce.12641).

References

Aho, K., D. Derryberry, and T. Peterson. 2014. Model selection for ecologists: the worldviews of AIC and BIC. Ecology **95**:631-636.

Ali, A. A., C. Xu, A. Rogers, N. G. Mcdowell, B. E. Medlyn, R. A. Fisher, S. D. Wullschleger, P. B. Reich, J. A. Vrugt, W. L. Bauerle, L. S. Santiago, and C. J. Wilson. 2015. Global scale environmental control of plant photosynthetic capacity. Ecological Applications **25**:2349-2365.

Bader, M.-F., R. Siegwolf, and C. Körner. 2010. Sustained enhancement of photosynthesis in mature deciduous forest trees after 8 years of free air CO_2 enrichment. Planta **232**:1115-1125.

Bauerle, W. L., J. D. Bowden, and G. G. Wang. 2007. The influence of temperature on within-canopy acclimation and variation in leaf photosynthesis: spatial acclimation to microclimate gradients among climatically divergent *Acer rubrum* L. genotypes. J Exp Bot **58**:3285-3298.

Bernacchi, C. J., J. E. Bagley, S. P. Serbin, U. M. Ruiz-Vera, D. M. Rosenthal, and A. Vanloocke. 2013. Modelling C_3 photosynthesis from the chloroplast to the ecosystem. Plant Cell Environ **36**:1641-1657.

Bernacchi, C. J., E. L. Singsaas, C. Pimentel, A. R. Portis Jr, and S. P. Long. 2001. Improved temperature response functions for models of Rubisco-limited photosynthesis. Plant Cell Environ **24**:253-259.

Berry, J., and O. Bjorkman. 1980. Photosynthetic response and adaptation to temperature in higher-plants. Annual Review of Plant Physiology and Plant Molecular Biology **31**:491-543.

Brugnoli, E., and O. Björkman. 1992. Chloroplast movements in leaves: Influence on chlorophyll fluorescence and measurements of light-induced absorbance changes related to ΔpH and zeaxanthin formation. Photosynthesis Research **32**:23-35.

Buckley, T. N., and A. Diaz-Espejo. 2015. Reporting estimates of maximum potential electron transport rate. New Phytologist **205**:14-17.

Burnham, K., and D. R. Anderson. 2002. Model Selection and Multimodel Inference: A Practical Information-Theoretic Approach. 2nd edition. Springer, New York.

Caemmerer, S., and J. Evans. 1991. Determination of the average partial pressure of CO_2 in chloroplasts from leaves of several C_3 plants. Functional Plant Biology **18**:287-305.

Canham, C. D., A. C. Finzi, S. W. Pacala, and D. H. Burbank. 1994. Causes and consequences of resource heterogeneity in forests: interspecific variation in light transmission by canopy trees. Canadian Journal of Forest Research **24**:337-349.

Cano, F. J., D. Sánchez-Gómez, J. Rodríguez-Calcerrada, C. R. Warren, L. Gil, and I. Aranda. 2013. Effects of drought on mesophyll conductance and photosynthetic limitations at different tree canopy layers. Plant Cell Environ **36**:1961-1980.

De Pury, D. G. G., and G. D. Farquhar. 1997. Simple scaling of photosynthesis from leaves to canopies without the errors of big-leaf models. Plant Cell Environ **20**:537-557.

Diaz-Espejo, A., C. J. Bernacchi, G. J. Collatz, and T. D. Sharkey. 2012. Models of photosynthesis.*in* J. Flexas, F. Loreto, and H. Medrano, editors. Terrestrial Photosynthesis in a Changing Environment: A Molecular, Physiological and Ecological Approach. Cambridge University Press, Cambridge University.

Dietze, M. 2014. Gaps in knowledge and data driving uncertainty in models of photosynthesis. Photosynthesis Research **119**:3-14.
Dillen, S. Y., M. O. De Beeck, K. Hufkens, M. Buonanduci, and N. G. Phillips. 2012. Seasonal patterns of foliar reflectance in relation to photosynthetic capacity and color index in two co-occurring tree species, *Quercus rubra* and *Betula papyrifera*. Agricultural and Forest Meteorology **160**:60-68.
Dreyer, E., X. Le Roux, P. Montpied, F. A. Daudet, and F. Masson. 2001. Temperature response of leaf photosynthetic capacity in seedlings from seven temperate tree species. Tree Physiol **21**:223-232.
Dungan, R. J., D. Whitehead, and R. P. Duncan. 2003. Seasonal and temperature dependence of photosynthesis and respiration for two co-occurring broad-leaved tree species with contrasting leaf phenology. Tree Physiol **23**:561-568.
Ellsworth, D. S., and P. B. Reich. 1993. Canopy structure and vertical patterns of photosynthesis and related leaf traits in a deciduous forest. Oecologia **96**:169-178.
Ellsworth, D. S., P. B. Reich, E. S. Naumburg, G. W. Koch, M. E. Kubiske, and S. D. Smith. 2004. Photosynthesis, carboxylation and leaf nitrogen responses of 16 species to elevated pCO_2 across four free-air CO_2 enrichment experiments in forest, grassland and desert. Global Change Biology **10**:2121-2138.
Evans, J. R. 1989. Photosynthesis and nitrogen relationships in leaves of C_3 plants. Oecologia **78**:9-19.
Farquhar, G. D., S. Von Caemmerer, and J. A. Berry. 1980. A biochemical model of photosynthetic CO_2 assimilation in leaves of C_3 species. Planta **149**:78-90.
Frelich, L. E., and P. B. Reich. 1995. Spatial Patterns and Succession in a Minnesota Southern-Boreal Forest. Ecological Monographs **65**:325-346.
Gough, C. M., B. S. Hardiman, L. E. Nave, G. Bohrer, K. D. Maurer, C. S. Vogel, K. J. Nadelhoffer, and P. S. Curtis. 2013. Sustained carbon uptake and storage following moderate disturbance in a Great Lakes forest. Ecological Applications **23**:1202-1215.
Grassi, G., E. Vicinelli, F. Ponti, L. Cantoni, and F. Magnani. 2005. Seasonal and interannual variability of photosynthetic capacity in relation to leaf nitrogen in a deciduous forest plantation in northern Italy. Tree Physiol **25**:349-360.
Harley, P. C., and D. D. Baldocchi. 1995. Scaling carbon dioxide and water vapour exchange from leaf to canopy in a deciduous forest. I. Leaf model parametrization. Plant Cell Environ **18**:1146-1156.
Harley, P. C., and T. D. Sharkey. 1991. An improved model of C_3 photosynthesis at high CO_2: Reversed O_2 sensitivity explained by lack of glycerate reentry into the chloroplast. Photosynthesis Research **27**:169-178.
Harley, P. C., R. B. Thomas, J. F. Reynolds, and B. R. Strain. 1992. Modelling photosynthesis of cotton grown in elevated CO2. Plant Cell Environ **15**:271-282.
Hikosaka, K., K. Ishikawa, A. Borjigidai, O. Muller, and Y. Onoda. 2006. Temperature acclimation of photosynthesis: mechanisms involved in the changes in temperature dependence of photosynthetic rate. J Exp Bot **57**:291-302.
Hikosaka, K., E. Nabeshima, and T. Hiura. 2007. Seasonal changes in the temperature response of photosynthesis in canopy leaves of *Quercus crispula* in a cool-temperate forest. Tree Physiol **27**:1035-1041.
Hollinger, D. Y. 1996. Optimality and nitrogen allocation in a tree canopy. Tree Physiol **16**:627-634.

Ishii, H., and S. Asano. 2010. The role of crown architecture, leaf phenology and photosynthetic activity in promoting complementary use of light among coexisting species in temperate forests. Ecological Research **25**:715-722.

Jensen, R. G. 2000. Activation of Rubisco regulates photosynthesis at high temperature and CO_2. Proceedings of the National Academy of Sciences **97**:12937-12938.

Kattge, J., and W. Knorr. 2007. Temperature acclimation in a biochemical model of photosynthesis: a reanalysis of data from 36 species. Plant Cell Environ **30**:1176-1190.

Kattge, J., W. Knorr, T. Raddatz, and C. Wirth. 2009. Quantifying photosynthetic capacity and its relationship to leaf nitrogen content for global-scale terrestrial biosphere models. Global Change Biology **15**:976-991.

Kim, Y., P. R. Moorcroft, I. Aleinov, M. J. Puma, and N. Y. Kiang. 2015. Variability of phenology and fluxes of water and carbon with observed and simulated soil moisture in the Ent Terrestrial Biosphere Model (Ent TBM version 1.0.1.0.0). Geosci. Model Dev. **8**:3837-3865.

Kirkpatrick, S. 1984. Optimization by simulated annealing: Quantitative studies. Journal of Statistical Physics **34**:975-986.

Kull, O., and Ü. Niinemets. 1998. Distribution of leaf photosynthetic properties in tree canopies: comparison of species with different shade tolerance. Functional Ecology **12**:472-479.

Le Quéré, C., G. P. Peters, R. J. Andres, R. M. Andrew, T. A. Boden, P. Ciais, P. Friedlingstein, R. A. Houghton, G. Marland, R. Moriarty, S. Sitch, P. Tans, A. Arneth, A. Arvanitis, D. C. E. Bakker, L. Bopp, J. G. Canadell, L. P. Chini, S. C. Doney, A. Harper, I. Harris, J. I. House, A. K. Jain, S. D. Jones, E. Kato, R. F. Keeling, K. Klein Goldewijk, A. Körtzinger, C. Koven, N. Lefèvre, F. Maignan, A. Omar, T. Ono, G. H. Park, B. Pfeil, B. Poulter, M. R. Raupach, P. Regnier, C. Rödenbeck, S. Saito, J. Schwinger, J. Segschneider, B. D. Stocker, T. Takahashi, B. Tilbrook, S. Van Heuven, N. Viovy, R. Wanninkhof, A. Wiltshire, and S. Zaehle. 2014. Global carbon budget 2013. Earth Syst. Sci. Data **6**:235-263.

Legner, N., S. Fleck, and C. Leuschner. 2014. Within-canopy variation in photosynthetic capacity, SLA and foliar N in temperate broad-leaved trees with contrasting shade tolerance. Trees **28**:263-280.

Leuning, R. 2002. Temperature dependence of two parameters in a photosynthesis model. Plant Cell Environ **25**:1205-1210.

Liberloo, M., I. Tulva, O. Raïm, O. Kull, and R. Ceulemans. 2007. Photosynthetic stimulation under long-term CO_2 enrichment and fertilization is sustained across a closed Populus canopy profile (EUROFACE). New Phytologist **173**:537-549.

Medlyn, B. E., F. W. Badeck, D. G. G. De Pury, C. V. M. Barton, M. Broadmeadow, R. Ceulemans, P. De Angelis, M. Forstreuter, M. E. Jach, S. Kellomäki, E. Laitat, M. Marek, S. Philippot, A. Rey, J. Strassemeyer, K. Laitinen, R. Liozon, B. Portier, P. Roberntz, K. Wang, and P. G. Jstbid. 1999. Effects of elevated [CO_2] on photosynthesis in European forest species: a meta-analysis of model parameters. Plant Cell Environ **22**:1475-1495.

Medlyn, B. E., E. Dreyer, D. Ellsworth, M. Forstreuter, P. C. Harley, M. U. F. Kirschbaum, X. Le Roux, P. Montpied, J. Strassemeyer, A. Walcroft, K. Wang, and D. Loustau. 2002. Temperature response of parameters of a biochemically based model of photosynthesis. II. A review of experimental data. Plant Cell Environ **25**:1167-1179.

Medvigy, D., S. Jeong, K. L. Clark, N. S. Skowronski, and K. V. R. Schäfer. 2013. Effects of seasonal variation of photosynthetic capacity on the carbon fluxes of a temperate deciduous forest. Journal of Geophysical Research: Biogeosciences **118**:1703-1714.

Meir, P., B. Kruijt, M. Broadmeadow, E. Barbosa, O. Kull, F. Carswell, A. Nobre, and P. G. Jarvis. 2002. Acclimation of photosynthetic capacity to irradiance in tree canopies in relation to leaf nitrogen concentration and leaf mass per unit area. Plant Cell Environ **25**:343-357.

Miao, Z., M. Xu, R. G. Lathrop, and Y. Wang. 2009. Comparison of the A–C_c curve fitting methods in determining maximum ribulose 1,5-bisphosphate carboxylase/oxygenase carboxylation rate, potential light saturated electron transport rate and leaf dark respiration. Plant Cell Environ **32**:109-122.

Montpied, P., A. Granier, and E. Dreyer. 2009. Seasonal time-course of gradients of photosynthetic capacity and mesophyll conductance to CO_2 across a beech (*Fagus sylvatica* L.) canopy. J Exp Bot **60**:2407-2418.

Murphy, L. 2014. likelihood: Methods for maximum likelihood estimation.

Nave, L. E., C. M. Gough, K. D. Maurer, G. Bohrer, B. S. Hardiman, J. Le Moine, A. B. Munoz, K. J. Nadelhoffer, J. P. Sparks, B. D. Strahm, C. S. Vogel, and P. S. Curtis. 2011. Disturbance and the resilience of coupled carbon and nitrogen cycling in a north temperate forest. Journal of Geophysical Research: Biogeosciences **116**:G04016.

Niinemets, Ü., T. F. Keenan, and L. Hallik. 2015. A worldwide analysis of within-canopy variations in leaf structural, chemical and physiological traits across plant functional types. New Phytologist **205**:973-993.

Oleson, K. W., D. M. Lawrence, G. B. Bonan, B. Drewniak, M. Huang, C. D. Koven, S. Levis, F. Li, W. J. Riley, Z. M. Subin, S. C. Swenson, P. E. Thornton, A. Bozbiyik, R. A. Fisher, C. L. Heald, E. Kluzek, J.-F. Lamarque, P. J. Lawrence, L. R. Leung, W. Lipscomb, S. Muszala, D. M. Ricciuto, W. Sacks, Y. Sun, J. Tang, and Y. Zong-Liang. 2013. Technical Description of version 4.5 of the Community Land Model (CLM). National Center for Atmospheric Research, Boulder, CO.

R Core Team. 2014. R: A language and environment for statistical computing. R Foundation for Statistical Computing, Vienna, Austria.

Raven, J. A. 2013. Rubisco: still the most abundant protein of Earth? New Phytologist **198**:1-3.

Reich, P. B., K. M. Sendall, K. Rice, R. L. Rich, A. Stefanski, S. E. Hobbie, and R. A. Montgomery. 2015. Geographic range predicts photosynthetic and growth response to warming in co-occurring tree species. Nature Clim. Change **5**:148-152.

Reich, P. B., M. B. Walters, B. D. Kloeppel, and D. S. Ellsworth. 1995. Different photosynthesis-nitrogen relations in deciduous hardwood and evergreen coniferous tree species. Oecologia **104**:24-30.

Ripullone, F., G. Grassi, M. Lauteri, and M. Borghetti. 2003. Photosynthesis–nitrogen relationships: interpretation of different patterns between *Pseudotsuga menziesii* and *Populus* × *euroamericana* in a mini-stand experiment. Tree Physiol **23**:137-144.

Rogers, A. 2014. The use and misuse of $V_{c,max}$ in Earth System Models. Photosynthesis Research **119**:15-29.

Rogers, A., B. E. Medlyn, and J. S. Dukes. 2014. Improving representation of photosynthesis in Earth System Models. New Phytologist **204**:12-14.

Sage, R. F., and D. S. Kubien. 2007. The temperature response of C_3 and C_4 photosynthesis. Plant Cell Environ **30**:1086-1106.

Sharkey, T. D. 1985. Photosynthesis in intact leaves of C_3 plants: Physics, physiology and rate limitations. The Botanical Review **51**:53-105.
Sharkey, T. D. 2015. Commentary: what gas exchange data can tell us about photosynthesis. Plant Cell Environ **39**:1161–1163.
Sharkey, T. D., C. J. Bernacchi, G. D. Farquhar, and E. L. Singsaas. 2007. Fitting photosynthetic carbon dioxide response curves for C_3 leaves. Plant Cell Environ **30**:1035-1040.
Silim, S., N. Ryan, and D. Kubien. 2010. Temperature responses of photosynthesis and respiration in *Populus balsamifera L.*: acclimation versus adaptation. Photosynthesis Research **104**:19-30.
Smith, N. G., and J. S. Dukes. 2013. Plant respiration and photosynthesis in global-scale models: incorporating acclimation to temperature and CO_2. Global Change Biology **19**:45-63.
Stuart-Haëntjens, E. J., P. S. Curtis, R. T. Fahey, C. S. Vogel, and C. M. Gough. 2015. Net primary production of a temperate deciduous forest exhibits a threshold response to increasing disturbance severity. Ecology **96**:2478-2487.
Sun, Y., L. Gu, R. E. Dickinson, S. G. Pallardy, J. Baker, Y. Cao, F. M. Damatta, X. Dong, D. Ellsworth, D. Van Goethem, A. M. Jensen, B. E. Law, R. Loos, S. C. V. Martins, R. J. Norby, J. Warren, D. Weston, and K. Winter. 2014. Asymmetrical effects of mesophyll conductance on fundamental photosynthetic parameters and their relationships estimated from leaf gas exchange measurements. Plant Cell Environ **37**:978-994.
Tjoelker, M. G., J. Oleksyn, and P. B. Reich. 2001. Modelling respiration of vegetation: evidence for a general temperature-dependent Q_{10}. Global Change Biology **7**:223-230.
Turnbull, M., D. Whitehead, D. Tissue, W. Schuster, K. Brown, V. Engel, and K. Griffin. 2002. Photosynthetic characteristics in canopies of *Quercus rubra*, *Quercus prinus* and *Acer rubrum* differ in response to soil water availability. Oecologia **130**:515-524.
Vaz, M., J. Maroco, N. Ribeiro, L. C. Gazarini, J. S. Pereira, and M. M. Chaves. 2010. Leaf-level responses to light in two co-occurring Quercus (Quercus ilex and Quercus suber): leaf structure, chemical composition and photosynthesis. Agroforestry Systems **82**:173-181.
Verheijen, L. M., R. Aerts, V. Brovkin, J. Cavender-Bares, J. H. C. Cornelissen, J. Kattge, and P. M. Van Bodegom. 2015. Inclusion of ecologically based trait variation in plant functional types reduces the projected land carbon sink in an earth system model. Global Change Biology: 3074–3086.
Verheijen, L. M., V. Brovkin, R. Aerts, G. Bönisch, J. H. C. Cornelissen, J. Kattge, P. B. Reich, I. J. Wright, and P. M. Van Bodegom. 2013. Impacts of trait variation through observed trait–climate relationships on performance of an Earth system model: a conceptual analysis. Biogeosciences **10**:5497-5515.
Von Caemmerer, S. 2000. Biochemical models of leaf photosynthesis. Csiro publishing.
Walcroft, A. S., D. Whitehead, W. B. Silvester, and F. M. Kelliher. 1997. The response of photosynthetic model parameters to temperature and nitrogen concentration in Pinus radiata D. Don. Plant Cell Environ **20**:1338-1348.
Williams, M., E. B. Rastetter, D. N. Fernandes, M. L. Goulden, S. C. Wofsy, G. R. Shaver, J. M. Melillo, J. W. Munger, S. M. Fan, and K. J. Nadelhoffer. 1996. Modelling the soil-plant-atmosphere continuum in a *Quercus–Acer* stand at Harvard Forest: the regulation of stomatal conductance by light, nitrogen and soil/plant hydraulic properties. Plant Cell Environ **19**:911-927.

Wilson, K. B., D. D. Baldocchi, and P. J. Hanson. 2000. Spatial and seasonal variability of photosynthetic parameters and their relationship to leaf nitrogen in a deciduous forest. Tree Physiol **20**:565-578.

Wright, I. J., P. B. Reich, M. Westoby, D. D. Ackerly, Z. Baruch, F. Bongers, J. Cavender-Bares, T. Chapin, J. H. C. Cornelissen, M. Diemer, J. Flexas, E. Garnier, P. K. Groom, J. Gulias, K. Hikosaka, B. B. Lamont, T. Lee, W. Lee, C. Lusk, J. J. Midgley, M.-L. Navas, U. Niinemets, J. Oleksyn, N. Osada, H. Poorter, P. Poot, L. Prior, V. I. Pyankov, C. Roumet, S. C. Thomas, M. G. Tjoelker, E. J. Veneklaas, and R. Villar. 2004. The worldwide leaf economics spectrum. Nature **428**:821-827.

Wullschleger, S. D. 1993. Biochemical Limitations to Carbon Assimilation in C_3 Plants—A Retrospective Analysis of the A/Ci Curves from 109 Species. J Exp Bot **44**:907-920.

Wullschleger, S. D., H. E. Epstein, E. O. Box, E. S. Euskirchen, S. Goswami, C. M. Iversen, J. Kattge, R. J. Norby, P. M. Van Bodegom, and X. Xu. 2014. Plant functional types in Earth system models: past experiences and future directions for application of dynamic vegetation models in high-latitude ecosystems. Ann Bot **114**:1-16.

Chapter 5

Conclusions and Synthesis

The Earth holds an expansive array of habitats that support a dynamic number and diversity of organisms. We find life at the great depths of the Atlantic Ocean (Sogin et al. 2006), in the canopy tops of the Amazon rainforest (Moura et al. 2013), and within the extreme, cold and dry environment of Antarctic soils (Cowan 2009). Whether with our eyes or with more refined scientific tools, we see evidence at different spatial and temporal scales of how biomes differ in organisms, climate, and their interactions. These differences partially arise from a common set of processes that move energy, carbon, water, and nutrients across the globe. Photosynthesis is one of these processes, and is the nearly universal foundation that supports differences in population, community, and ecosystem dynamics, because it converts sunlight into a form of energy that is useable by living organisms.

My dissertation reveals that the role of light in photosynthesis and ecosystem carbon cycling is not as straightforward as previously thought. Photosynthesis at the leaf and ecosystem scales depends not only on the amount of solar radiation that reaches the Earth's surface, but also on the physical and ecological differences within a plant canopy. I reach this conclusion by answering three questions that mechanistically demonstrate how this canopy heterogeneity modifies the effects of light on gross ecosystem CO_2 uptake, which conceptually, is the integration of photosynthetic activity across all leaves within a plant canopy.

5.1 Summary of Dissertation Goals and Conclusions

This dissertation uses theory and tools from atmospheric science, ecosystem ecology, and plant physiology to empirically test how three physical, biophysical, and ecological processes alter the effects of light (photosynthetically active radiation; 400-700 nm) on photosynthetic processes tied to gross ecosystem CO_2 uptake. The primary goals and findings of each chapter are listed below.

Chapter 2: *Determine how clouds change the amount and type of light available for plant canopies to use in photosynthesis.* Before plants can absorb light and use it in photosynthesis, clouds reflect, transmit, and scatter incoming solar radiation (Fritz 1954, Twomey 1991). As a result, the interaction between clouds and incoming solar radiation is the first process to modify the relationship between light and gross ecosystem CO_2 uptake. However, a mechanistic link between cloud properties and the effects of scattered, diffuse light on ecosystem carbon cycling has not been previous demonstrated with observations from multiple plant canopies. In this chapter, I combined NASA satellite-retrieved data on cloud optical thickness, an integrative measure of how strongly clouds scatter and absorb light, with ground-based measurements of above-canopy light and gross primary production (GPP). Using these datasets, I tested for links between clouds, surface light, and GPP and also quantified the response of GPP to cloud optical thickness in different ecosystems (Cheng et al. in review-a).

Conclusions: Across the entire range of cloud optical thickness measured by NASA (0 to 100; unitless), total light (i.e, the sum of diffuse and direct light) decreased nonlinearly. However, diffuse light increased under a narrow range of optically thin clouds (optical thickness < 7) and then decreased under optically thick clouds (optical thickness > 7). Under thin clouds, the increase in diffuse light compensated for the decrease in total light because canopies used diffuse light more efficiently than they used direct light. This led to no net change in GPP in temperate forest and maize canopies under optically thin clouds, but a decrease in GPP under optically thick clouds. These results suggest that future GPP is unlikely to change if the optical thickness of thin clouds stays below 7. However, future GPP could decrease if the optical thickness of thin clouds increases to above 7.

In addition, optically thin clouds only accounted for 7-24% of the variation in surface diffuse light, suggesting that other cloud properties and atmospheric constituents may be more important drivers of canopy light availability. For example, aerosols produced from natural sources and anthropogenic fossil fuel combustion can scatter and absorb light (Mahowald et al. 2011). Aerosols have a smaller range of optical thickness than clouds do, where events with optical thickness > 1.5 are considered a high aerosol event (Eck et al. 2003). Aerosol optical thickness thereby generally falls within the range of optical thickness where GPP does not decline (optical thickness < 7). This suggests that aerosols may more frequently have a positive effect on GPP than clouds do, as is hypothesized in Mercado et al. (2009) and Oliphant et al.

(2011). However, because many forests are in remote locations and have a low frequency of high aerosol optical thickness events (Steiner et al. 2013), I did not examine the separate role of aerosols in this dissertation. This chapter expands on previous understanding of atmospheric controls of canopy light by 1) empirically demonstrating a mechanistic link between clouds and surface diffuse light, 2) quantifying the characteristics of clouds that increase or decrease surface light conditions, and 3) calculating the magnitude of change in GPP under clouds.

Chapter 3: *Identify how GPP responds to diffuse light and canopy structure, independent of co-varying environmental variables.* Previous research on diffuse light and ecosystem productivity heavily relied on theoretical estimates of diffuse light and did not isolate this relationship from other environmental factors that co-vary with diffuse light. These analysis methods can bias estimates of how GPP responds to diffuse light. In this chapter, I use ground-based measurements of above-canopy light and GPP to empirically demonstrate and quantify the response of GPP to diffuse light, after removing the effects of total light, vapor pressure deficit, and air temperature on GPP (Cheng et al. 2015).

Conclusions: After removing the effect of direct light on GPP, diffuse light explained up to 17% of variation in forest GPP and up to 41% of variation in crop GPP. After additionally accounting for impacts of vapor pressure deficit and air temperature on GPP, I found that GPP increased with diffuse light for most hours of the day. However, the rate of increase in GPP ranged from 0.003 to 0.050 μmol CO_2 per μmol photons of diffuse light and varied with time of day. The increases in GPP with diffuse light also differed across ecosystems in this study, even between plant canopies of the same plant functional type. This variation may result from an interaction between the angle of incoming light (i.e., zenith angle) and plant canopy structure, which could change the proportions of leaves within canopies that intercept incoming light. This suggests that a canopy's physical structure or community composition alters the response of GPP to incoming solar radiation. This chapter expands our understanding of how light influences gross ecosystem CO_2 uptake by empirically demonstrating that plant canopy structure interacts with zenith angle to alter the effects of incoming light on GPP. The calculated rates of increase in GPP to diffuse light in this chapter can also be used to calculate the global impact of diffuse light on GPP while accounting for 1) how time of day and plant canopy structure modify the response

of GPP to diffuse light and 2) how other environmental factors that co-occur with diffuse light conditions affect GPP.

Chapter 4: *Examine how leaf biochemical limitations in photosynthesis change with within-canopy heterogeneity in species, leaf light, and leaf temperature.* After light moves through the atmosphere and is distributed through plant canopies, it is intercepted by leaves and used in photosynthesis. The interaction between incoming radiation and canopy structure creates a wide range of microclimates within the canopy, particularly in light and air temperature. Both air temperature and the amount of light a leaf absorbs can change leaf temperature and subsequently, alter rates of photosynthesis. Because plants can produce leaves adapted to their microclimate, leaves within the canopy could photosynthesize differently and scale up to alter gross ecosystem CO_2 uptake. Photosynthesis is primarily limited by three biochemical reactions, the maximum rate of carboxylation ($V_{c,max}$), maximum rate of electron transport (J_{max}), and triose phosphate utilization (*TPU*). However, data on how $V_{c,max}$, J_{max}, and *TPU* change within a plant canopy are limited. In this chapter, I measured net photosynthesis at different CO_2 concentrations on leaves from high and low light environments and from three species in a temperate, broadleaf forest. I used the data to derive $V_{c,max}$, J (which is calculated using J_{max}), and *TPU* and to identify whether the limitations in photosynthesis vary in the canopy through species-specific responses to leaf light environment and leaf temperature (Cheng et al. in review-b).

Conclusions: $V_{c,max}$, J, and *TPU* in leaves from different species and light environments increased with leaf temperature at similar rates. In addition, differences in $V_{c,max}$ within the canopy varied with leaf nitrogen per area, which is known to decrease from the top to the bottom of a plant canopy (Ellsworth and Reich 1993). However, this nitrogen gradient was not enough to explain the within-canopy variation in J or *TPU*. Generally, J was higher in early successional species (*Populus grandidenta*) and lower in later successional species (*Quercus rubra*, *Acer rubrum*), but species did not differ in *TPU*. In addition, leaves exposed to more light had higher J and *TPU* than leaves exposed to low light. An ecosystem scale experiment at the forest where I conducted this study indicates that ecological succession changes the distribution of foliage within the canopy (Hardiman et al. 2013). As a result, values of J and *TPU* within a canopy could change in the future as succession alters both the distribution of species and microclimates within a plant canopy.

This chapter adds to our understanding of how light influences gross ecosystem CO_2 uptake by providing evidence that the biochemical limits to photosynthesis vary with canopy heterogeneity. In addition, simplified representations of how $V_{c,max}$, J_{max}, and *TPU* respond to environmental and ecological variation are used in Earth system models to scale photosynthesis from the leaf to canopy. This chapter showed that some of the simplifications used to scale photosynthesis from the leaf to ecosystem is not supported by field-based data collected from a temperate forest canopy. If these patterns are found in other canopies, these simplifications of photosynthesis in Earth system models may be leading to errors in calculations of CO_2 fluxes into terrestrial ecosystems. However, to assess the impact of within-canopy variation in *J* and *TPU* on model estimates of CO_2 fluxes into plant canopies, sensitivity studies need to be conducted. Variation in *J* and *TPU* with species or light environment would only affect model estimates if these two rates more frequently limit photosynthesis than does within-canopy variation in $V_{c,max}$. This chapter provides suggestions for how experiments with Earth system models can identify whether leaf-level biochemical variations within plant canopies impact ecosystem and global-level CO_2 flux calculations.

5.2 Application to Earth System Modeling

The outcomes of this dissertation have two important applications to Earth system modeling. First, Chapters 2 and 3 demonstrate the importance of using data to test conclusions from model experiments. For example, a site-based empirical model estimated an 8-23% increase in photosynthesis and an offline global land surface model estimated a 25% increase in the land carbon sink when there was an increase in diffuse light produced predominately by aerosols (Gu et al. 2003, Mercado et al. 2009). Similarly, other studies used measurements or derivations of diffuse light to claim that clouds increase CO_2 fluxes into ecosystems (Hollinger et al. 1994, Gu et al. 1999). These results led to the inference that clouds and aerosols substantially alter the magnitude of the global land carbon sink. However, other studies testing this inference with various combinations of radiative transfer models, light use efficiency models, and a limited set of field measurements came to inconsistent conclusions about the impact of diffuse light on ecosystem productivity (Hollinger et al. 1994, Rocha et al. 2004, Urban et al. 2007, Alton 2008, Knohl and Baldocchi 2008). My dissertation research tested these hypotheses using satellite and ground-based data and demonstrated that the mechanistic links between clouds, diffuse light, and

ecosystem productivity do exist. However, these processes do not have as large of an effect as some studies previously found. Overall, models are useful for identifying potentially significant drivers of Earth system patterns (i.e., land-atmosphere CO_2 fluxes) across temporal and spatial scales. However, models should be used in concert with empirical studies to test if these patterns are mechanistically observable *in situ*.

Second, Chapter 4 demonstrates the importance of using field observations to improve Earth system model projections of land-atmosphere CO_2 fluxes. Earth system modelers are required to simplify photosynthesis, and in some cases, tweak key parameters (e.g., $V_{c,max}$) to minimize unrealistic model output as opposed to mechanistically representing processes (Rogers et al. 2014). The modeling community has suggested that additional leaf photosynthesis measurements would add to their capacity to improve representations of leaf photosynthesis in land surface models (Dietze 2014, Rogers 2014). Chapter 4 meets this request by providing a new set of net photosynthesis measurements across a range of CO_2 concentrations from mature, canopy-dominant trees taken from multiple species in one plant canopy. The results provided support for the current method of using leaf nitrogen and leaf temperature to scale $V_{c,max}$ within the canopy. However, results did not support the calculation of J_{max} and TPU from $V_{c,max}$ or from nitrogen per leaf area alone. Our results indicate that leaf traits that are not captured in a canopy nitrogen gradient influence J_{max} and TPU. This provides support for recent interest in moving away from the traditional groupings of plants in Earth system models and instead, creating a new set of plant functional types that capture dynamic patterns in plant canopies (Wullschleger et al. 2014).

Despite the *in situ* observation that canopy heterogeneity alters limitations to leaf photosynthesis in one canopy, these data alone are not enough to conclusively say that canopy heterogeneity is a dominant driver of gross ecosystem CO_2 uptake. Because the net rate of photosynthesis is calculated based on the most limiting of the three biochemical processes, plant trait variation in J_{max} and TPU may not affect gross ecosystem CO_2 uptake if $V_{c,max}$ is the dominant limitation to photosynthesis or if the gradient of change in J_{max} and TPU within a plant canopy is small. To quantify the global impact of canopy heterogeneity on the rate-limiting reactions in photosynthesis, model sensitivity experiments are required. Multi-layer canopy models are scale-appropriate tools for this research because they allow us to mechanistically link and quantify changes at the leaf-level to the ecosystem-level (Bonan et al. 2011, Bonan et al.

2014). Results of these canopy level simulations will provide evidence for whether changes in the parameterizations of J_{max} and *TPU* can narrow the range of uncertainty around future projections of the land carbon sink. This dissertation provides an example of how an iterative process of using models and *in situ* measurements to develop research questions is a more rigorous way of developing our understanding of the terrestrial carbon cycle, as suggested in Medlyn et al. (2015).

5.3 Synthesis

This dissertation demonstrates that several physical, biophysical, and ecological processes modify the impacts of light on photosynthetic processes (i.e., GPP and leaf photosynthesis) linked to gross ecosystem CO_2 uptake. Unlike previous research, this dissertation tests and finds evidence for mechanistic links between clouds, surface diffuse light, and ecosystem productivity that were previously assumed to exist. As a result, this dissertation addresses conflicting results in the literature about the impact of diffuse light on ecosystem carbon processing and suggests that the response of gross ecosystem CO_2 uptake to increases in cloud-produced diffuse light may be small. There are conditions when this relationship could be important, but other drivers of gross ecosystem CO_2 uptake (e.g., total light and leaf temperature) may have larger short-term and long-term impacts. Further analysis indicates that canopy heterogeneity (i.e., the distribution of leaves, gaps, and species within the entire canopy) influences the way ecosystems use light. First, the plant canopy alters the effect of incoming diffuse light on GPP. Second, the distribution of species and light within a plant canopy changes the rates of biochemical reactions that limit leaf photosynthesis. Both of these processes demonstrate how canopy heterogeneity influences carbon cycling at the leaf and ecosystem scales. They also illustrate how clouds and canopy structure influence land-atmosphere CO_2 fluxes and subsequently, Earth's climate.

This dissertation also provides an important framework for testing our assumptions about how living organisms form feedbacks with their environment. A model is not only a representation of how we understand an interactive system. It also shapes the way we ask questions about the drivers and patterns in that system. An opportunity arises, when we combine tools from multiple disciplines and questions from across temporal and spatial scales, to break apart that model, test assumptions, and reshape it with new, empirically based information. For

example, in atmospheric science, the discussion on the relationship between light and ecosystem carbon cycling is focused on atmospheric drivers. In ecology, the discussion is focused on how leaves and species process that light. This dissertation provides a third option of framing this relationship by demonstrating that canopy heterogeneity is a mediator of relationships that both atmospheric drivers and ecological drivers have with gross ecosystem CO_2 uptake. Thus, the conclusions in this dissertation support the current restructuring of methods used to represent canopy processes and plant functional types in Earth system models.

In addition, an iterative process, where models and observational data are used in tandem to develop and empirically answer questions, increases our mechanistic understanding of the global carbon cycle. This approach also applies to outstanding questions in ecosystem ecology, such as the response of ecosystems to changes in nitrogen cycling and how to best represent them in Earth system models (Galloway et al. 2008, Thomas et al. 2015). More broadly, this framework of testing assumptions with models and empirical data empowers us to question other assumptions about climate-species interactions. This is key to ensuring that the foundations in other models, such as ecological niche models (Araújo and Peterson 2012) or species distribution models (Elith and Leathwick 2009, Thuiller et al. 2011), are reliable, so that we can more accurately uncover the drivers of population, community, and ecosystem dynamics across the Earth.

References

Alton, P. B. 2008. Reduced carbon sequestration in terrestrial ecosystems under overcast skies compared to clear skies. Agricultural and Forest Meteorology **148**:1641-1653.

Araújo, M. B., and A. T. Peterson. 2012. Uses and misuses of bioclimatic envelope modeling. Ecology **93**:1527-1539.

Bonan, G. B., P. J. Lawrence, K. W. Oleson, S. Levis, M. Jung, M. Reichstein, D. M. Lawrence, and S. C. Swenson. 2011. Improving canopy processes in the Community Land Model version 4 (CLM4) using global flux fields empirically inferred from FLUXNET data. Journal of Geophysical Research: Biogeosciences **116**:G02014.

Bonan, G. B., M. Williams, R. A. Fisher, and K. W. Oleson. 2014. Modeling stomatal conductance in the earth system: linking leaf water-use efficiency and water transport along the soil-plant-atmosphere continuum. Geoscientific Model Development **7**:2193-2222.

Cheng, S. J., G. Bohrer, A. L. Steiner, D. Y. Hollinger, A. Suyker, R. P. Phillips, and K. J. Nadelhoffer. 2015. Variations in the influence of diffuse light on gross primary productivity in temperate ecosystems. Agricultural and Forest Meteorology **201**:98-110.

Cheng, S. J., A. L. Steiner, D. Y. Hollinger, G. Bohrer, and K. J. Nadelhoffer. in review-a. Using satellite-derived optical thickness to assess the influence of clouds on terrestrial carbon uptake. Journal of Geophysical Research: Biogeosciences.

Cheng, S. J., R. Q. Thomas, J. V. Wilkening, P. S. Curtis, T. D. Sharkey, and K. J. Nadelhoffer. in review-b. Photosynthesis from leaf to canopy: species and leaf light availability drive within-canopy variation in forest photosynthetic capacity. Journal of Geophysical Research: Biogeosciences.

Cowan, D. A. 2009. Cryptic microbial communities in Antarctic deserts. Proceedings of the National Academy of Sciences **106**:19749-19750.

Dietze, M. 2014. Gaps in knowledge and data driving uncertainty in models of photosynthesis. Photosynthesis Research **119**:3-14.

Eck, T. F., B. N. Holben, J. S. Reid, N. T. O'neill, J. S. Schafer, O. Dubovik, A. Smirnov, M. A. Yamasoe, and P. Artaxo. 2003. High aerosol optical depth biomass burning events: A comparison of optical properties for different source regions. Geophysical Research Letters **30**.

Elith, J., and J. R. Leathwick. 2009. Species Distribution Models: Ecological Explanation and Prediction Across Space and Time. Annual Review of Ecology, Evolution, and Systematics **40**:677-697.

Ellsworth, D. S., and P. B. Reich. 1993. Canopy structure and vertical patterns of photosynthesis and related leaf traits in a deciduous forest. Oecologia **96**:169-178.

Fritz, S. 1954. Scattering of solar energy by clouds of "large drops". Journal of Meteorology **11**:291-300.

Galloway, J. N., A. R. Townsend, J. W. Erisman, M. Bekunda, Z. Cai, J. R. Freney, L. A. Martinelli, S. P. Seitzinger, and M. A. Sutton. 2008. Transformation of the Nitrogen Cycle: Recent Trends, Questions, and Potential Solutions. Science **320**:889-892.

Gu, L., D. D. Baldocchi, S. C. Wofsy, J. W. Munger, J. J. Michalsky, S. P. Urbanski, and T. A. Boden. 2003. Response of a Deciduous Forest to the Mount Pinatubo Eruption: Enhanced Photosynthesis. Science **299**:2035-2038.

Gu, L., J. D. Fuentes, H. H. Shugart, R. M. Staebler, and T. A. Black. 1999. Responses of net ecosystem exchanges of carbon dioxide to changes in cloudiness: Results from two North American deciduous forests. Journal of Geophysical Research: Atmospheres **104**:31421-31434.

Hardiman, B. S., C. M. Gough, A. Halperin, K. L. Hofmeister, L. E. Nave, G. Bohrer, and P. S. Curtis. 2013. Maintaining high rates of carbon storage in old forests: A mechanism linking canopy structure to forest function. Forest Ecology and Management **298**:111-119.

Hollinger, D. Y., F. M. Kelliher, J. N. Byers, J. E. Hunt, T. M. Mcseveny, and P. L. Weir. 1994. Carbon Dioxide Exchange between an Undisturbed Old-Growth Temperate Forest and the Atmosphere. Ecology **75**:134-150.

Knohl, A., and D. D. Baldocchi. 2008. Effects of diffuse radiation on canopy gas exchange processes in a forest ecosystem. Journal of Geophysical Research: Biogeosciences **113**:G02023.

Mahowald, N., D. S. Ward, S. Kloster, M. G. Flanner, C. L. Heald, N. G. Heavens, P. G. Hess, J.-F. Lamarque, and P. Y. Chuang. 2011. Aerosol Impacts on Climate and Biogeochemistry. Annual Review of Environment and Resources **36**:45-74.

Medlyn, B. E., S. Zaehle, M. G. De Kauwe, A. P. Walker, M. C. Dietze, P. J. Hanson, T. Hickler, A. K. Jain, Y. Luo, W. Parton, I. C. Prentice, P. E. Thornton, S. Wang, Y.-P. Wang, E. Weng, C. M. Iversen, H. R. Mccarthy, J. M. Warren, R. Oren, and R. J. Norby. 2015. Using ecosystem experiments to improve vegetation models. Nature Clim. Change **5**:528-534.

Mercado, L. M., N. Bellouin, S. Sitch, O. Boucher, C. Huntingford, M. Wild, and P. M. Cox. 2009. Impact of changes in diffuse radiation on the global land carbon sink. Nature **458**:1014-1017.

Moura, N. G., A. C. Lees, C. B. Andretti, B. J. W. Davis, R. R. C. Solar, A. Aleixo, J. Barlow, J. Ferreira, and T. A. Gardner. 2013. Avian biodiversity in multiple-use landscapes of the Brazilian Amazon. Biological Conservation **167**:339-348.

Oliphant, A. J., D. Dragoni, B. Deng, C. S. B. Grimmond, H. P. Schmid, and S. L. Scott. 2011. The role of sky conditions on gross primary production in a mixed deciduous forest. Agricultural and Forest Meteorology **151**:781-791.

Rocha, A. V., H.-B. Su, C. S. Vogel, H. P. Schmid, and P. S. Curtis. 2004. Photosynthetic and Water Use Efficiency Responses to Diffuse Radiation by an Aspen-Dominated Northern Hardwood Forest. Forest Science **50**:793-801.

Rogers, A. 2014. The use and misuse of $V_{c,max}$ in Earth System Models. Photosynthesis Research **119**:15-29.

Rogers, A., B. E. Medlyn, and J. S. Dukes. 2014. Improving representation of photosynthesis in Earth System Models. New Phytologist **204**:12-14.

Sogin, M. L., H. G. Morrison, J. A. Huber, D. M. Welch, S. M. Huse, P. R. Neal, J. M. Arrieta, and G. J. Herndl. 2006. Microbial diversity in the deep sea and the underexplored "rare biosphere". Proceedings of the National Academy of Sciences **103**:12115-12120.

Steiner, A. L., D. Mermelstein, S. J. Cheng, T. E. Twine, and A. Oliphant. 2013. Observed Impact of Atmospheric Aerosols on the Surface Energy Budget. Earth Interactions **17**:1-22.

Thomas, R. Q., E. N. J. Brookshire, and S. Gerber. 2015. Nitrogen limitation on land: how can it occur in Earth system models? Global Change Biology **21**:1777-1793.

Thuiller, W., S. Lavergne, C. Roquet, I. Boulangeat, B. Lafourcade, and M. B. Araujo. 2011. Consequences of climate change on the tree of life in Europe. Nature **470**:531-534.

Twomey, S. 1991. Symposium on Global Climatic Effects of Aerosols Aerosols, clouds and radiation. Atmospheric Environment. Part A. General Topics **25**:2435-2442.

Urban, O., D. Janouš, M. Acosta, R. Czerný, I. Marková, M. Navrátil, M. Pavelka, R. Pokorný, M. Šprtová, R. U. I. Zhang, V. Špunda, J. Grace, and M. V. Marek. 2007. Ecophysiological controls over the net ecosystem exchange of mountain spruce stand. Comparison of the response in direct vs. diffuse solar radiation. Global Change Biology **13**:157-168.

Wullschleger, S. D., H. E. Epstein, E. O. Box, E. S. Euskirchen, S. Goswami, C. M. Iversen, J. Kattge, R. J. Norby, P. M. Van Bodegom, and X. Xu. 2014. Plant functional types in Earth system models: past experiences and future directions for application of dynamic vegetation models in high-latitude ecosystems. Ann Bot **114**:1-16.

APPENDICES

Appendix A

Supplementary Figures for Chapter 2

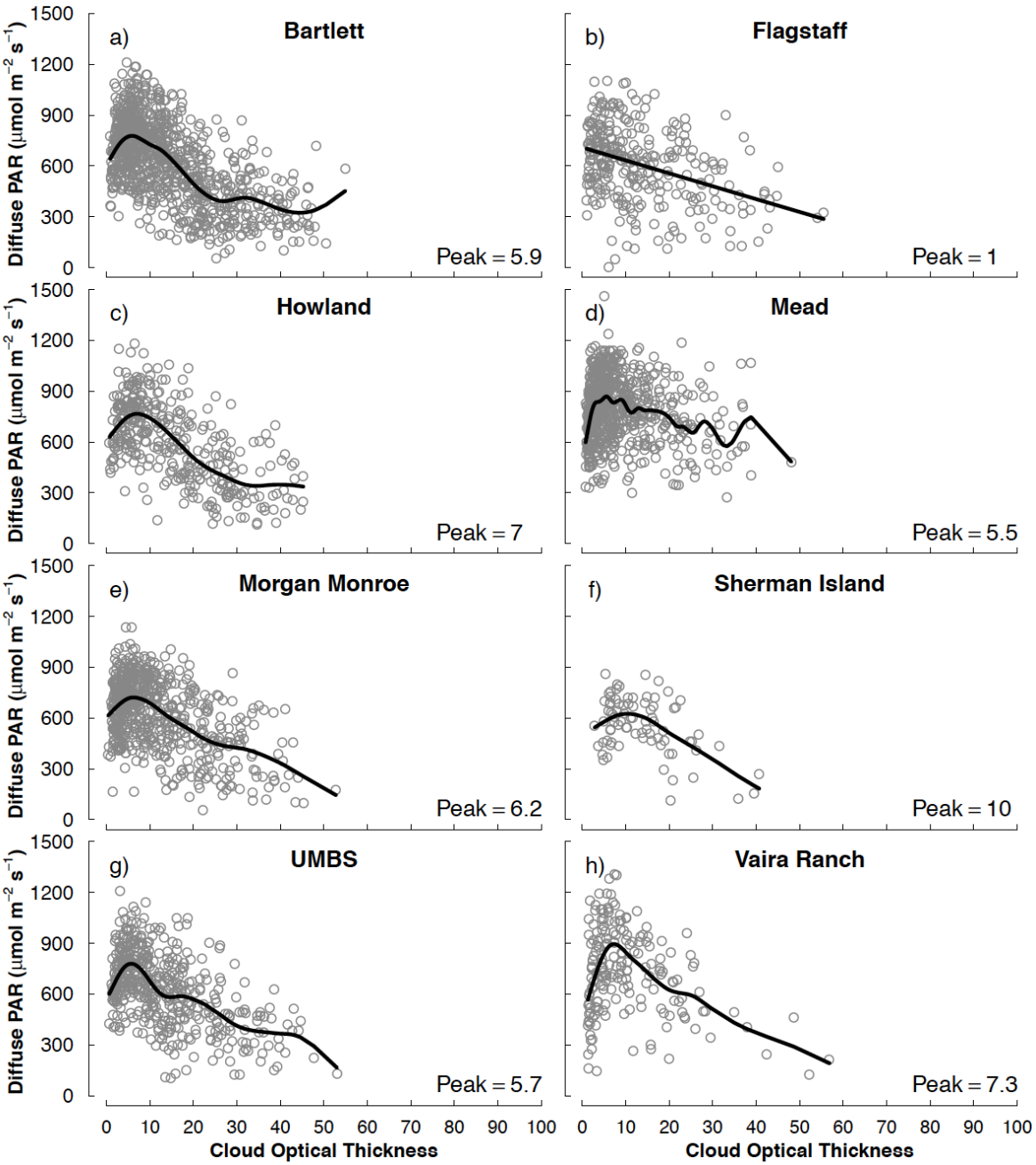

Figure A1: The response of Ameriflux-tower measured diffuse PAR to increases in 1x1 km average cloud optical thickness (τ_c; unitless) retrieved from MODIS satellites. "Peak" refers to the highest value of τ_c that is associated with an increase in diffuse PAR. Data points include measurements from May through September from years with available data (Table 2.1). For Howland Forest, April data are included when this month is calculated as part of the site's growing season.

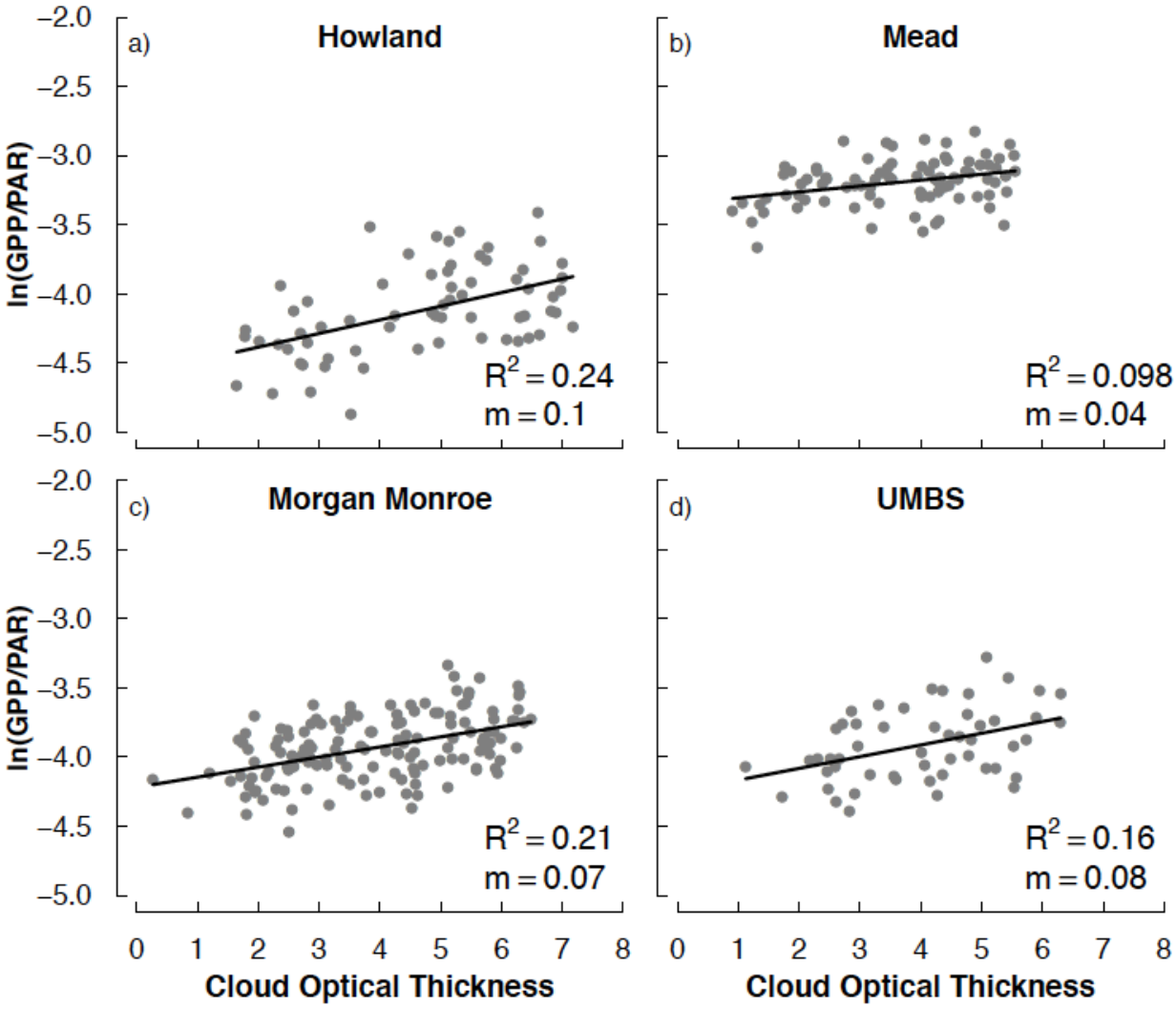

Figure A2: During the peak growing season, light use efficiency (gross primary productivity per unit total photosynthetically active radiation - PAR) increases with cloud optical thickness (τ_c) at a) Howland Forest, b) Mead, c) Morgan Monroe, and d) UMBS. UMBS. Light use efficiency is plotted on a natural log scale to meet statistical assumptions for linear regressions. Regression lines are drawn for relationships with $p < 0.01$.

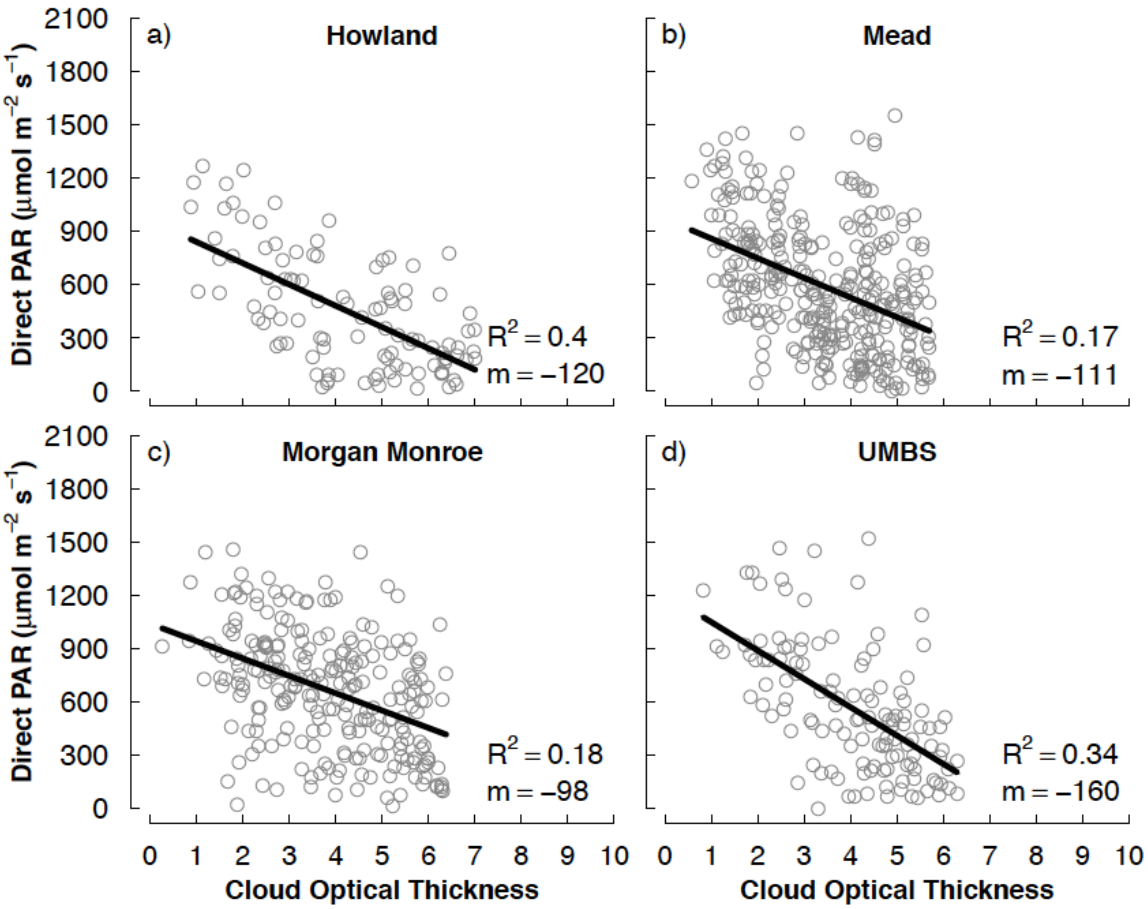

Figure A3: Relationships between cloud optical thickness and direct PAR at a) Howland, b) Mead, c) Morgan Monroe, and 3) UMBS. Regression lines are drawn for relationships with $p < 0.05$

Appendix B

Supplementary Table for Chapter 3

Table B1: Values of α and γ predicted by best-fit rectangular hyperbolas describing the response of GPP to direct PAR. The α represents the quantum yield and γ represents the maximum GPP value. All α and γ values listed have $p < 6.02 \times 10^{-4}$ (Bonferroni-corrected critical value), except for those in italics, which have $p < 0.01$ and those in **bold**, which were not significant because $p > 0.05$. NS indicates we were unable to fit a light response curve.

Site		Zenith Angle (°)								
		AM					PM			
		76-100	61-75	46-60	31-45	16-30	31-45	46-60	61-75	76-100
Howland Forest Logged	α	1.16	2.64	2.82	2.74	3.41	2.58	2.61	2.07	1.10
	γ	7.41	11.84	14.67	16.52	18.12	14.57	12.93	10.04	6.39
	R^2	0.39	0.37	0.34	0.26	0.27	0.29	0.33	0.37	0.39
Howland Forest Reference	α	1.28	2.15	2.41	2.30	2.27	2.21	2.13	1.89	1.91
	γ	4.74	9.89	14.15	16.16	17.15	13.93	11.64	8.35	4.53
	R^2	0.23	0.34	0.34	0.34	0.35	0.33	0.38	0.39	0.21
Howland Forest N Fertilized	α	1.81	2.85	2.93	2.38	2.82	3.28	3.79	2.85	2.01
	γ	5.27	10.32	14.20	17.14	17.77	14.71	12.05	8.82	5.04
	R^2	0.25	0.32	0.35	0.37	0.29	0.24	0.21	0.27	0.18
Morgan Monroe	α	*2.01*	1.43	1.59	1.50	2.03	1.99	2.09	2.58	NS
	γ	4.66	12.39	19.83	25.72	27.29	22.99	16.78	10.31	NS
	R^2	0.06	0.13	0.23	0.32	0.29	0.31	0.22	0.25	NS
UMBS	α	1.05	*3.57*	4.06	3.08	2.99	3.96	1.59	1.43	3.00
	γ	6.07	12.36	20.38	25.32	27.10	23.78	19.17	13.25	6.94
	R^2	0.28	0.09	0.11	0.15	0.12	0.14	0.24	0.34	0.21
Mead Irrigated Maize	α	0.73	3.95	4.49	3.35	2.98	3.51	1.61	2.07	NS
	γ	16.11	30.91	48.21	59.92	64.10	49.94	35.94	17.71	NS
	R^2	0.49	0.21	0.22	0.31	0.23	0.29	0.20	0.13	NS
Mead Irrigated Rotation: Maize	α	0.40	1.65	2.60	2.48	3.30	1.20	1.29	0.64	NS
	γ	17.61	32.62	48.64	58.70	65.20	50.15	38.13	21.68	NS
	R^2	0.51	0.47	0.43	0.38	0.42	0.41	0.36	0.38	NS
Mead Irrigated Rotation: Soybean	α	0.59	2.24	6.35	5.37	5.29	6.48	*3.51*	NS	NS
	γ	12.20	23.63	31.62	37.67	36.42	31.74	23.52	NS	NS
	R^2	0.59	0.45	0.27	0.29	0.27	0.21	0.23	NS	NS

Mead Rainfed Rotation: Maize	α	0.54	3.39	4.67	4.21	3.78	3.23	2.31	0.94	NS
	γ	17.47	31.51	44.79	55.53	56.19	46.60	33.49	18.65	NS
	R^2	0.66	0.53	0.48	0.53	0.37	0.39	0.29	0.44	NS
Mead Rainfed Rotation: Soybean	α	0.75	4.69	*16.67*	*9.43*	**15.38**	**31.88**	**5.89**	1.35	NS
	γ	13.11	23.44	29.27	34.98	30.74	29.40	20.29	13.47	NS
	R^2	0.53	0.16	0.08	0.05	0.01	0.00	0.04	0.18	NS

Appendix C

Supplementary Tables for Chapter 4

Table C1: List of equations, maximum likelihood parameter estimates, differences in AIC_c scores compared to the model with the lowest AIC_c (ΔAIC_c), standard deviation (sd) and R^2 for the models used to test for patterns in $V_{c,max}$ (n=36).

Model #	Model Equation[a]	# of Parameters	V1[b]	V2[b]	V3[b]	V4[b]	V5[b]	$Q_{10,1}$	$Q_{10,2}$	$Q_{10,3}$	$Q_{10,4}$	$Q_{10,5}$	sd	AIC_c	R^2
4	$V_{c,max} = V \times Q_{10}^{(T-25)/10} \times N_{area}$	3	750.74	--	--	--	--	3.73	--	--	--	--	39.18	0.00	0.64
10	$V_{c,max} = V[spp] \times Q_{10}^{(T-25)/10} \times N_{area}$	5	796.38	921.18	739.63	--	--	3.18	--	--	--	--	38.74	2.09	0.68
7	$V_{c,max} = V[loc] \times Q_{10}^{(T-25)/10} \times N_{area}$	4	746.98	795.25	--	--	--	3.63	--	--	--	--	39.87	2.14	0.65
20	$V_{c,max} = V \times Q_{10}[loc]^{(T-25)/10} \times N_{area}$	4	742.52	--	--	--	--	3.67	3.94	--	--	--	39.59	2.61	0.64
6	$V_{c,max} = V[loc] \times Q_{10}^{(T-25)/10}$	4	122.79	77.99	--	--	--	3.67	--	--	--	--	40.29	3.13	0.64
16	$V_{c,max} = V \times Q_{10}[spp]^{(T-25)/10} \times N_{area}$	5	760.18	--	--	--	--	3.85	3.87	3.36	--	--	39.58	4.62	0.65
19	$V_{c,max} = V \times Q_{10}[loc]^{(T-25)/10}$	4	107.37	--	--	--	--	4.89	1.68	--	--	--	40.58	5.18	0.62
11	$V_{c,max} = V[spp\_loc] \times Q_{10}^{(T-25)/10}$	7	106.34	73.24	129.31	137.36	93.28	3.46	--	--	--	--	34.82	5.44	0.70
12	$V_{c,max} = V[spp\_loc] \times Q_{10}^{(T-25)/10} \times N_{area}$	7	734.92	911.41	902.78	717.42	839.68	3.15	--	--	--	--	37.60	6.76	0.69
17	$V_{c,max} = V \times Q_{10}[spp\_loc]^{(T-25)/10}$	7	108.18	--	--	--	--	3.91	0.74	4.72	7.26	2.28	39.38	10.52	0.65
18	$V_{c,max} = V \times Q_{10}[spp\_loc]^{(T-25)/10} \times N_{area}$	7	763.72	--	--	--	--	4.00	4.04	4.20	3.41	4.07	40.49	11.27	0.65
9	$V_{c,max} = V[spp] \times Q_{10}^{(T-25)/10}$	5	89.82	128.68	116.28	--	--	3.48	--	--	--	--	45.22	14.71	0.54

3	$V_{c,max} = V \times Q_{10}^{(T-25)/10}$	3	104.41	--	--	--	--	3.76	--	--	--	--	49.82	16.89	0.43
15	$V_{c,max} = V \times Q_{10}[spp]^{(T-25)/10}$	5	106.68	--	--	--	--	2.40	4.82	3.85	--	--	47.62	17.21	0.51
2	$V_{c,max} = V \times N_{area}$	2	1012.10	--	--	--	--	--	--	--	--	--	59.99	28.02	0.17
5	$V_{c,max} = V[loc]$	3	164.10	105.62	--	--	--	--	--	--	--	--	59.60	30.42	0.17
14	$V_{c,max} = V[spp\_loc] \times N_{area}$	6	859.56	1239.07	1407.58	919.84	1075.72	--	--	--	--	--	56.21	33.12	0.29
1	$V_{c,max} = V$	2	141.60	--	--	--	--	--	--	--	--	--	65.91	34.87	0.00
8	$V_{c,max} = V[spp]$	4	118.21	176.89	148.29	--	--	--	--	--	--	--	63.30	35.46	0.11
13	$V_{c,max} = V[spp\_loc]$	6	139.59	86.23	175.96	181.59	118.60	--	--	--	--	--	59.68	35.53	0.24

[a]Model equations containing "spp" estimate parameters for each species, where V1 and $Q_{10,1}$ are parameters for red maple, V2 and $Q_{10,2}$ are for bigtooth aspen, and V3 and $Q_{10,3}$ are for red oak. Model equations containing "loc" estimate parameters for each canopy location, where V1 and $Q_{10,1}$ are parameters for sun leaves and V_2 and $Q_{10,2}$ are parameters for shade leaves. Model equations containing "spp_loc" estimate parameters for each species-specific canopy location, where V1 and $Q_{10,1}$ are parameters for red maple sun leaves, V2 and $Q_{10,2}$ are parameters for red maple shade leaves, V3 and $Q_{10,3}$ are parameters for bigtooth aspen sun leaves, V4 and $Q_{10,4}$ are parameters for red oak sun leaves, and V5 and $Q_{10,5}$ are parameters for red oak shade leaves.
[b]Parameters of V are in units of μmol CO_2 / (10,000 mg N s).

Table C2: List of equations, maximum likelihood parameter estimates, differences in AIC_c scores compared to the model with the lowest AIC_c (ΔAIC_c), standard deviation (sd) and R^2 for the models used to test for patterns in *J* (n=36).

Model #	Model Equation	# of Parameters	C_{J1}[b]	C_{J2}[b]	C_{J3}[b]	C_{J4}[b]	C_{J5}[b]	$Q_{10,1}$	$Q_{10,2}$	$Q_{10,3}$	$Q_{10,4}$	$Q_{10,5}$	C_V	sd	AICc
11	$J = C_J[spp\_loc] \times Q_{10}^{(T-25)/10}$	7	116.02	69.42	148.92	134.37	102.23	1.79	--	--	--	--	--	21.25	0.00
22	$J = C_J \times V_{c,max}$	2	0.86	--	--	--	--	--	--	--	--	--	--	28.62	6.45
6	$J = C_J[loc] \times Q_{10}^{(T-25)/10}$	4	134.23	89.60	--	--	--	1.80	--	--	--	--	--	27.30	6.84
19	$J = C_J \times Q_{10}[loc]^{(T-25)/10}$	4	117.46	--	--	--	--	2.42	0.85	--	--	--	--	30.03	13.85
10	$J = C_J[spp] \times Q_{10}^{(T-25)/10} \times N_{area}$	5	845.76	1134.42	765.60	--	--	1.57	--	--	--	--	--	28.48	13.90
12	$J = C_J[spp\_loc] \times Q_{10}^{(T-25)/10} \times N_{area}$	7	827.47	912.62	1163.37	735.27	905.15	1.54	--	--	--	--	--	27.09	14.34
9	$J = C_J[spp] \times Q_{10}^{(T-25)/10}$	5	95.80	157.34	120.75	--	--	1.66	--	--	--	--	--	29.30	15.21
13	$J = C_J[spp\_loc]$	6	130.15	82.26	173.29	150.09	116.90	--	--	--	--	--	--	27.58	15.76
5	$J = C_J[loc]$	3	151.72	101.54	--	--	--	--	--	--	--	--	--	32.22	17.83
17	$J = C_J \times Q_{10}[spp\_loc]^{(T-25)/10}$	7	117.53	--	--	--	--	2.10	0.58	2.89	2.75	1.09	--	26.29	18.09
14	$J = C_J[spp\_loc] \times N_{area}$	6	836.42	1117.89	1268.55	785.34	1037.22	--	--	--	--	--	--	31.92	21.82
15	$J = C_J \times Q_{10}[spp]^{(T-25)/10}$	5	121.37	--	--	--	--	0.97	2.60	1.71	--	--	--	32.64	22.89
8	$J = C_J[spp]$	4	109.07	171.58	132.78	--	--	--	--	--	--	--	--	33.58	23.12
4	$J = C_J \times Q_{10}^{(T-25)/10} \times N_{area}$	3	815.79	--	--	--	--	1.84	--	--	--	--	--	36.08	24.45
16	$J = C_J \times Q_{10}[spp]^{(T-25)/10} \times N_{area}$	5	843.49	--	--	--	--	1.82	2.27	1.26	--	--	--	31.72	24.93
7	$J = C_J[loc] \times Q_{10}^{(T-25)/10} \times N_{area}$	4	806.69	887.74	--	--	--	1.77	--	--	--	--	--	35.12	26.13
21	$J = C_J \times C_V \times Q_{10}^{(T-25)/10} \times N_{area}$	4	5492.60	--	--	--	--	1.78	--	--	--	--	0.15	35.65	26.99
20	$J = C_J \times Q_{10}[loc]^{(T-25)/10} \times N_{area}$	4	833.02	--	--	--	--	1.74	1.73	--	--	--	--	34.93	27.10
3	$J = C_J \times Q_{10}^{(T-25)/10}$	3	117.13	--	--	--	--	1.75	--	--	--	--	--	37.20	27.28
18	$J = C_J \times Q_{10}[spp\_loc]^{(T-25)/10} \times N_{area}$	7	855.80	--	--	--	--	1.99	1.05	2.44	0.78	2.15	--	33.44	29.37
2	$J = C_J \times N_{area}$	2	926.21	--	--	--	--	--	--	--	--	--	--	40.13	30.63
1	$J = C_J$	2	131.54	--	--	--	--	--	--	--	--	--	--	40.83	31.73

[a]Model equations containing "spp" estimate parameters for each species, where C_{J1} and $Q_{10,1}$ are parameters for red maple, C_{J2} and $Q10_2$ are parameters for bigtooth aspen, and C_{J3} and $Q_{10,3}$ are parameters for red oak. Model equations containing "loc" estimate parameters for each canopy location, where C_{J1} and $Q_{10,1}$ are parameters for sun leaves and C_{J2} and $Q_{10,2}$ are parameters for shade leaves. Model equations containing "spp_loc" estimate parameters for each species-specific canopy location, where C_{J1} and $Q_{10,1}$ are parameters for red maple sun leaves, C_{J2} and $Q_{10,2}$ are parameters for red maple shade leaves, C_{J3} and $Q_{10,3}$ are parameters for bigtooth aspen sun leaves, C_{J4} and $Q_{10,4}$ are parameters for red oak sun leaves, and C_{J5} and $Q_{10,5}$ are parameters for red oak shade leaves. $V_{c,max}$

is the maximum rate of carboxylation as derived from the A/C_i curves shown in Figure 4.1. C_V is the parameter estimate for $V_{c,max}$.
[b]Parameters of V are in units of μmol CO_2 m^{-2} s^{-1}.

Table C3: List of equations, maximum likelihood parameter estimates, differences in AIC_c scores compared to the model with the lowest AIC_c (ΔAIC_c), standard deviation (sd) and R^2 for the models used to test for patterns in *TPU* (n=36).

Model #	Model Equation[a]	# of Parameters	C_{TPU1}	C_{TPU2}	C_{TPU3}	C_{TPU4}	C_{TPU5}	$Q_{10,1}$	$Q_{10,2}$	$Q_{10,3}$	$Q_{10,4}$	$Q_{10,5}$	C_V	sd	AIC_c	R^2
5	$TPU = C_{TPU}[loc]$	3	9.41	6.21	--	--	--	--	--	--	--	--	--	1.73	0.00	0.44
6	$TPU = C_{TPU}[loc] \times Q_{10}^{(T-25)/10}$	4	9.09	6.04	--	--	--	1.16	--	--	--	--	--	1.74	1.56	0.46
13	$TPU = C_{TPU}[spp\_loc]$	6	9.25	5.98	10.35	9.10	6.49	--	--	--	--	--	--	1.71	5.49	0.48
19	$TPU = C_{TPU} \times Q_{10}[loc]^{(T-25)/10}$	4	8.00	--	--	--	--	1.64	0.46	--	--	--	--	1.83	5.78	0.39
11	$TPU = C_{TPU}[spp\_loc] \times Q_{10}^{(T-25)/10}$	7	8.57	5.46	9.95	8.38	6.22	1.19	--	--	--	--	--	1.75	8.03	0.49
17	$TPU = C_{TPU} \times Q10[spp\_loc]^{(T-25)/10}$	7	8.00	--	--	--	--	1.86	0.57	1.81	1.48	0.41	--	1.81	13.86	0.40
8	$TPU = C_{TPU}[spp]$	4	7.59	10.42	7.61	--	--	--	--	--	--	--	--	2.09	16.01	0.19
9	$TPU = C_{TPU}[spp] \times Q_{10}^{(T-25)/10}$	5	7.58	10.15	7.30	--	--	1.16	--	--	--	--	--	2.09	18.58	0.19
1	$TPU = C_{TPU}$	2	8.14	--	--	--	--	--	--	--	--	--	--	2.34	18.69	0.00
10	$TPU = C_{TPU}[spp] \times Q_{10}^{(T-25)/10} \times N_{area}$	5	63.23	73.92	47.59	--	--	1.07	--	--	--	--	--	2.25	20.60	0.15
14	$TPU = C_{TPU}[spp\_loc] \times N_{area}$	6	61.26	76.42	73.18	44.89	55.29	--	--	--	--	--	--	2.11	20.73	0.21
3	$TPU = C_{TPU} \times Q_{10}^{(T-25)/10}$	3	8.04	--	--	--	--	1.08	--	--	--	--	--	2.33	20.89	0.01
15	$TPU = C_{TPU} \times Q_{10}[spp]^{(T-25)/10}$	5	8.05	--	--	--	--	1.13	1.71	0.82	--	--	--	2.32	22.03	0.12
12	$TPU = C_{TPU}[spp\_loc] \times Q_{10}^{(T-25)/10} \times N_{area}$	7	62.14	75.82	71.08	44.95	54.65	1.03	--	--	--	--	--	2.05	23.86	0.21
16	$TPU = C_{TPU} \times Q_{10}[spp]^{(T-25)/10} \times N_{area}$	5	57.11	--	--	--	--	1.81	1.59	0.56	--	--	--	2.24	24.75	0.04
2	$TPU = C_{TPU} \times N_{area}$	2	56.58	--	--	--	--	--	--	--	--	--	--	2.68	28.27	0.00
4	$TPU = C_{TPU} \times Q_{10}^{(T-25)/10} \times N_{area}$	3	55.15	--	--	--	--	1.16	--	--	--	--	--	2.66	30.29	0.00
18	$TPU = C_{TPU} \times Q_{10}[spp\_loc]^{(T-25)/10} \times N_{area}$	7	59.18	--	--	--	--	1.81	1.07	1.22	0.52	0.31	--	2.33	31.48	0.02
7	$TPU = C_{TPU}[loc] \times Q_{10}^{(T-25)/10} \times N_{area}$	4	54.35	59.69	--	--	--	1.16	--	--	--	--	--	2.64	32.40	0.00
20	$TPU = C_{TPU} \times Q_{10}[loc]^{(T-25)/10} \times N_{area}$	4	55.54	--	--	--	--	1.16	0.89	--	--	--	--	2.64	32.44	0.00
21	$TPU = C_{TPU} \times C_V \times Q_{10}^{(T-25)/10} \times N_{area}$	4	8066.87	--	--	--	--	1.13	--	--	--	--	0.01	2.67	32.83	0.00
22	$TPU = C_{TPU} \times V_{c,max}$	2	0.05	--	--	--	--	--	--	--	--	--	--	3.26	42.35	0.00

[a]Model equations containing "spp" estimate parameters for each species, where C_{TPU1} and $Q_{10,1}$ are parameters for red maple, C_{TPU2} and $Q_{10,2}$ are parameters for bigtooth aspen, and C_{TPU3} and $Q_{10,3}$ are parameters for red oak. Model equations containing "loc" estimate parameters for each canopy location, where C_{TPU1} and $Q_{10,1}$ are parameters for sun leaves and C_{TPU2} and $Q_{10,2}$ are parameters for shade leaves. Model equations containing "spp_loc" estimate parameters for each species-specific canopy location, where C_{TPU1} and $Q_{10,1}$ are parameters for red maple sun leaves, C_{TPU2} and $Q_{10,2}$ are parameters for red maple shade leaves, C_{TPU3} and $Q_{10,3}$ are parameters for bigtooth aspen sun leaves, C_{TPU4} and $Q_{10,4}$ are parameters for red oak sun leaves, and C_{TPU5} and $Q_{10,5}$ are parameters for red oak. $V_{c,max}$

is the maximum rate of carboxylation as derived from the A/C_i curves shown in Figure 4.1. C_V is the parameter estimate for $V_{c,max}$.
[b]Parameters of V are in units of μmol CO_2 m^{-2} s^{-1}.